

XYZ-SU3 Breakings from Laplace Sum Rules at Higher Orders

R. Albuquerque

Faculty of Technology, Rio de Janeiro State University (FAT, UERJ), Brazil

Email address: raphael.albuquerque@uerj.br

S. Narison*

*Laboratoire Univers et Particules de Montpellier (LUPM), CNRS-IN2P3,
Case 070, Place Eugène Bataillon, 34095 - Montpellier, France.*

Email address: snarison@gmail.com

D. Rabetiarivony** and G. Randriamananjara**

Institute of High-Energy Physics of Madagascar (iHEPMAD)

University of Antakatso, Antananarivo 101, Madagascar

We present new compact integrated expressions of SU3 breaking corrections to QCD spectral functions of heavy-light molecules and four-quark *XYZ*-like states at lowest order (LO) of perturbative (PT) QCD and up to $d = 8$ condensates of the Operator Product Expansion (OPE). Including next-to-next-to-leading order (N2LO) PT corrections in the chiral limit and next-to-leading order (NLO) SU3 PT corrections, which we have estimated by assuming the factorization of the four-quark spectral functions, we improve previous LO results for the *XYZ*-like masses and decay constants from QCD spectral sum rules (QSSR). Systematic errors are estimated from a geometric growth of the higher order PT corrections and from some partially known $d = 8$ non-perturbative contributions. Our optimal results, based on stability criteria, are summarized in Tables 18 to 21 while the 0^{++} and 1^{++} channels are compared with some existing LO results in Table 22. One can notice that, in most channels, the SU3 corrections on the meson masses are tiny: $\leq 10\%$ (resp. $\leq 3\%$) for the c (resp. b)-quark channel but can be large for the couplings ($\leq 20\%$). Within the lowest dimension currents, most of the 0^{++} and 1^{++} states are below the physical thresholds while our predictions cannot discriminate a molecule from a four-quark state. A comparison with the masses of some experimental candidates indicates that the 0^{++} X(4500) might have a large $\bar{D}_{s0}^* D_{s0}^*$ molecule component while an interpretation of the 0^{++} candidates as four-quark ground states is not supported by our findings. The 1^{++} X(4147) and X(4273) are compatible with the $\bar{D}_s^* D_s$, $\bar{D}_{s0}^* D_{s1}$ molecules and/or with the axial-vector A_c four-quark ground state. Our results for the $0^{-\pm}$, $1^{-\pm}$ and for different beauty states can be tested in the future data. Finally, we revisit our previous estimates¹ for the $\bar{D}_0^* D_0^*$ and $\bar{D}_0^* D_1$ and present new results for the $\bar{D}_1 D_1$.

Keywords: QCD spectral sum rules, Perturbative and Non-Perturbative calculations, Exotic mesons masses and decay constants.

Pac numbers: 11.55.Hx, 12.38.Lg, 13.20-v

* ICTP-Trieste consultant for Madagascar.

** PhD Students.

1. Introduction and Experimental Facts

In recent papers,^{1–4} we have used QCD spectral (Laplace^{5–10} and FESR^{11,12}) sum rules^{13–19} to improve our previous results for the masses and decay constants (couplings) of the XYZ exotic heavy-light and charmonium-like mesons obtained in the chiral limit $m_q = 0$ ^{20–24}^a. In so doing, we include up to next-to-next-leading (N2LO) PT factorizable corrections to the heavy-light exotic (molecule and four-quark) correlators which are necessary for giving more sense on the input values of the heavy quark masses which play an important rôle in the analysis.

In this paper^b, we pursue our investigation by including analogous N2LO PT corrections in the chiral limit and adding to these the SU3 NLO PT corrections to the heavy-light exotic correlators. To these new higher order (HO) PT contributions, we add the contributions of condensates having a dimension ($d \leq 6$) already available in the literature but rederived in this paper. Due to the uncertainties on the size (violation of the factorization assumption,^{29–33} mixing of operators³⁴) and incomplete contributions (only one class of contributions are only computed in the literature) of higher dimension ($d \geq 8$), we do not include them into the analysis but only consider their effects as a source of systematic errors due to the truncation of the Operator Product Expansion (OPE). The contributions of the unknown order α_s^3 N2LO contribution are estimated from a geometric growth of the PT series³⁵ and are added as a source of systematic uncertainties in the truncation of the PT series. In this sense, we consider this work as an improvement of previous related works in the literature and, in particular, our works in.^{23,24}

Recent measurements of the $J/\psi\phi$ invariant masses from $B^+ \rightarrow J/\psi\phi K^+$ decays by the LHCb collaboration³⁶ confirmed the existence of the $X(4147)$ and $X(4273)$ with quantum numbers 1^{++} within 8.4 and 6.0σ significance found earlier by the CDF,^{37,38} the CMS³⁹ and the D0⁴⁰ collaborations. In the same time, the LHCb collaboration has reported the existence of the 0^{++} states in the analogous $J/\psi\phi$ invariant masses. On the other, the BELLE collaboration⁴¹ has found a $J/\psi\phi$ narrow structure within a 3.2σ , the $Y(4351)$ with a width of 13 MeV [but not the $X(4140)$ found earlier by the CDF collaboration³⁷] from $\gamma\gamma$ scattering which can be a 0^{++} or a 2^{++} state. These experimental results are summarized in Table 1.

Our results are summarized in Tables 18 to 21 and in the last section : Summary and Conclusions. A comparison with some other lowest order (LO) QCD spectral sum rules for the 0^{++} and 1^{++} states is given in Table 22 of Section 10. A confrontation with different experimental candidates is also given in this section.

^aFor reviews, see e.g.^{25–27}

^bA compact form of the paper can be found in²⁸

Table 1. Experimental 1^{++} and 0^{++} observed states from the $J/\psi\phi$ invariant masses of the $B^\pm \rightarrow J/\psi\phi K^\pm$ decays and $\gamma\gamma \rightarrow J/\psi\phi$ scattering process.

States	J^{PC}	Mass [MeV]	Total width [MeV]	Refs.
	1^{++}			
X(4147)		$4146.5 \pm 4.5^{+4.6}_{-2.8}$	$83 \pm 21^{+21}_{-14}$	36–40
X(4273)		$4273.3 \pm 8.3^{+17.2}_{-3.6}$	$56 \pm 11^{+8}_{-11}$	36, 38
	0^{++} or 2^{++}			
X(4350)		$4350.6^{+4.6}_{-5.1} \pm 0.7$	$13^{+18}_{-9} \pm 4$	41
	0^{++}			
X(4500)		$4506 \pm 11^{+12}_{-15}$	$92 \pm 21^{+21}_{-21}$	36
X(4700)		$4704 \pm 10^{+14}_{-24}$	$120 \pm 31^{+42}_{-33}$	36

2. QCD expressions of the Spectral Functions

Compared to previous LO QCD expressions of the spectral functions given in the literature, we provide new integrated compact expressions which are more elegant and easier to handle for the numerical analysis. These expressions are tabulated in the Appendices.

The PT expression of the spectral function obtained using on-shell renormalization has been transformed into the \overline{MS} -scheme by using the relation between the \overline{MS} running mass $\overline{m}_Q(\mu)$ and the on-shell mass (pole) M_Q , to order α_s^2 :^{42–51}

$$\begin{aligned} M_Q = \overline{m}_Q(\mu) & \left[1 + \frac{4}{3}a_s + (16.2163 - 1.0414n_l)a_s^2 \right. \\ & + \text{Log}\left(\frac{\mu}{M_Q}\right)^2 (a_s + (8.8472 - 0.3611n_l)a_s^2) \\ & \left. + \text{Log}^2\left(\frac{\mu}{M_Q}\right)^2 (1.7917 - 0.0833n_l)a_s^2 \dots \right], \end{aligned} \quad (1)$$

for n_l light flavours where μ is the arbitrary subtraction point and $a_s \equiv \alpha_s/\pi$.

Higher order PT corrections are obtained using the factorization assumption of the four-quark correlators into a convolution of bilinear current correlators as we shall discuss later on.

3. QSSR analysis of the Heavy-Light Molecules

3.1. Molecule currents and the QCD two-point function

For describing these molecule states, we shall consider the usual lowest dimension local interpolating currents where each bilinear current has the quantum number of the corresponding open $D_s(0^-)$, $D_{s0}^*(0^+)$, $D_s^*(1^-)$, $D_{s1}(1^+)$ states and the anal-

ogous states in the b -quark channel^c. The previous assignment is consistent with the definition of a molecule to be a weakly bound state of two mesons within a Van der Waals force other than a gluon exchange. This feature can justify the approximate use (up to order $1/N_c$) of the factorization of the four-quark currents as a convolution of two bilinear quark-antiquark currents when estimating the HO PT corrections. These states and the corresponding interpolating currents are given in Table 2.

Table 2. Interpolating currents with a definite C -parity describing the molecule-like states. $Q \equiv c$ (resp. b) for the $\bar{D}_s D_s$ (resp. $\bar{B}_s B_s$)-like molecules.

States	J^{PC}	Molecule Currents $\equiv \mathcal{O}_{mol}(x)$
Scalar	0^{++}	
$\bar{D}_s D_s, \bar{B}_s B_s$		$(\bar{s}\gamma_5 Q)(\bar{Q}\gamma_5 s)$
$\bar{D}_s^* D_s^*, \bar{B}_s^* B_s^*$		$(\bar{s}\gamma_\mu Q)(\bar{Q}\gamma^\mu s)$
$\bar{D}_{s0}^* D_{s0}^*, \bar{B}_{s0}^* B_{s0}^*$		$(\bar{s}Q)(\bar{Q}s)$
$\bar{D}_{s1} D_{s1}, \bar{B}_{s1} B_{s1}$		$(\bar{s}\gamma_\mu \gamma_5 Q)(\bar{Q}\gamma^\mu \gamma_5 s)$
Axial-vector	1^{++}	
$\bar{D}_s^* D_s, \bar{B}_s^* B_s$		$\frac{i}{\sqrt{2}} \left[(\bar{Q}\gamma_\mu s)(\bar{s}\gamma_5 Q) - (\bar{s}\gamma_\mu Q)(\bar{Q}\gamma_5 s) \right]$
$\bar{D}_{s0}^* D_{s1}, \bar{B}_{s0}^* B_{s1}$		$\frac{1}{\sqrt{2}} \left[(\bar{s}Q)(\bar{Q}\gamma_\mu \gamma_5 s) + (\bar{Q}s)(\bar{s}\gamma_\mu \gamma_5 Q) \right]$
Pseudoscalar	$0^{-\pm}$	
$\bar{D}_{s0}^* D_s, \bar{B}_{s0}^* B_s$		$\frac{1}{\sqrt{2}} \left[(\bar{s}Q)(\bar{Q}\gamma_5 s) \pm (\bar{Q}s)(\bar{q}\gamma_5 Q) \right]$
$\bar{D}_s^* D_{s1}, \bar{B}_s^* B_{s1}$		$\frac{1}{\sqrt{2}} \left[(\bar{Q}\gamma_\mu s)(\bar{s}\gamma^\mu \gamma_5 Q) \mp (\bar{Q}\gamma_\mu \gamma_5 s)(\bar{s}\gamma^\mu Q) \right]$
Vector	$1^{-\pm}$	
$\bar{D}_{s0}^* D_s^*, \bar{B}_{s0}^* B_s^*$		$\frac{1}{\sqrt{2}} \left[(\bar{s}Q)(\bar{Q}\gamma_\mu s) \mp (\bar{Q}s)(\bar{q}\gamma_\mu Q) \right]$
$\bar{D}_s D_{s1}, \bar{B}_s B_{s1}$		$\frac{i}{\sqrt{2}} \left[(\bar{Q}\gamma_\mu \gamma_5 s)(\bar{s}\gamma_5 Q) \pm (\bar{s}\gamma_\mu \gamma_5 Q)(\bar{Q}\gamma_5 s) \right]$

The two-point correlators associated to the (axial)-vector interpolating operators are:

$$\begin{aligned} \Pi_{mol}^{\mu\nu}(q) &\equiv i \int d^4x e^{iq \cdot x} \langle 0 | T[\mathcal{O}_{mol}^\mu(x) \mathcal{O}_{mol}^{\nu\dagger}(0)] | 0 \rangle \\ &= -\Pi_{mol}^{(1)}(q^2)(g^{\mu\nu} - \frac{q^\mu q^\nu}{q^2}) + \Pi_{mol}^{(0)}(q^2) \frac{q^\mu q^\nu}{q^2}, \end{aligned} \quad (2)$$

^cFor convenience, we shall not consider colored and more general combinations of interpolating operators discussed e.g in^{52,53} as well as higher dimension ones involving derivatives.

The two invariants, $\Pi_{mol}^{(1)}$ and $\Pi_{mol}^{(0)}$, appearing in Eq. (2) are independent and have respectively the quantum numbers of the spin 1 and 0 mesons.

$\Pi_{mol}^{(0)}$ is related via Ward identities^{13,14} to the (pseudo)scalar two-point functions $\psi_{mol}^{(s,p)}(q^2)$ built directly from the (pseudo)scalar currents given in Table 2:

$$\psi_{mol}^{(s,p)}(q^2) = i \int d^4x e^{iq.x} \langle 0 | T[\mathcal{O}_{mol}^{(s,p)}(x) \mathcal{O}_{mol}^{(s,p)}(0)] | 0 \rangle , \quad (3)$$

with which we shall work in the following.

Thanks to their analyticity properties, the invariant functions $\Pi_{mol}^{(1,0)}(q^2)$ in Eq. (2) and the two-point correlator $\psi_{mol}^{(s,p)}(q^2)$ in Eq. 3 obey the dispersion relation:

$$\Pi_{mol}^{(1,0)}(q^2), \psi_{mol}^{(s,p)}(q^2) = \frac{1}{\pi} \int_{4M_Q^2}^{\infty} dt \frac{\text{Im}\{\Pi_{mol}^{(1,0)}(t), \psi_{mol}^{(s,p)}(t)\}}{t - q^2 - i\epsilon} + \dots , \quad (4)$$

where $\text{Im}\Pi_{mol}^{(1,0)}(t)$, $\text{Im}\psi_{mol}^{(s,p)}(t)$ are the spectral functions and \dots indicate subtraction points which are polynomial in q^2 .

3.2. LO PT and NP corrections to the molecule spectral functions

The new different LO integrated expressions including non-perturbative (NP) corrections up to dimension $d=6-8$ used in the analysis are tabulated in Appendix A.

Compared to the ones in the literature, the expressions of the spectral functions are in integrated and compact forms which are more easier to handle for the numerical phenomenological analysis.

However, one should note that some of the expressions given in the literature do not agree each others. Due to the few informations given by the authors on their derivation, it is difficult to trace back the origin of such discrepancies^d. Hopefully, within the accuracy of the approach, such discrepancies affect only slightly the final results if the errors are taken properly.

In the chiral limit $m_q = 0$ and $\langle \bar{u}u \rangle = \langle \bar{d}d \rangle$, we have checked that the orthogonal combinations of $\bar{D}^*D, \bar{B}^*B(1^{++}), \bar{D}_0^*D_1, \bar{B}_0^*B_1(0^{--})$ and $\bar{D}^*D_1, \bar{B}^*B_1(0^{--})$ molecules give the same results up to the $d = 6$ contributions. This is due to the presence of one γ_5 matrix in the current which neutralizes the different traces appearing in each pair. This is not the case of the $\bar{D}_0^*D^*, \bar{B}_0^*B^*$ (without γ_5) and $\bar{D}D_1, \bar{B}B_1$ (with two γ_5).

3.3. N2LO PT corrections using factorization

Assuming a factorization of the four-quark interpolating current as a natural consequence of the molecule definition of the state, we can write the corresponding

^dA numerical comparison in some specific channels is given in Section 10.

spectral function as a convolution of the spectral functions associated to quark bilinear current^e as illustrated by the Feynman diagrams in Fig. 1. In this way, we obtain⁵⁴^f for the $\bar{D}D^*$ - and $\bar{D}_0^*D^*$ -like spin 1 states:

$$\frac{1}{\pi} \text{Im}\Pi_{mol}^{(1)}(t) = \theta(t - 4M_Q^2) \left(\frac{1}{4\pi}\right)^2 t^2 \int_{M_Q^2}^{(\sqrt{t}-M_Q)^2} dt_1 \int_{M_Q^2}^{(\sqrt{t}-\sqrt{t_1})^2} dt_2 \\ \times \lambda^{3/2} \frac{1}{\pi} \text{Im}\Pi^{(1)}(t_1) \frac{1}{\pi} \text{Im}\psi^{(s,p)}(t_2). \quad (5)$$

For the $\bar{D}D$ -like spin 0 state, one has:

$$\frac{1}{\pi} \text{Im}\psi_{mol}^{(s)}(t) = \theta(t - 4M_Q^2) \left(\frac{1}{4\pi}\right)^2 t^2 \int_{M_Q^2}^{(\sqrt{t}-M_Q)^2} dt_1 \int_{M_Q^2}^{(\sqrt{t}-\sqrt{t_1})^2} dt_2 \\ \times \lambda^{1/2} \left(\frac{t_1}{t} + \frac{t_2}{t} - 1\right)^2 \\ \times \frac{1}{\pi} \text{Im}\psi^{(p)}(t_1) \frac{1}{\pi} \text{Im}\psi^{(p)}(t_2), \quad (6)$$

and for the \bar{D}^*D^* -like spin 0 state:

$$\frac{1}{\pi} \text{Im}\psi_{mol}^{(s)}(t) = \theta(t - 4M_Q^2) \left(\frac{1}{4\pi}\right)^2 t^2 \int_{M_Q^2}^{(\sqrt{t}-M_Q)^2} dt_1 \int_{M_Q^2}^{(\sqrt{t}-\sqrt{t_1})^2} dt_2 \\ \times \lambda^{1/2} \left[\left(\frac{t_1}{t} + \frac{t_2}{t} - 1\right)^2 + \frac{8t_1 t_2}{t^2}\right] \\ \times \frac{1}{\pi} \text{Im}\Pi^{(1)}(t_1) \frac{1}{\pi} \text{Im}\Pi^{(1)}(t_2), \quad (7)$$

where:

$$\lambda = \left(1 - \frac{(\sqrt{t_1} - \sqrt{t_2})^2}{t}\right) \left(1 - \frac{(\sqrt{t_1} + \sqrt{t_2})^2}{t}\right), \quad (8)$$

is the phase space factor and M_Q is the on-shell heavy quark mass. $\text{Im } \Pi^{(1)}(t)$ is the spectral function associated to the bilinear $\bar{c}\gamma_\mu(\gamma_5)q$ vector or axial-vector current, while $\text{Im } \psi^{(5)}(t)$ is associated to the $\bar{c}(\gamma_5)q$ scalar or pseudoscalar current^g. This representation simplifies the evaluation of the PT α_s^n -corrections as we can use the PT expression of the spectral functions for heavy-light bilinear currents known to order α_s (NLO) from⁵⁸^h. Order α_s^2 (N2LO) corrections are known in the chiral limit $m_q = 0$ from^{59,60} which are available as a Mathematica Program

^eIt is called properly sesquilinear instead of bilinear current as it is formed by a quark field and its anti-particle.

^fFor some applications to the $\bar{B}B$ mixing, see e.g.^{55–57}

^gIn the limit where the light quark mass $m_q = 0$, the PT expressions of the vector (resp. scalar) and axial-vector (resp. pseudoscalar) spectral functions are the same.

^hWithin the above procedure, we have checked that we reproduce the factorized PT LO contributions obtained using for example the PT expressions of $\bar{D}_0^*D_0^*$ and $\bar{D}_0^*D^*$ given in Appendix A.

named Rvsⁱ. We shall use the NLO SU3 breaking PT corrections obtained in⁶¹ from the two-point function formed by bilinear currents. From the above representation, the anomalous dimensions of the molecule correlators come from the (pseudo)scalar current. Therefore, the corresponding renormalization group invariant interpolating current reads to NLO^j:

$$\bar{\mathcal{O}}_{mol}^{(s,p)}(\mu) = a_s(\mu)^{4/\beta_1} \mathcal{O}_{mol}^{(s,p)}, \quad \bar{\mathcal{O}}_{mol}^{(v,a)}(\mu) = a_s(\mu)^{2/\beta_1} \mathcal{O}_{mol}^{(v,a)}, \quad (9)$$

with $-\beta_1 = (1/2)(11 - 2n_f/3)$ is the first coefficient of the QCD β -function for n_f flavours and $a_s \equiv (\alpha_s/\pi)$.

3.4. $1/q^2$ tachyonic gluon mass and large order PT corrections

The $1/q^2$ corrections due to a tachyonic gluon mass discussed in^{62,63} (for reviews see: ^{64,65}) will not be included here. Instead, we shall consider the fact that they are dual to the sum of the large order PT series³⁵ such that, with the inclusion of the N3LO terms estimated from the geometric growth of the QCD PT series³⁵ as a source of the PT errors, we expect to give a good approximation of these uncalculated higher order terms. The estimate of these errors is given in Tables 7 to 16.

3.5. Parametrization of the Spectral Function within MDA

We shall use the Minimal Duality Ansatz (MDA) given in Eq. 10 for parametrizing the spectral function (generic notation):

$$\frac{1}{\pi} \text{Im}\Pi_{mol}(t) \simeq f_{mol}^2 M_{mol}^8 \delta(t - M_{mol}^2) + \text{"QCD continuum"} \theta(t - t_c), \quad (10)$$

where f_{mol} is the decay constant defined as:

$$\langle 0 | \mathcal{O}_{mol}^{(s,p)} | mol \rangle = f_{mol}^{(s,p)} M_{mol}^4, \quad \langle 0 | \mathcal{O}_{mol}^\mu | mol \rangle = f_{mol}^{(v,a)} M_{mol}^5 \epsilon_\mu, \quad (11)$$

respectively for spin 0 and 1 molecule states with ϵ_μ the vector polarization. The higher states contributions are smeared by the "QCD continuum" coming from the discontinuity of the QCD diagrams and starting from a constant threshold t_c . This *simple model* has been tested successfully in the $e^+e^- \rightarrow hadrons$ (ρ and ϕ mesons) channels where complete data are available.^{13,14} Finite width corrections to this simple model has been e.g studied in^{66–68} and have been found to be negligible. We then expect that such results also hold here.

Noting that, in the previous definition in Table 2, the bilinear (pseudo)scalar current acquires an anomalous dimension due to its normalization, thus the decay

ⁱWe have seen in¹ that these N2LO corrections are relatively small which demonstrates the good convergence of the PT series.

^jThe spin 0 current built from two (axial)-vector currents has no anomalous dimension. We have introduced the super-indices (v, a) for denoting the vector and axial-vector spin 1 channels.

constants run to order α_s^2 as^k:

$$f_{mol}^{(s,p)}(\mu) = \hat{f}_{mol}^{(s,p)}(-\beta_1 a_s)^{4/\beta_1} / r_m^2, \quad f_{mol}^{(v,a)}(\mu) = \hat{f}_{mol}^{(v,a)}(-\beta_1 a_s)^{2/\beta_1} / r_m, \quad (12)$$

where we have introduced the renormalization group invariant coupling \hat{f}_{mol} . The QCD corrections numerically read to N2LO:

$$r_m(n_f = 4) = 1 + 1.014 a_s + 1.389 a_s^2, \quad r_m(n_f = 5) = 1 + 1.176 a_s + 1.501 a_s^2. \quad (13)$$

This coupling is the analogue of the pion decay constant $f_\pi = 132$ MeV where the corresponding hadronic coupling behaves as $1/f_{mol}$. This behaviour can be understood from a three-point sum rule analysis (for reviews, see e.g^{13, 14, 25}), à la Golberger-Treiman like-relation⁶⁹ or from some low-energy theorems.^{66, 117, 118}

3.6. The inverse Laplace transform sum rule (LSR)

The exponential sum rules firstly derived by SVZ^{5, 6} have been called Borel sum rules due to the factorial suppression factor of the condensate contributions in the OPE. Their quantum mechanics version have been studied by Bell-Bertlmann in^{8–10} through the harmonic oscillator where τ has the property of an imaginary time. The derivation of their radiative corrections has been firstly shown by Narison-de Rafael⁷ to have the properties of the inverse Laplace sum rule (LSR). The LSR and its ratio read¹:

$$\mathcal{L}_{mol}(\tau, t_c, \mu) = \frac{1}{\pi} \int_{4M_Q^2}^{t_c} dt e^{-t\tau} \text{Im}\{\Pi_{mol}^{(v,a)}, \psi_{mol}^{(s,p)}\}(t, \mu), \quad (14)$$

$$\mathcal{R}_{mol}(\tau, t_c, \mu) = \frac{\int_{4M_Q^2}^{t_c} dt t e^{-t\tau} \text{Im}\{\Pi_{mol}^{(v,a)}, \psi_{mol}^{(s,p)}\}(t, \mu)}{\int_{4M_Q^2}^{t_c} dt e^{-t\tau} \text{Im}\{\Pi_{mol}^{(v,a)}, \psi_{mol}^{(s,p)}\}(t, \mu)} \simeq M_R^2, \quad (15)$$

where μ is the subtraction point which appears in the approximate QCD series when radiative corrections are included and τ is the sum rule variable replacing q^2 . The variables τ, μ and t_c are, in principle, free parameters. We shall use stability criteria (if any), with respect to these free 3 parameters, for extracting the optimal results.

3.7. Double ratios of inverse Laplace transform sum rules (DRSR)

Double ratios of sum rules (DRSR)⁷⁰ are also useful for extracting the SU3 breaking effects on couplings and mass ratios. They read:

$$f_{mol}^{sd} \equiv \frac{\mathcal{L}_{mol}^s(\tau, t_c, \mu)}{\mathcal{L}_{mol}^d(\tau, t_c, \mu)}, \quad r_{mol}^{sd} \equiv \frac{\mathcal{R}_{mol}^s(\tau, t_c, \mu)}{\mathcal{R}_{mol}^d(\tau, t_c, \mu)}. \quad (16)$$

^kThe coupling of the (pseudo)scalar molecule built from two (axial)-vector currents has no anomalous dimension and does not run.

^lThe last equality in Eq. 15 is obtained when one uses MDA in Eq. 10 for parametrizing the spectral function.

The upper indices s, d indicate the s and d quark channels. These DRSR can be used when each sum rule optimizes at the same values of the parameters (τ, t_c, μ) . In this case, they lead to a more precise determination of the SU3 breaking effects on the couplings and mass ratios as obtained in some other channels.^{22, 71–80}

3.8. Tests of MDA and Stability Criteria

In the standard Minimal Duality Ansatz (MDA) given in Eq. 10 for parametrizing the spectral function, the “QCD continuum” threshold t_c is constant and is independent on the subtraction point μ ^m. One should notice that this standard MDA with constant t_c describes quite well the properties of the lowest ground state as explicitly demonstrated in^{82,83} and in various examples,^{13,14} while it has been also successfully tested in the large N_c limit of QCD in.^{84,85}

Refs.^{82,83} have explicitly tested this simple model by confronting the predictions of the integrated spectral function within this simple parametrization with the full data measurements. One can notice in Figs. 1 and 2 of Ref.^{82,83} the remarkable agreement of the model predictions and of the measured data of the J/ψ charmonium and Υ bottomonium systems for a large range of the inverse sum rule variable τ . Though it is difficult to estimate with a good precision the systematic error related to this simple model, this feature indicates the ability of the model for reproducing accurately the data. We expect that the same feature is reproduced for the case of the XYZ discussed here where complete data are still lacking.

In order to extract an optimal information for the lowest resonance parameters from this rather crude description of the spectral function and from the approximate QCD expression, one often applies the stability criteria at which an optimal result can be extracted. This stability is signaled by the existence of a stability plateau, an extremum or an inflexion point (so-called “sum rule window”) versus the changes of the external sum rule variables τ and t_c where the simultaneous requirement on the dominance over the continuum contribution and on the convergence of the OPE is automatically satisfied. This optimization criterion demonstrated in series of papers by Bell-Bertlmann,^{8–10} in the case of the τ -variable, by taking the examples of harmonic oscillator and charmonium sum rules and extended to the case of the t_c -parameter in^{13,14} gives a more precise meaning of the so-called “sum rule window” originally discussed by SVZ^{5,6} and used in the sum rules literature. Similar applications of the optimization method to the pseudoscalar D and B open meson states have been successful when comparing these results with the ones from some other determinations as discussed in Refs.^{82,83} and reviewed in^{13,14,86–88} and in some other recent reviews.^{89,90}

In this paper, we shall add to the previous well-known τ - and t_c -stability criteria, the one associated to the requirement of stability versus the arbitrary subtraction constant μ often put by hand in the current literature and which is often the source

^mSome model with a μ -dependence of t_c has been discussed e.g in.⁸¹

of large errors from the PT series in the sum rule analysis. The μ -stability procedure has been applied recently in^{82, 83, 87, 88, 91–94}ⁿ which gives a much better meaning on the choice of μ -value at which the observable is extracted, while the errors in the determinations of the results have been reduced due to a better control of the μ region of variation which is not the case in the existing literature.

Table 3. QCD input parameters: the original errors for $\langle \alpha_s G^2 \rangle$, $\langle g^3 G^3 \rangle$ and $\rho \langle \bar{q}q \rangle^2$ have been multiplied by about a factor 3 for a conservative estimate of the errors (see also the text).

Parameters	Values	Ref.
$\alpha_s(M_\tau)$	0.325(8)	29, 100, 101
\hat{m}_s	(0.114 ± 0.006) GeV	13, 29, 75, 76, 92, 102, 103
$\overline{m}_c(m_c)$	1261(12) MeV	average ^{104–110}
$\overline{m}_b(m_b)$	4177(11) MeV	average ^{104–107, 110}
$\hat{\mu}_q$	(253 ± 6) MeV	13, 75, 76, 92, 102, 103
$\kappa \equiv \langle \bar{s}s \rangle / \langle \bar{d}d \rangle$	$(0.74^{+0.34}_{-0.12})$	13, 79, 80
M_0^2	(0.8 ± 0.2) GeV ²	31–33, 77, 111–113
$\langle \alpha_s G^2 \rangle$	$(7 \pm 3) \times 10^{-2}$ GeV ²	8–10, 29, 30, 105–107, 114–119
$\langle g^3 G^3 \rangle$	(8.2 ± 2.0) GeV ² $\times \langle \alpha_s G^2 \rangle$	105–107
$\rho \alpha_s \langle \bar{q}q \rangle^2$	$(5.8 \pm 1.8) \times 10^{-4}$ GeV ⁶	29–33

3.9. QCD Input Parameters

The QCD parameters which shall appear in the following analysis will be the charm and bottom quark masses $m_{c,b}$, the strange quark m_s (we shall neglect the light quark masses $m_{u,d}$), the light quark condensates $\langle \bar{q}q \rangle$ ($q \equiv u, d, s$), the gluon condensates $\langle \alpha_s G^2 \rangle \equiv \langle \alpha_s G_{\mu\nu}^a G_a^{\mu\nu} \rangle$ and $\langle g^3 G^3 \rangle \equiv \langle g^3 f_{abc} G_{\mu\nu}^a G_{\rho}^{b,\nu} G_{\sigma}^{c,\rho} \rangle$, the mixed quark condensate $\langle \bar{q}Gq \rangle \equiv \langle \bar{q}g\sigma^{\mu\nu}(\lambda_a/2)G_{\mu\nu}^a q \rangle = M_0^2 \langle \bar{q}q \rangle$ and the four-quark condensate $\rho \alpha_s \langle \bar{q}q \rangle^2$, where $\rho \simeq 3 – 4$ indicates the deviation from the four-quark vacuum saturation. Their values are given in Table 3^o

We shall work with the running light quark condensates, which read to leading order in α_s :

$$\langle \bar{q}q \rangle(\tau) = -\hat{\mu}_q^3 (-\beta_1 a_s)^{2/\beta_1}, \quad \langle \bar{q}Gq \rangle(\tau) = -M_0^2 \hat{\mu}_q^3 (-\beta_1 a_s)^{1/3\beta_1}, \quad (17)$$

and the running strange quark mass to NLO (for the number of flavours $n_f = 3$):

$$\overline{m}_s(\tau) = \hat{m}_s (-\beta_1 a_s)^{-2/\beta_1} (1 + 0.8951 a_s), \quad (18)$$

ⁿSome other alternative approaches for optimizing the PT series can be found in.^{95–99}

^oA recent analysis⁹⁴ confirms the quoted values of m_c, b , α_s and improve the one of $\langle \alpha_s G^2 \rangle$.

where $\beta_1 = -(1/2)(11 - 2n_f/3)$ is the first coefficient of the β function for n_f flavours; $a_s \equiv \alpha_s(\tau)/\pi$; \hat{m}_q and \hat{m}_s are the spontaneous RGI light quark condensate and strange quark mass.¹²⁰ We shall use:

$$\alpha_s(M_\tau) = 0.325(8) \implies \alpha_s(M_Z) = 0.1192(10) \quad (19)$$

from τ -decays^{29,100,101}^P which agree with the 2016 world average:¹²²

$$\alpha_s(M_Z) = 0.1181(11) . \quad (20)$$

The value of the running $\langle \bar{q}q \rangle$ condensate is deduced from the well-known GMOR relation:

$$(m_u + m_d)\langle \bar{u}u + \bar{d}d \rangle = -m_\pi^2 f_\pi^2 , \quad (21)$$

where $f_\pi = 130.4(2)$ MeV.⁸⁹ The value of $(\bar{m}_u + \bar{m}_d)(2) = (7.9 \pm 0.6)$ MeV obtained in^{75,76} agrees with the PDG in¹¹⁰ and lattice averages in.⁹⁰ Then, we deduce the RGI light quark spontaneous mass \hat{m}_q given in Table 3.

For the heavy quarks, we shall use the running mass^q and the corresponding value of α_s evaluated at the scale μ . These sets of correlated parameters are given in Table 4 for different values of μ and for a given number of flavours n_f . The value of μ used here corresponds to the optimal one obtained in.¹

For the $\langle \alpha_s G^2 \rangle$ condensate, we have enlarged the original error by a factor about 3 in order to have a conservative result for recovering the original SVZ estimate and the alternative extraction in^{108,109} from charmonium sum rules. However, a direct naive comparison of this range of values obtained within short QCD series (few terms) with the one from lattice calculations¹²³ obtained within a long QCD series¹²⁴ can be misleading.

We shall see later on that the effects of the gluon and four-quark condensates on the values of the decay constants and masses are relatively small though they play an important rôle in the stability analysis.

4. Accuracy of the Factorization Assumption

4.1. PT Lowest order tests

To lowest order of PT QCD, the four-quark correlator can be subdivided into its factorized (Fig. 1a) and its non-factorized (Fig. 1b) parts.

We have tested in¹ the factorization assumption at LO by taking the example of the $\bar{M}_0^* M^*(1^-)$ molecule states where $M \equiv D$ (resp. B) meson in the charm (resp. bottom) quark channels. We concluded from the previous two examples that assuming a factorization of the PT contributions at LO induces an almost negligible

^PA recent update is done in¹²¹ where the same central value is obtained and where more complete references can be found.

^qThis choice is not justified if one works at lowest order (LO) like in the existing literature due to the ill-defined mass definition at LO. Effects of the use of the running or the on-shell mass at LO has been explicitly shown in.^{1,23,24}

Table 4. $\alpha_s(\mu)$ and correlated values of $\overline{m}_Q(\mu)$ used in the analysis for different values of the subtraction scale μ . The error in $\overline{m}_Q(\mu)$ has been induced by the one of $\alpha_s(\mu)$ to which one has added the error on their determination given in Table 3.

Input for $\bar{D}_s D_s, \dots, [c s \bar{c} \bar{s}]$, : $n_f = 4$

$\mu[\text{GeV}]$	$\alpha_s(\mu)$	$\overline{m}_c(\mu)[\text{GeV}]$
Input: $\overline{m}_c(m_c)$	0.4084(144)	1.26
1.5	0.3649(110)	1.176(5)
2	0.3120(77)	1.069(9)
2.5	0.2812(61)	1.005(10)
3.0	0.2606(51)	0.961(10)
3.5	0.2455(45)	0.929(11)
4.0	0.2339(41)	0.903(11)
4.5	0.2246(37)	0.882(11)
5.0	0.2169(35)	0.865(11)
5.5	0.2104(33)	0.851(12)
6.0	0.2049(30)	0.838(12)

Input for $\bar{B}_s B_s, \dots, [b s \bar{b} \bar{s}]$: $n_f = 5$

$\mu[\text{GeV}]$	$\alpha_s(\mu)$	$\overline{m}_b(\mu)[\text{GeV}]$
3	0.2590(26)	4.474(4)
3.5	0.2460(20)	4.328(2)
Input: $\overline{m}_b(m_b)$	0.2320(20)	4.177
4.5	0.2267(20)	4.119(1)
5.0	0.2197(18)	4.040(1)
5.5	0.2137(17)	3.973(2)
6.0	0.2085(16)	3.914(2)
6.5	0.2040(15)	3.862(2)
7.0	0.2000(15)	3.816(3)

effect on the decay constant ($\simeq 1.5\%$) and mass ($\simeq 7 \times 10^{-4}$) determinations for the $\bar{D}_0^* D^*$ and $\bar{B}_0^* B^*$ vector molecules.

4.2. Factorization tests for PT \oplus NP contributions at LO

We have noticed in¹ that the effect of factorization of the PT \oplus NP at LO is about 2.2% for the decay constant and 0.5% for the mass which is quite tiny. However, to avoid this (small) effect, we shall work in the following with the full non-factorized PT \oplus NP of the LO expressions.

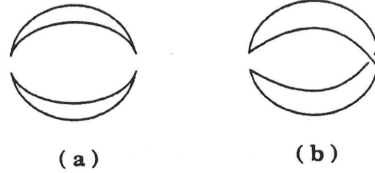


Fig. 1. (a) Factorized contribution to the four-quark correlator at lowest order of PT; (b) Non-factorized contribution at lowest order of PT (the figure comes from ⁵⁴).

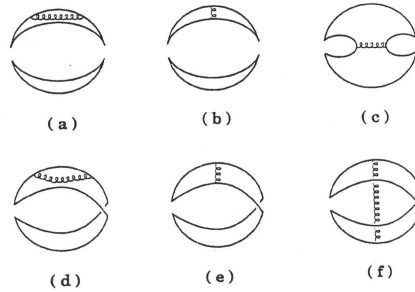


Fig. 2. (a,b) Factorized contributions to the four-quark correlator at NLO of PT; (c to f) Non-factorized contributions at NLO of PT (the figure comes from ⁵⁴).

4.3. Test at NLO of PT from the $B^0\bar{B}^0$ four-quark correlator

For extracting the PT α_s^n corrections to the correlator and due to the technical complexity of the calculations, we shall assume that these radiative corrections are dominated by the ones from the factorized diagrams (Fig. 2a,b) while we neglect the ones from non-factorized diagrams (Fig. 2c to f). This fact has been proven explicitly by ^{56,57} in the case of the \bar{B}^0B^0 systems (very similar correlator as the ones discussed in the following) where the non-factorized α_s corrections do not exceed 10% of the total α_s contributions.

4.4. Conclusions of the factorization tests

We expect from the previous LO examples that the masses of the molecules are known with a good accuracy while, for the coupling, we shall have in mind the systematics induced by the radiative corrections estimated by keeping only the factorized diagrams. The contributions of the factorized diagrams will be extracted from the convolution integrals given in Eq. 5. Here, the suppression of the NLO corrections will be more pronounced for the extraction of the meson masses from the ratio of sum rules compared to the case of the \bar{B}^0B^0 systems.

5. The Heavy-light Charm Molecule States

They are described by the interpolating currents given in Table 2. The corresponding spectral functions are given to LO of PT QCD in Appendix A. The different sources of the errors from the analysis are given in Table 5 to 8.

5.1. The (0^{++}) Charm Scalar Molecule States

We shall study the $\bar{D}_s D_s$, $\bar{D}_s^* D_s^*$, $\bar{D}_{s0}^* D_{s0}^*$ and their beauty analogue. Noticing that the qualitative behaviours of the curves in these channels are very similar, we shall illustrate the analysis in the case of $\bar{D}_s D_s$ and $\bar{B}_s B_s$ molecule states by working with the SU3 ratios f_{DD}^{sd} and r_{DD}^{sd} of couplings and masses defined in Eq.16.

The $\bar{D}_s D_s$ molecule state

– $\bar{D}_s D_s$ coupling and mass

The analysis of the μ subtraction point behaviour of the $\bar{D}_s D_s$ coupling and mass is very similar to the chiral limit case discussed in detail in¹ and will not be repeated here. We use the optimal choice obtained there:

$$\mu = (4.5 \pm 0.5) \text{ GeV}. \quad (22)$$

Taking the previous value of μ , we study, in Fig. 3a), the behaviour of the $\bar{D}_s D_s$ coupling^r and in Fig. 3b) its mass in terms of the LSR variable τ at different values of t_c at NLO of PT QCD by including the contributions of condensates up to dimension 6. Higher dimension ($d = 8$) though partially known (see Appendix A) will not be included in the OPE but serves as an estimate of the errors induced by unknown higher dimension condensates. We shall use, for the estimate of the coupling, the input $\bar{D}_s D_s$ mass value obtained iteratively from the sum rule.

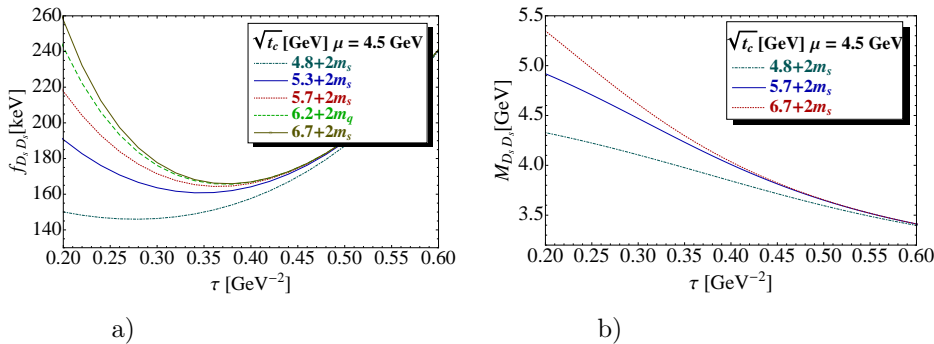


Fig. 3. **a)** The coupling $f_{D_s D_s}$ at NLO as function of τ for different values of t_c , for $\mu = 4.5$ GeV and for the QCD parameters in Tables 3 and 4; **b)** The same as a) but for the mass $M_{D_s D_s}$.

^rHere and in the following “decay constant” is the same as “coupling”.

– $\bar{D}_s D_s / \bar{D} D$ SU3 ratios of couplings and masses

Taking the previous value of input parameters, we study, in Fig. 4a), the behaviour of the SU3 ratio of couplings f_{DD}^{sd} and in Fig. 4b) the ratio of masses r_{DD}^{sd} (see Eq. 16) in terms of the LSR variable τ at different values of t_c . Noticing from Fig. 4 that the value of τ at which the decay constant $f_{D_s D_s}$ reaches a minimum is about the same as the one of f_{DD} (Fig. 6 of Ref. ¹), then, it is legitimate to use the ratio or double ratio of sum rules (DRSR) for extracting with a good accuracy the SU3 breaking corrections to the coupling and mass in this channel. We show this ratio in Fig. 4 where only the mass ratio presents τ -stability.

– Results

From the previous analysis, we consider as an optimal estimate the mean value of the coupling, mass and their SU3 ratios obtained at the minimum or inflexion point for the common range of t_c -values ($\sqrt{t_c} \simeq 4.8 + 2\bar{m}_s$ GeV) corresponding to the starting of the τ -stability f and the one where (almost) t_c -stability ($\sqrt{t_c} \simeq 6.7 + 2\bar{m}_s$ GeV) is reached for $\tau \simeq (0.38 \pm 0.02)$ GeV⁻². In these stability regions, the requirement that the pole contribution is larger than the one of the continuum is automatically satisfied (see e.g. ²⁵). In this way, we obtain from a direct determination of the mass and coupling in Fig. 3 and for $\mu = 4.5$ GeV at NLO:

$$f_{D_s D_s}(4.5) \simeq 156(10)_{t_c}(1)_\tau \cdots \text{keV}, \quad M_{D_s D_s} \simeq 4144(10)_{t_c}(38)_\tau \cdots \text{MeV}, \quad (23)$$

at $\tau \simeq 0.28$ (resp. 0.38) GeV⁻² for $\sqrt{t_c} \simeq 4.8 + 2m_s$ (resp. $6.7 + 2m_s$) GeV. ... correspond to errors given in Table 5 induced by the QCD input parameters. Using the input values of $f_{DD} = 164(8)$ keV and $M_{DD} = 3901(6)$ MeV at NLO from Ref. ¹s, we deduce:

$$f_{DD}^{sd} \equiv \frac{f_{D_s D_s}}{f_{DD}} \simeq 0.95(4)_f(6)_{t_c}(0)_\tau \cdots, \quad r_{DD}^{sd} \equiv \frac{M_{D_s D_s}}{M_{DD}} \simeq 1.062(2)_M(3)_{t_c}(10)_\tau \cdots, \quad (24)$$

where the first errors come from the determination of the $\bar{D} D$ coupling and mass.¹ A direct determination of the SU3 ratios of couplings and masses from Fig. 4 shows τ and t_c -stabilities from which we deduce a more accurate determination:

$$f_{DD}^{sd} \simeq 0.950(8)_{t_c}(1)_\tau \cdots, \quad r_{DD}^{sd} \simeq 1.069(1)_{t_c}(0)_\tau \cdots, \quad (25)$$

in perfect agreement within the errors with the ones in Eq. 24. Using the input values of $M_{DD} = 3901(6)$ MeV and $f_{DD} = 164(8)$ keV at NLO from Ref.,¹ we can deduce:

$$f_{D_s D_s} \simeq 156(8)_f(1)_{t_c}(0)_\tau \cdots \text{keV}, \quad M_{D_s D_s} \simeq 4170(6)_M(4)_{t_c}(0)_\tau \cdots \text{MeV}, \quad (26)$$

^sIn order to avoid double counting, we retain only the error due to (τ, t_c) for these inputs.

which agree with the direct determination in Eq. 23. We take as a final estimate the mean:

$$\begin{aligned} f_{DD}^{sd} &\simeq 0.950(5) \cdots, & f_{D_s D_s} &\simeq 156(8) \cdots \text{keV}, \\ r_{DD}^{sd} &\simeq 1.069(1) \cdots, & M_{D_s D_s} &\simeq 4169(7) \cdots \text{MeV}, \end{aligned} \quad (27)$$

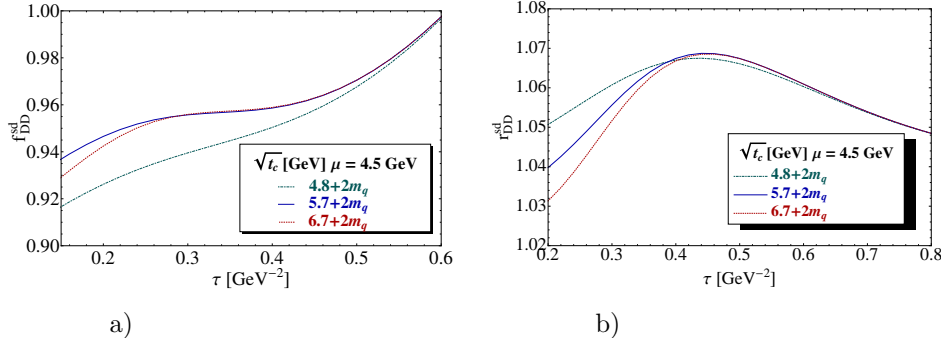


Fig. 4. **a)** SU3 ratio of couplings f_{DD}^{sd} at NLO as function of τ for different values of t_c , for $\mu = 4.5$ GeV and for the QCD parameters in Tables 3 and 4; **b)** The same as a) but for the SU3 ratio of masses r_{DD}^{sd} .

The $\bar{D}_s^ D_s^*$ molecule state*

– $\bar{D}_s^ D_s^*$ coupling and mass*

The qualitative behaviour of different curves are very similar to the case of the $\bar{D}_s D_s$ state. From these curves, one can see that the ones of the coupling present stabilities, while the ones of the mass have inflection points which cannot be precisely located. We deduce from the analysis a direct determination of the coupling:

$$f_{D_s^* D_s^*}(4.5) \simeq 259(23)_{t_c}(0)_{\tau} \cdots \text{keV}, \quad (28)$$

where one has stability at $\tau \simeq 0.24$ (resp. 0.36) GeV^{-2} for $\sqrt{t_c} \simeq 4.8 + 2\bar{m}_s$ (resp. $6.7 + 2\bar{m}_s$) GeV.

– $\bar{D}_s^ D_s^*/\bar{D}^* D^*$ SU3 ratios of couplings and masses*

In this channel, the ratios of masses present extrema at $\tau \simeq 0.36$ (resp. 0.38) GeV^{-2} like in the case of $D_s D_s$ but more pronounced while the ratio of couplings presents net inflection points at $\tau \simeq 0.28$ (resp. 0.36) GeV^{-2} as shown in Fig. 5. We deduce:

$$f_{D_s^* D_s^*}^{sd} \equiv \frac{f_{D_s^* D_s^*}}{f_{D^* D^*}} \simeq 0.929(8)_{t_c}(0)_{\tau} \cdots, \quad r_{D_s^* D_s^*}^{sd} \equiv \frac{M_{D_s^* D_s^*}}{M_{D^* D^*}} \simeq 1.074(1)_{t_c}(0)_{\tau} \cdots. \quad (29)$$

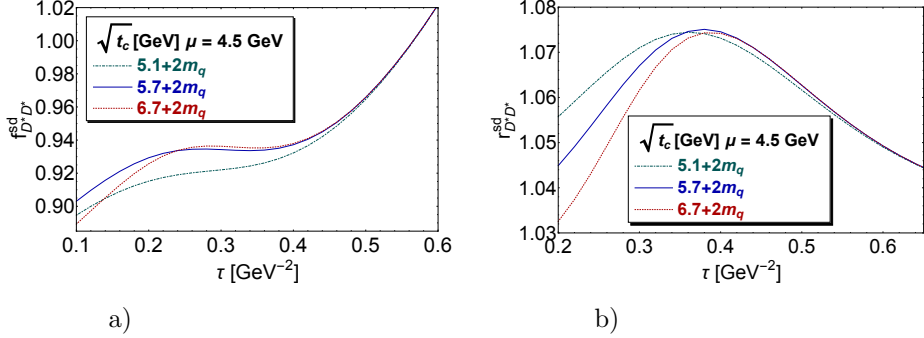


Fig. 5. **a)** SU3 ratio of couplings $f_{D^* D^*}^{sd}$ at NLO as function of τ for different values of t_c , for $\mu = 4.5$ GeV and for the QCD parameters in Tables 3 and 4; **b)** The same as a) but for the SU3 ratio of masses $r_{D^* D^*}^{sd}$.

– Results at NLO

Combining the previous value of $f_{D_s^* D_s^*}$ and the ratio $r_{D^* D}^{sd}$ with the ones at NLO from:¹ $f_{D^* D^*} = 288(9)$ keV and $M_{D^* D^*} = 3903(17)$ MeV, one can deduce:

$$f_{D^* D^*}^{sd} \equiv \frac{f_{D_s^* D_s^*}}{f_{D^* D^*}} \simeq 0.90(3)_f(8)_{t_c}(0)_\tau \cdots, \quad M_{D_s^* D_s^*} \simeq 4192(18)_M(4)_{t_c}(0)_\tau \cdots \text{MeV}, \quad (30)$$

where the first errors come from the determination of the $\bar{D}^* D^*$ coupling and mass.¹ Taking the mean of the ratio of couplings and re-using the value $f_{D^* D^*} = 288(9)$ keV, we deduce our final estimate:

$$f_{D_s^* D_s^*}^{sd} \simeq 0.929(8) \cdots \implies f_{D_s^* D_s^*}(4.5) \simeq 265(8.3)(2.9) \text{ keV} . \quad (31)$$

The $\bar{D}_{s0}^ D_{s0}^*$ and $\bar{D}_0^* D_0^*$ molecule states*

- The $\bar{D}_{s0}^* D_{s0}^*$ molecule

The analysis is very similar to the above (see Fig. 4), where the SU3 ratio of masses presents maxima at $\tau \simeq 0.28$ (resp. 0.32) GeV^{-2} for $\sqrt{t_c} \simeq 5.3$ (resp. 7) $+2\bar{m}_s$ GeV , while the decay constant presents τ and t_c -stabilities (see Fig. 3) for $\tau \simeq 0.18$ (resp. 0.28) GeV^{-2} for the previous range of t_c -values. In this way, we obtain at NLO:

$$f_{D_{s0}^* D_{s0}^*}(4.5) \simeq 86(8)_{t_c}(0)_\tau \cdots \text{ keV , } \quad r_{D_0^* D_0^*}^{sd} \equiv \frac{M_{D_{s0}^* D_{s0}^*}}{M_{D_0^* D_0^*}} \simeq 1.069(68)_{t_c}(13)_\tau \cdots . \quad (32)$$

A direct determination of the ratio of coupling shows net inflexion points as in Fig. 4 at $\tau \simeq 0.24$ (resp. 0.30) GeV^{-2} for $\sqrt{t_c} \simeq 5.3 + 2\bar{m}_q$ (resp. $7 + 2\bar{m}_q$) GeV . In this way, we obtain:

$$f_{D_0^* D_0^*}^{sd} \simeq 0.875(6)_{t_c}(0)_\tau \dots \quad (33)$$

The analysis of the mass presents an inflexion point as in Fig. 3 which is sensitive to the τ -values. We fix this range as the one from $r_{D_0^* D_0^*}^{sd}$ which is $\tau \simeq 0.28$ (resp.

0.32) GeV⁻² for $\sqrt{t_c} \simeq 5.3$ (resp. 7) +2 \bar{m}_s GeV. In this way, we obtain:

$$M_{D_{s0}^* D_{s0}^*} \simeq 4277(102)_{t_c}(92)_\tau \cdots \text{MeV}. \quad (34)$$

– Revisiting the $\bar{D}_0^* D_0^*$ molecule

Here, we cross-check our results obtained in the chiral limit in¹ and we notice an error as the τ -stability of the coupling $f_{D_0^* D_0^*}$ starts earlier from $\sqrt{t_c} = 5.3$ GeV and for $\tau \simeq 0.24$ GeV⁻² than the one used in.¹ Taking this larger range of $\sqrt{t_c}$ values from 5.3 to 6.8 GeV, we deduce at NLO:

$$f_{D_0^* D_0^*} \simeq 96(10) \cdots \text{keV}, \quad (35)$$

instead of 116 keV obtained in.¹ This change of the low- t_c values also affects the direct mass determination. The curves present inflexion points around $\tau \simeq 0.29$ GeV⁻² which leads at NLO to:

$$M_{D_0^* D_0^*} \simeq 4008(411)_{t_c}(35)_\tau \cdots \text{MeV}, \quad (36)$$

with a large error instead of 4402(54) MeV quoted in.¹

– Final Results

We also deduce from the SU3 ratios and the result from $\bar{D}_{s0}^* D_{s0}^*$, the value of the coupling:

$$f_{D_{s0}^* D_{s0}^*}(4.5) \simeq 84(9) \cdots \text{keV}, \quad M_{D_0^* D_0^*} \simeq 4001(95)_{t_c}(255)_f \cdots \text{MeV}, \quad (37)$$

Taking the mean of the two values of couplings and masses, we deduce the final value at NLO:

$$\begin{aligned} f_{D_{s0}^* D_{s0}^*}(4.5) &\simeq 85(6) \cdots \text{keV} \implies f_{D_0^* D_0^*}(4.5) \simeq 97(7) \cdots \text{keV}, \\ M_{D_0^* D_0^*} &\simeq 4003(227) \cdots \text{MeV}. \end{aligned} \quad (38)$$

The $\bar{D}_{s1} D_{s1}$ and $\bar{D}_1 D_1$ molecule states

We perform a similar analysis. The behaviours of the different curves are very similar to the case of the $\bar{D}_s D_s$ molecule states and will not be shown here. They present stabilites for $\sqrt{t_c} \simeq 5.1+2\bar{m}_s$ to 6.7+2 \bar{m}_s GeV for $\tau \simeq 0.28 - 0.34$ (resp. 0.32–0.34) (resp. 0.28–0.34) GeV⁻² for the coupling $f_{D_{s1} D_{s1}}$ (resp. SU3 ratio of couplings $f_{D_1 D_1}^{sd}$) (resp. SU3 ratio of masses $r_{D_1 D_1}^{sd}$) leading to the values at NLO:

$$f_{D_{s1} D_{s1}} \simeq 209(14) \cdots \text{keV}, \quad f_{D_1 D_1}^{sd} \simeq 0.906(9) \cdots, \quad r_{D_1 D_1}^{sd} \simeq 1.097(6) \cdots, \quad (39)$$

where the quoted errors come from the correlated values of (t_c, τ) and \cdots are QCD corrections given in Table 5. The mass presents an inflexion point which is difficult to localize. To fix the τ -values, we take the range where the SU3 ratio of masses optimizes, which corresponds to $\tau \simeq 0.32 - 0.34$ GeV⁻². In this way, we obtain:

$$M_{D_{s1} D_{s1}} \simeq 4187(34) \cdots \text{MeV}. \quad (40)$$

Using the previous values of the SU3 ratio, we can deduce for the $\bar{D}_1 D_1$ molecule at NLO:

$$f_{D_1 D_1} \simeq 231(16) \cdots \text{keV}, \quad M_{D_1 D_1} \simeq 3838(37) \cdots \text{MeV}. \quad (41)$$

5.2. The $(1^{+\pm})$ Charm Axial-Vector Molecule States

Here, within our choice of interpolating currents, the (1^{++}) and (1^{+-}) are degenerate in masses and have the same couplings like in the case of the pseudoscalar molecules.

The $\bar{D}_s^ D_s$ molecule state*

The curves are very similar to the case of the scalar molecules where the coupling presents a minimum for $\tau \simeq 0.26$ (resp. 0.36) GeV^{-2} for $\sqrt{t_c} \simeq 4.8+2\bar{m}_s$ (resp. $6.7+2\bar{m}_s$) GeV , while the SU3 ratio of masses presents a maximum both for $\tau = 0.42$ GeV^{-2} and for $\sqrt{t_c} \simeq 5.7+2\bar{m}_q$ GeV , ($q \equiv d, s$). We obtain:

$$f_{D_s^* D_s}(4.5) \simeq 145(10)_{t_c}(0)_\tau \cdots \text{keV}, \quad r_{D^* D}^{sd} \equiv \frac{M_{D_s^* D_s}}{M_{D^* D}} \simeq 1.070(1)_{t_c}(0)_\tau \cdots. \quad (42)$$

Using the values: $M_{D^* D} = 3901(3.4)$ MeV and $f_{D^* D} = 154(7.6)$ keV from Ref. 1, we deduce:

$$f_{D^* D}^{sd} \simeq 0.94(5)_f(7)_{t_c}(0)_\tau \cdots, \quad M_{D_s^* D_s} \simeq 4174(3)_M(4)_{t_c}(0)_\tau \cdots \text{MeV}. \quad (43)$$

One can improve the determination of the ratio of couplings by its direct determination. At the inflection points for $\tau \simeq 0.30$ (resp. 0.34) GeV^{-2} for $\sqrt{t_c} \simeq 4.8+2\bar{m}_q$ (resp. $6.7+2\bar{m}_q$) GeV , one deduces:

$$f_{D^* D}^{sd} \simeq 0.934(10)_{t_c}(0)_\tau \cdots. \quad (44)$$

Taking the mean value of the SU3 ratio of coupling, we deduce at NLO:

$$f_{D^* D}^{sd} \simeq 0.930(7) \cdots \implies f_{D_s^* D_s}(4.5) \simeq 143(7)_f(1.1)_{t_c}(0)_\tau \cdots \text{keV} \quad (45)$$

The $\bar{D}_{s0}^ D_{s1}$ and $\bar{D}_0^* D_1$ molecule states*

– The $\bar{D}_{s0}^ D_{s1}$ molecule*

The coupling and SU3 ratio of masses stabilizes for $\tau \simeq 0.26$ (resp. 0.32) GeV^{-2} for $\sqrt{t_c} \simeq 5.3+2\bar{m}_q$ (resp. $6.7+2\bar{m}_q$) GeV . The SU3 ratio of coupling stabilizes for $\tau \simeq 0.27$ (resp. 0.28) GeV^{-2} . We obtain at NLO:

$$\begin{aligned} f_{D_{s0}^* D_{s1}}(4.5) &\simeq 87(7)_{t_c}(0)_\tau \cdots \text{keV}, \quad f_{D_0^* D_1}^{sd} \simeq 0.904(9)_{t_c}(0)_\tau, \\ r_{D_0^* D_1}^{sd} &\simeq 1.119(18)_{t_c}(0)_\tau \cdots \end{aligned} \quad (46)$$

Using the previous range of values of $\tau \simeq 0.26$ (resp. 0.32) GeV^{-2} , we deduce at NLO:

$$M_{D_{s0}^* D_{s1}} \simeq 4269(7)_{t_c}(0)_\tau \cdots \text{MeV}. \quad (47)$$

– *Revisiting the $\bar{D}_0^* D_1$ molecule*

Here we revise our previous result in Ref.¹ by correcting the range of t_c and of τ used there. The coupling stabilizes at $\tau \simeq 0.26$ (resp. 0.32) GeV⁻² for $\sqrt{t_c} \simeq 5.3+2\bar{m}_q$ (resp. $6.7+2\bar{m}_q$) GeV. Within these ranges of values, a direct determination gives:

$$f_{D_0^* D_1}(4.5) \simeq 96(7)_{t_c}(0)_\tau \cdots \text{ keV}, \quad M_{D_0^* D_1} \simeq 3857(29)_{t_c}(0)_\tau \cdots \text{ MeV}. \quad (48)$$

Combining the previous values of $M_{D_{s0}^* D_{s1}}$, $f_{D_{s0}^* D_{s1}}$ with $r_{D_0^* D_1}^{sd}$ and $f_{D_0^* D_1}^{sd}$, one can also deduce:

$$f_{D_0^* D_1}(4.5) \simeq 96(7)_{t_c}(0)_\tau \cdots \text{ keV}, \quad M_{D_0^* D_1} \simeq 3815(61)_{t_c}(0)_\tau \cdots \text{ MeV}. \quad (49)$$

Taking the mean of the two determinations lead to our final estimate at NLO:

$$f_{D_0^* D_1}(4.5) \simeq 96(7) \cdots \text{ keV}, \quad M_{D_0^* D_1} \simeq 3849(26) \cdots \text{ MeV}. \quad (50)$$

These corrected values replace the ones obtained in Ref.¹ at NLO :

$$f_{D_0^* D_1}(4.5) \simeq 118(16) \text{ keV}, \quad M_{D_0^* D_1} \simeq 4395(164) \text{ MeV}. \quad (51)$$

These revisited values together with the ones of $D_0^* D_0^*$ given in Eq. 38 and the new value of the ones of $D_1 D_1$ in Eq. 41 are quoted in Table 18 to NLO and N2LO.

Table 5. Different sources of errors for the estimate of the 0^+ and 1^+ $\bar{D}_s D_s$ -like molecule masses (in units of MeV) and couplings $f_{M_s M_s}(\mu)$ (in units of keV). We use $\mu = 4.5(5)$ GeV.

	$D_s D_s$		$D_s^* D_s^*$		$D_{s0}^* D_{s0}^*$		$D_{s1} D_{s1}$		$D_s^* D_s$		$D_{s0}^* D_{s1}$	
	ΔM	Δf	ΔM	Δf	ΔM	Δf	ΔM	Δf	ΔM	Δf	ΔM	Δf
Inputs												
<i>LSR parameters</i>												
(t_c, τ)	7	10	18	23	59	4	34	14	5	10	7	7
μ	24.56	0.16	24.14	0.60	28.31	0.61	25.50	8.65	27.89	0.63	30.33	2.87
<i>QCD inputs</i>												
M_Q	11.19	4.82	7.98	7.67	8.63	2.83	4.61	5.45	11.07	3.17	5.05	1.99
α_s	12.45	3.50	12.30	5.79	15.65	1.33	11.76	3.68	12.63	4.26	18.68	1.21
$N3LO$	0.0	0.77	0.28	1.33	3.64	1.19	4.41	1.40	0.98	0.91	0.42	1.61
$\langle \bar{q}q \rangle$	11.20	1.93	9.32	1.68	38.38	5.16	4.58	2.26	8.51	1.70	32.09	3.09
$\langle \alpha_s G^2 \rangle$	5.66	1.04	1.32	0.58	0.06	2.54	4.31	1.82	0.46	0.11	2.02	0.17
M_0^2	9.93	0.20	8.28	2.59	15.18	1.00	14.28	2.81	6.32	1.17	13.19	1.67
$\langle \bar{q}^2 \rangle^2$	11.01	7.47	9.95	18.08	51.01	13.29	27.77	20.46	10.24	7.41	38.73	12.90
$\langle g_s^2 G^3 \rangle$	0.08	0.11	0.12	0.25	0.57	0.23	0.16	0.31	0.30	0.10	1.54	0.16
$d \geq 8$	32.0	9.62	196.5	4.80	95.5	2.74	29.9	6.39	56.0	8.10	194.8	1.22
<i>Total errors</i>	48.31	17.01	199.97	31.33	134.32	12.22	62.41	28.14	66.62	15.95	204.94	13.97

Table 6. Different sources of errors for the estimate of the 0^+ and 1^+ $\bar{D}D$ -like molecule SU(3) ratios of masses r_{MM}^{sd} and SU(3) ratios of couplings f_{MM}^{sd} . We use $\mu = 4.5(5)$ GeV.

	$D_s D_s$	$D_s^* D_s^*$	$D_{s0}^* D_{s0}^*$	$D_{s1} D_{s1}$	$D_{s0}^* D_s$	$D_{s0}^* D_{s1}$
	r^{sd}	f^{sd}	r^{sd}	f^{sd}	r^{sd}	f^{sd}
Inputs						
<i>LSR parameters</i>						
(t_c, τ)	0.001	0.005	0.001	0.008	0.013	0.036
μ	0.0	0.001	0.0	0.001	0.0	0.002
<i>QCD inputs</i>						
M_Q	0.0	0.002	0.0	0.003	0.0	0.003
α_s	0.0	0.001	0.0	0.0	0.0	0.0
$N3LO$	0.00	0.00	0.00	0.00	0.001	0.001
$\langle \bar{q}q \rangle$	0.001	0.0	0.001	0.0	0.008	0.004
$\langle \alpha_s G^2 \rangle$	0.001	0.002	0.0	0.001	0.0	0.007
M_D^0	0.001	0.0	0.002	0.0	0.0	0.002
$\langle \bar{q}q \rangle^2$	0.002	0.025	0.001	0.025	0.010	0.031
$\langle g^3 G^3 \rangle$	0.0	0.0	0.0	0.0	0.001	0.0
$d \geq 8$	0.003	0.009	0.002	0.010	0.010	0.002
<i>Total errors</i>	0.004	0.028	0.003	0.028	0.021	0.050
	0.007	0.007	0.007	0.007	0.007	0.009
	0.001	0.001	0.001	0.001	0.001	0.002

5.3. The $(0^{-\pm})$ Charm Pseudoscalar Molecule States

Here, within our choice of interpolating currents, the (0^{--}) and (0^{-+}) are degenerate in masses and have the same couplings.

The $\bar{D}_{s0}^* D_s$ molecule state

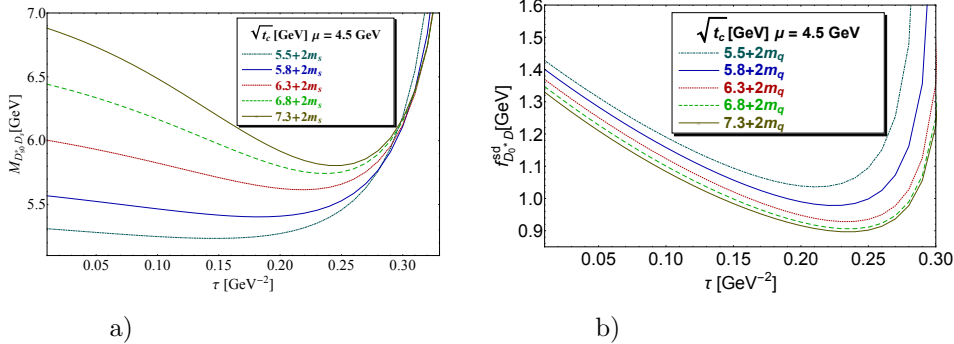


Fig. 6. **a)** The mass $M_{D_s^* D}$ at NLO as function of τ for different values of t_c , for $\mu = 4.5$ GeV and for the QCD parameters in Tables 3 and 4; **b)** The same as a) but for the SU3 ratio of couplings $f_{D_s^* D}^{sd}$.

The mass presents minima (but not the coupling) for $\tau=0.18$ (resp. 0.25) GeV^{-2} corresponding to $\sqrt{t_c} = 5.8 + 2\bar{m}_q$ (resp. $\sqrt{t_c} = 7.3 + 2\bar{m}_q$) GeV as shown in Fig. 6. Within the same range of t_c , the ratio of couplings has minima for $\tau=0.22$ (resp. 0.24) GeV^{-2} . In these regions, we deduce:

$$f_{D_s^* D}^{sd} \simeq 0.938(41)_{t_c}(2)_\tau \cdots, \quad M_{D_s^* D} \simeq 5604(201)_{t_c}(17)_\tau \cdots \text{ MeV.} \quad (52)$$

Using the values: $M_{D_0^* D} = 5800(115)$ MeV and $f_{D_0^* D} = 240(16)$ keV from,¹ we deduce at NLO:

$$r_{D_0^* D}^{sd} \simeq 0.97(2)_M(5)_{t_c}(0)_\tau \cdots, \quad f_{D_{s0}^* D_s} \simeq 225(15)_f(10)_{t_c}(1)_\tau \cdots \text{ keV.} \quad (53)$$

The $\bar{D}_s^* D_{s1}$ molecule state

The shapes of different curves for the mass and SU3 ratio of couplings are very similar to the case of the $\bar{D}_{s0}^* D_s$ and will not be shown here. Unlike the previous case of $D_{s0}^* D_s$, the coupling presents τ -stabilities as shown in Fig. 7 from $\sqrt{t_c} = 6.0 + 2\bar{m}_q$ (resp. $\sqrt{t_c} = 7.3 + 2\bar{m}_q$) GeV and for $\tau = 0.14$ (resp. 0.21) GeV^{-2} . Within the above

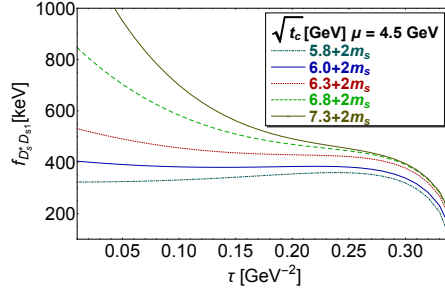


Fig. 7. The coupling $f_{D_s^* D_{s1}}$ at NLO as function of τ for different values of t_c , for $\mu = 4.5$ GeV and for the QCD parameters in Tables 3 and 4.

range of t_c , the ratio of couplings presents stability for $\tau = 0.22$ (resp. 0.24) GeV^{-2} from $\sqrt{t_c} = 6 + 2\bar{m}_q$ (resp. $\sqrt{t_c} = 7.3 + 2\bar{m}_q$) GeV, while the minima for the mass occur at $\tau = 0.19$ (resp. 0.25) GeV^{-2} . In these regions, we deduce:

$$\begin{aligned} f_{D_s^* D_{s1}} &\simeq 431(51)_{t_c}(8)_\tau \cdots \text{ keV,} \\ f_{D^* D_1}^{sd} &\simeq 0.94(1)_{t_c}(0)_\tau \cdots, \quad M_{D_s^* D_{s1}} \simeq 5724(176)_{t_c}(14)_\tau \cdots \text{ MeV.} \end{aligned} \quad (54)$$

Using the values: $M_{D^* D_1} = 5898(89)$ MeV and $f_{D^* D_1} = 490(25)$ keV from,¹ we deduce at NLO:

$$r_{D^* D_1}^{sd} \simeq 0.97(1.5)_M(5)_{t_c}(0)_\tau \cdots, \quad f_{D_s^* D_{s1}} \simeq 460(23.5)_f(5)_{t_c}(0)_\tau \cdots \text{ keV,} \quad (55)$$

where the coupling agrees within the errors with the previous direct determination. Taking the mean of the couplings and re-using $f_{D^* D_1} = 490(25)$ keV, we deduce the final estimate:

$$f_{D_s^* D_{s1}} \simeq 455(22) \cdots \text{ keV,} \implies f_{D^* D_1}^{sd} \simeq 0.93(1) \cdots, \quad (56)$$

where we have taken the error on the ratio from the direct determination.

5.4. The (1^{--}) Charm Vector Molecule States

The $(1^{--}) \bar{D}_{s0}^ D_s^*$ molecule state*

The results are similar to the previous ones. The coupling presents τ -stabilities from $\sqrt{t_c} = 6.0 + 2\bar{m}_q$ to $\sqrt{t_c} = 7.3 + 2\bar{m}_q$ GeV and for $\tau = 0.21$ - 0.24 (resp. 0.24) GeV^{-2} . Within these range of t_c -values, the mass stabilizes for $\tau \simeq 0.18$ (resp. 0.24) GeV^{-2} and the SU3 ratio of couplings for $\tau \simeq 0.23$ (resp. 0.24) GeV^{-2} . We obtain:

$$\begin{aligned} f_{D_{s0}^* D_s^*} &\simeq 201(13)_{t_c}(2)_\tau \cdots \text{ keV ,} \\ f_{D_0^* D^*}^{sd} &\simeq 0.90(3)_{t_c}(0)_\tau \cdots , \quad M_{D_{s0}^* D_s^*} \simeq 5708(170)_{t_c}(12)_\tau \text{ MeV.} \end{aligned} \quad (57)$$

Using the values: $M_{D_0^* D^*} = 5861(83.4)$ MeV and $f_{D_0^* D^*} = 238(11.4)$ keV from,¹ we can deduce:

$$r_{D_0^* D^*}^{sd} \simeq 0.98(1.4)_M(3)_{t_c}(0)_\tau \cdots , \quad f_{D_{s0}^* D_s^*} \simeq 214(10)_f(7)_{t_c}(0)_\tau \cdots \text{ keV .} \quad (58)$$

Taking the mean value of the couplings and re-using $f_{D_0^* D^*} = 238(11.4)$ keV, we deduce the final estimate:

$$f_{D_{s0}^* D_s^*} \simeq 208(9) \cdots \text{ keV} \implies f_{D_0^* D^*}^{sd} \simeq 0.87(3) \cdots , \quad (59)$$

where again the error of the SU3 ratio comes from the precise direct determination.

The $(1^{--}) \bar{D}_s D_{s1}$ molecule state

The results of the analysis are similar to the previous $D_s^* D_{s1}$ pseudoscalar case and the figures will not be shown. The coupling presents τ -stabilities from $\sqrt{t_c} = 6.0 + 2\bar{m}_q$ to $\sqrt{t_c} = 7.3 + 2\bar{m}_q$ GeV and for $\tau = 0.14$ (resp. 0.24) GeV^{-2} . Within these range of t_c -values, the mass stabilizes for $\tau \simeq 0.28 \text{ GeV}^{-2}$ and the ratio of couplings for $\tau \simeq 0.28 \text{ GeV}^{-2}$. We obtain:

$$\begin{aligned} f_{D_s D_{s1}} &\simeq 202(8)_{t_c}(0)_\tau \cdots \text{ keV ,} \\ f_{DD_1}^{sd} &\simeq 0.96(2)_{t_c}(0)_\tau \cdots , \quad M_{D_s D_{s1}} \simeq 5459(100)_{t_c}(0)_\tau \text{ MeV.} \end{aligned} \quad (60)$$

Using the values: $M_{DD_1} = 5639(150)$ MeV and $f_{DD_1} = 209(19)$ keV from,¹ we can deduce:

$$r_{DD_1}^{sd} \simeq 0.97(2.6)_M(2)_{t_c}(0)_\tau \cdots , \quad f_{D_s D_{s1}} \simeq 201(18)_f(4)_{t_c}(0)_\tau \cdots \text{ keV .} \quad (61)$$

Taking the mean of the couplings, we deduce our final result:

$$f_{D_s D_{s1}} \simeq 202(7) \cdots \text{ keV} \implies f_{DD_1}^{sd} \simeq 0.97(2) \cdots . \quad (62)$$

5.5. The (1^{-+}) Charm Vector Molecule States

The $(1^{-+}) \bar{D}_{s0}^ D_s^*$ molecule state*

The results are similar to the previous ones. The coupling presents τ -stabilities from $\sqrt{t_c} = 6.0 + 2\bar{m}_q$ to $\sqrt{t_c} = 7.2 + 2\bar{m}_q$ GeV and for $\tau = 0.12$ (resp. 0.21) GeV^{-2} . Within

these range of t_c -values, the mass stabilizes for $\tau \simeq 0.18$ (resp. 0.23) GeV^{-2} and the ratio of couplings for $\tau \simeq 0.18$ (resp. 0.19) GeV^{-2} . We obtain:

$$\begin{aligned} f_{D_{s0}^* D_s^*} &\simeq 203(20)_{t_c}(2)_\tau \cdots \text{ keV ,} \\ f_{D_0^* D^*}^{sd} &\simeq 1.021(44)_{t_c}(12)_\tau \cdots , \quad M_{D_{s0}^* D_s^*} \simeq 5699(169)_{t_c}(3)_\tau \text{ MeV.} \end{aligned} \quad (63)$$

Using the values: $M_{D_0^* D^*} = 5920(83.4)$ MeV and $f_{D_0^* D^*} = 224(11.4)$ keV from,¹ we can deduce:

$$r_{D_0^* D^*}^{sd} \simeq 0.963(14)_M(29)_{t_c}(0)_\tau \cdots , \quad f_{D_{s0}^* D_s^*} \simeq 229(12)_f(10)_{t_c}(3)_\tau \cdots \text{ keV .} \quad (64)$$

Taking the mean value of the couplings and re-using $f_{D_0^* D^*} = 224(11.4)$ keV, we deduce the final estimate:

$$f_{D_{s0}^* D_s^*} \simeq 219(13) \cdots \text{ keV} \implies f_{D_0^* D^*}^{sd} \simeq 0.98(5) \cdots , \quad (65)$$

where again the error of the ratio comes from the precise direct determination.

The (1^{-+}) $\bar{D}_s D_{s1}$ molecule state

The results of the analysis are similar to the previous $D_s^* D_{s1}$ pseudoscalar case and the figures will not be shown. The coupling presents τ -stabilities from $\sqrt{f_c} = 6.0 + 2\bar{m}_q$ to $\sqrt{f_c} = 7.3 + 2\bar{m}_q$ GeV and for $\tau=0.14$ (resp. 0.24) GeV^{-2} . Within these range of t_c -values, the mass stabilizes for $\tau \simeq 0.28$ GeV^{-2} and the ratio of couplings for $\tau \simeq 0.28$ GeV^{-2} . We obtain:

$$\begin{aligned} f_{D_s D_{s1}} &\simeq 193.4(55)_{t_c}(3)_\tau \cdots \text{ keV ,} \\ f_{DD_1}^{sd} &\simeq 1.054(123)_{t_c}(0)_\tau \cdots , \quad M_{D_s D_{s1}} \simeq 5599(139)_{t_c}(5)_\tau \cdots \text{ MeV.} \end{aligned} \quad (66)$$

Using the values: $M_{DD_1} = 5840(150)$ MeV and $f_{DD_1} = 213(19)$ keV from,¹ we can deduce:

$$r_{DD_1}^{sd} \simeq 0.959(34)_M(2)_{t_c}(1)_\tau \cdots , \quad f_{D_s D_{s1}} \simeq 224.5(20.0)_f(26.2)_{t_c}(0.)_\tau \cdots \text{ keV .} \quad (67)$$

Taking the mean of the couplings, we deduce our final result:

$$f_{D_s D_{s1}} \simeq 194(5) \cdots \text{ keV ,} \implies f_{DD_1}^{sd} \simeq 0.911(106) \cdots , \quad (68)$$

where we have taken the error from the direct determination of $f_{DD_1}^{sd}$.

6. The Heavy-light Charm Four-Quark States

6.1. Interpolating currents

The four-quark states are described by the interpolating currents given in Table 9. The corresponding spectral functions are given to LO of PT QCD in Appendix B. The different sources of the errors are given in Table 10 and Table 11.

Table 7. Different sources of errors for the estimate of the 0^- and 1^- $\bar{D}_s D_s$ -like molecule masses (in units of MeV) and couplings $f_{M_s M_s}$ (in units of keV). We use $\mu = 4.5(5)$ GeV.

Inputs	$\Delta M_{D_s^* D_s}$	$\Delta f_{D_s^* D_s}$	$\Delta M_{D_s^* D_{s1}}$	$\Delta f_{D_s^* D_{s1}}$	$\Delta M_{D_s^* D_s^*}$	$\Delta f_{D_s^* D_s^*}$	$\Delta M_{D_s D_{s1}}$	$\Delta f_{D_s D_{s1}}$
<i>LSR parameters</i>								
(t_c, τ)	202	18	177	22	170	9	100	7
μ	10	4.07	8	10.33	11	3.36	12	4.39
<i>QCD inputs</i>								
M_Q	26.51	5.73	26.46	12.23	27.09	5.36	30.28	5.11
α_s	5.51	2.20	5.20	4.68	7.1	2.14	6.51	2.16
$N3LO$	15.33	0.49	6.44	3.71	9.59	0.56	13.09	0.77
$\langle \bar{q}q \rangle$	6.65	0.48	5.72	0.98	11.92	0.21	0.0	0.0
$\langle \alpha_s G^2 \rangle$	15.0	1.75	6.25	0.98	3.94	0.19	0.0	0.0
M_0^2	1.02	0.0	3.75	0.49	6.33	0.76	10.78	1.72
$\langle \bar{q}q \rangle^2$	83.12	12.61	74.5	25.47	61.18	8.94	59.11	8.11
$\langle g^3 G^3 \rangle$	2.36	0.11	2.45	0.24	2.24	0.09	2.47	0.12
$d \geq 8$	17.05	5.54	15.84	8.53	2.8	0.36	9.4	1.96
<i>Total errors</i>	223.12	23.57	195.06	33.88	183.97	10.93	122.38	11.86

Table 8. Different sources of errors for the direct estimate of the 0^- and 1^- $\bar{D}_s D_s$ -like molecule SU(3) ratio of couplings f_{MM}^{sd} (the SU3 ratio of masses are not determined directly). We use $\mu = 4.5(5)$ GeV.

Inputs	$\Delta f_{D_0^* D}^{sd}$	$\Delta f_{D^* D_1}^{sd}$	$\Delta f_{D_0^* D^*}^{sd}$	$\Delta f_{DD_1}^{sd}$
<i>LSR parameters</i>				
(t_c, τ)	0.04	0.01	0.03	0.02
μ	0.001	0.002	0.001	0.004
<i>QCD inputs</i>				
M_Q	0.003	0.003	0.002	0.003
α_s	0.0	0.0	0.0	0.0
$N3LO$	0.003	0.006	0.001	0.003
$\langle \bar{q}q \rangle$	0.002	0.002	0.001	0.0
$\langle \alpha_s G^2 \rangle$	0.001	0.0	0.0	0.0
M_0^2	0.0	0.001	0.003	0.003
$\langle \bar{q}q \rangle^2$	0.033	0.032	0.025	0.024
$\langle g^3 G^3 \rangle$	0.0	0.0	0.0	0.0
$d \geq 8$	0.007	0.004	0.0	0.006
<i>Total errors</i>	0.053	0.036	0.039	0.032

6.2. The $S_{sc}(0^+)$ Charm Scalar Four-Quark State

The behaviours of the corresponding curves are very similar to some of the previous molecule ones. They are shown in Figs. 8 and 9. The SU3 ratio of coupling presents τ -stabilities from $\sqrt{t_c} = 5 + 2\bar{m}_q$ to $\sqrt{t_c} = 6.5 + 2\bar{m}_q$ GeV and for $\tau=0.28$ (resp. 0.36) GeV^{-2} . Within these range of t_c -values, the SU3 ratio of masses stabilizes for $\tau \simeq 0.4$ (resp. 0.4) GeV^{-2} and the coupling for $\tau \simeq 0.28$ (resp. 0.36) GeV^{-2} . We obtain:

$$f_{S_c}^{sd} \simeq 0.924(15)_{t_c}(3)_\tau \dots, r_{S_c}^{sd} \simeq 1.085(2)_{t_c}(0)_\tau \dots, f_{S_{sc}} \simeq 162(10)_{t_c}(1)_\tau \dots \text{keV}, \quad (69)$$

Using the NLO values: $M_{S_c} = 3901(0.2)$ MeV, $f_{S_c} = 184(9)$ keV from¹ and $f_{S_c}^{sd}$, we can deduce:

$$M_{S_{sc}} \simeq 4233(0.2)_M(7)_{t_c}(0)_\tau \dots \text{MeV}, f_{S_{sc}} \simeq 170(8)_f(3)_{t_c}(1)_\tau \dots \text{keV}. \quad (70)$$

Table 9. Interpolating currents describing the four-quark states. $Q \equiv c$ (resp. b). k is an arbitrary current mixing where the optimal value is found to be $k = 0$ from.^{23,24}

States	J^P	Four-Quark Currents $\equiv \mathcal{O}_{4q}(x)$
Scalar	0^+	$\epsilon_{abc}\epsilon_{dec} \left[(s_a^T C \gamma_5 Q_b)(\bar{s}_d \gamma_5 C \bar{Q}_e^T) + k(s_a^T C Q_b)(\bar{s}_d C \bar{Q}_e^T) \right]$
Axial-vector	1^+	$\epsilon_{abc}\epsilon_{dec} \left[(s_a^T C \gamma_5 Q_b)(\bar{s}_d \gamma_\mu C \bar{Q}_e^T) + k(s_a^T C Q_b)(\bar{s}_d \gamma_\mu \gamma_5 C \bar{Q}_e^T) \right]$
Pseudoscalar	0^-	$\epsilon_{abc}\epsilon_{dec} \left[(s_a^T C \gamma_5 Q_b)(\bar{s}_d C \bar{Q}_e^T) + k(s_a^T C Q_b)(\bar{s}_d \gamma_5 C \bar{Q}_e^T) \right]$
Vector	1^-	$\epsilon_{abc}\epsilon_{dec} \left[(s_a^T C \gamma_5 Q_b)(\bar{s}_d \gamma_\mu \gamma_5 C \bar{Q}_e^T) + k(s_a^T C Q_b)(\bar{s}_d \gamma_\mu C \bar{Q}_e^T) \right]$

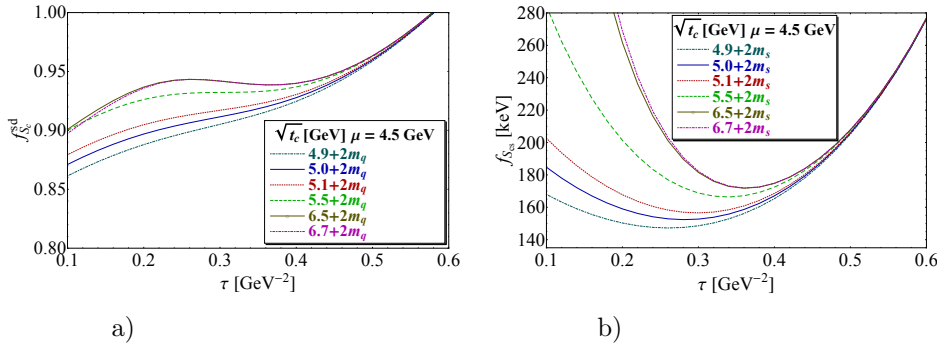


Fig. 8. **a)** SU3 ratio of couplings $f_{S_c}^{sd}$ at NLO as function of τ for different values of t_c , for $\mu = 4.5$ GeV and for the QCD parameters in Tables 3 and 4; **b)** The same as a) but for the couplings $f_{S_{sc}}$.

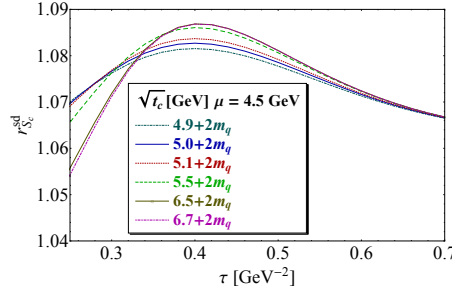


Fig. 9. SU3 ratio of masses $r_{S_c}^{sd}$ at NLO as function of τ for different values of t_c , for $\mu = 4.5$ GeV and for the QCD parameters in Tables 3 and 4.

Taking the mean of $f_{S_{sc}}$ and re-using $f_{S_c} \simeq 184(9)$ keV, we deduce the final estimate:

$$f_{S_{sc}} \simeq 166(7) \cdots \text{ keV} \implies f_{S_c}^{sd} \simeq 0.902(17) \cdots , \quad (71)$$

where the error of $f_{S_c}^{sd}$ comes from the direct determination.

6.3. The $A_{sc}(1^+)$ Charm Axial-Vector Four-Quark State

The behaviours of the corresponding curves are very similar to the previous ones. The SU3 ratio of coupling presents τ -stabilities from $\sqrt{t_c} = 5.1 + 2\bar{m}_q$ to $\sqrt{t_c} = 6.5 + 2\bar{m}_q$ GeV and for $\tau=0.26$ (resp. 0.36) GeV^{-2} . Within these range of t_c -values, the SU3 ratio of masses stabilizes for $\tau \simeq 0.34$ (resp. 0.34) GeV^{-2} and the coupling for $\tau \simeq 0.28$ (resp. 0.34) GeV^{-2} . We obtain:

$$f_{A_c}^{sd} \simeq 0.834(17)_{t_c}(2)_\tau \cdots , \quad r_{A_c}^{sd} \simeq 1.081(4)_{t_c}(1)_\tau \cdots , \quad f_{A_{sc}} \simeq 137(8)_{t_c}(5)_\tau \cdots \text{ keV} , \quad (72)$$

Using the NLO values: $M_{A_c} = 3890(27)$ MeV and $f_{A_c} = 176(9)$ keV from,¹ we can deduce:

$$M_{A_{sc}} \simeq 4205(29)_M(16)_{t_c}(4)_\tau \cdots \text{ MeV}, \quad f_{A_{sc}} \simeq 147(8)_f(30)_{t_c}(4)_\tau \cdots \text{ keV} . \quad (73)$$

Taking the mean of $f_{A_{sc}}$ and re-using $f_{A_c} \simeq 176(9)$ keV, we deduce the final estimate:

$$f_{A_{sc}} \simeq 141(6) \cdots \text{ keV} \implies f_{A_c}^{sd} \simeq 0.80(3) \cdots , \quad (74)$$

where the error of $f_{A_c}^{sd}$ comes from the direct determination.

6.4. The $\pi_{sc}(0^-)$ Charm Pseudoscalar State

The coupling presents τ -stabilities from $\sqrt{t_c} = 6.0 + 2\bar{m}_q$ to $\sqrt{t_c} = 7.3 + 2\bar{m}_q$ GeV and for $\tau=0.15$ (resp. 0.22) GeV^{-2} . Within these range of t_c -values, the mass stabilizes for $\tau \simeq 0.20$ (resp. 0.24) GeV^{-2} and the ratio of couplings for $\tau \simeq 0.23$ (resp. 0.24) GeV^{-2} . We obtain:

$$\begin{aligned} f_{\pi_{sc}} &\simeq 249(21)_{t_c}(6)_\tau \cdots \text{ keV} , \\ f_{\pi_c}^{sd} &\simeq 0.90(3)_{t_c}(4)_\tau \cdots , \quad M_{\pi_{sc}} \simeq 5671(159)_{t_c}(4)_\tau \cdots \text{ MeV} . \end{aligned} \quad (75)$$

Using the values: $M_{\pi_c} = 5872(101)$ MeV and $f_{\pi_c} = 292(5.7)$ keV from,¹ we can deduce:

$$r_{\pi_c}^{sd} \simeq 0.97(3) \cdots , \quad f_{\pi_{sc}} \simeq 263(5)_f(9)_{t_c}(3)_\tau \cdots \text{ keV} . \quad (76)$$

Taking the mean of $f_{\pi_{sc}}$ and re-using $f_{\pi_c} = 292(5.7)$ keV, we deduce the final estimate:

$$f_{\pi_{sc}} \simeq 256(9) \cdots \text{ keV} \implies f_{\pi_c}^{sd} \simeq 0.88(3) \cdots \quad (77)$$

6.5. The $V_{sc}(1^-)$ Charm Vector State

The behaviours of the corresponding curves are very similar to the previous ones. The coupling presents τ -stabilities from $\sqrt{t_c} = 6.0 + 2\bar{m}_q$ to $\sqrt{t_c} = 7.3 + 2\bar{m}_q$ GeV and for $\tau=0.11\text{-}0.15$ (resp. 0.24) GeV^{-2} . Within these range of t_c -values, the mass stabilizes for $\tau \simeq 0.19$ (resp. 0.24) GeV^{-2} and the ratio of couplings for $\tau \simeq 0.23$ (resp. 0.24) GeV^{-2} . We obtain:

$$\begin{aligned} f_{V_{sc}} &\simeq 235(21)_{t_c}(5)_\tau \dots \text{ keV ,} \\ f_{V_c}^{sd} &\simeq 0.94(4)_{t_c}(1)_\tau \dots , \quad M_{V_{sc}} \simeq 5654(222)_{t_c}(8)_\tau \dots \text{ MeV.} \end{aligned} \quad (78)$$

Using the NLO values: $M_{V_c} = 5904(90)$ MeV and $f_{V_c} = 268(14)$ keV from,¹ we can deduce:

$$r_{V_c}^{sd} \simeq 0.96(4) \dots , \quad f_{V_{sc}} \simeq 252(13)_f(11)_{t_c}(3)_\tau \dots \text{ keV .} \quad (79)$$

Taking the mean of $f_{V_{sc}}$ and re-using $f_{V_c} = 268(14)$ keV, we deduce the final estimate:

$$f_{V_{sc}} \simeq 245(14) \dots \text{ keV} \implies f_{V_c}^{sd} \simeq 0.91(4) \dots , \quad (80)$$

where the error of $f_{V_c}^{sd}$ comes from the direct determination.

Table 10. Different sources of errors for the estimate of the four-quarks [$c\bar{s}c\bar{s}$] pseudo (scalar) π_{sc} (S_{sc}) and axial (vector) A_{sc} (V_{sc}) masses (in units of MeV) and couplings (in units of keV). We use $\mu = 4.5(5)$ GeV.

Inputs	$\Delta M_{S_{sc}}$	$\Delta f_{S_{sc}}$	$\Delta M_{A_{sc}}$	$\Delta f_{A_{sc}}$	$\Delta M_{\pi_{sc}}$	$\Delta f_{\pi_{sc}}$	$\Delta M_{V_{sc}}$	$\Delta f_{V_{sc}}$
<i>LSR parameters</i>								
(t_c, τ)	7	8.6	33.4	5.5	159.1	9	222.1	14
μ	24.77	8.03	29.12	7.90	8.40	4.69	7.10	5.01
<i>QCD inputs</i>								
M_Q	11.87	5.20	10.88	4.09	27.18	6.49	27.01	6.17
α_s	15.69	4.20	16.61	3.81	5.39	2.46	3.99	2.26
$N3LO$	0.00	1.82	0.28	1.33	10.29	0.77	8.05	0.91
$\langle \bar{q}q \rangle$	15.75	2.33	20.45	2.47	6.17	0.58	5.47	0.46
$\langle \alpha_s G^2 \rangle$	0.56	0.56	0.54	0.16	9.17	0.62	1.70	0.21
M_0^2	14.94	1.60	18.30	2.17	0.3	0.0	5.17	1.37
$\langle \bar{q}q \rangle^2$	12.09	9.32	33.02	8.99	80.31	26.20	81.12	25.82
$\langle g^3 G^3 \rangle$	0.54	0.15	0.24	0.14	2.36	0.13	2.19	0.12
$d \geq 8$	45.09	0.91	91.51	1.30	9.7	2.70	22.5	7.26
<i>Total errors</i>	60.83	16.79	112.14	14.79	181.43	28.83	239.44	30.50

7. The Heavy-light Beauty Molecule States

We extend the previous analysis to the case of beauty molecule states. The strategy for obtaining the results is very similar to the one of the charm. The different sources of errors are given in Tables 12 to 15.

Table 11. Different sources of errors for the direct estimate of the four-quarks $[c\bar{s}\bar{c}\bar{s}]$ pseudo (scalar) π_{sc} (S_{sc}) and axial (vector) A_{sc} (V_{sc}) SU(3) ratio of masses r_M^{sd} and of couplings f_M^{sd} . We use $\mu = 4.5(5)$ GeV.

Inputs	$\Delta r_{S_c}^{sd}$	$\Delta f_{S_c}^{sd}$	$\Delta r_{A_c}^{sd}$	$\Delta f_{A_c}^{sd}$	$\Delta f_{\pi_c}^{sd}$	$\Delta f_{V_c}^{sd}$
<i>LSR parameters</i>						
(t_c, τ)	0.002	0.017	0.004	0.03	0.03	0.04
μ	0.0	0.005	0.0	0.007	0.002	0.003
<i>QCD inputs</i>						
M_Q	0.0	0.004	0.0	0.004	0.002	0.002
α_s	0.001	0.002	0.001	0.003	0.0	0.0
$N3LO$	0.0	0.005	0.0	0.005	0.001	0.003
$\langle \bar{q}q \rangle$	0.002	0.002	0.003	0.003	0.002	0.001
$\langle \alpha_s G^2 \rangle$	0.0	0.001	0.0	0.0	0.0	0.0
M_0^2	0.002	0.001	0.003	0.003	0.0	0.002
$\langle \bar{q}q \rangle^2$	0.003	0.029	0.004	0.024	0.045	0.049
$\langle g^3 G^3 \rangle$	0.0	0.0	0.0	0.0	0.0	0.0
$d \geq 8$	0.010	0.005	0.016	0.009	0.049	0.072
<i>Total errors</i>	0.011	0.035	0.018	0.041	0.073	0.096

7.1. The (0^{++}) Beauty Scalar Molecule States

The $\bar{B}_s B_s$ molecule state

We shall illustrate the analysis by showing the different figures (Figs. 10 and 11) in this channel. The subtraction point is taken at $\mu = 6$ GeV, where μ -stability has been obtained in¹ for the non-strange quark case. From these figures, we obtain

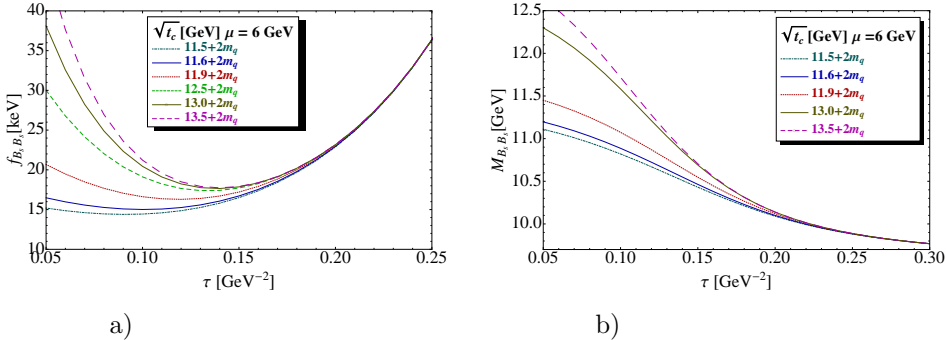


Fig. 10. **a)** The coupling $f_{B_s B_s}$ at NLO as function of τ for different values of t_c , for $\mu = 6$ GeV and for the QCD parameters in Tables 3 and 4; **b)** The same as a) but for the mass $M_{B_s B_s}$.

extrema or inflection points from $\sqrt{t_c} \simeq 11.6 + 2m_q$ to $13 + 2m_q$ GeV. The τ -stabilities occur at 0.10 (resp. 0.14), about 0.13–0.15 (resp. 0.16) and 0.13 (resp. 0.14) GeV^{-2} for the coupling, mass, SU3 ratio of couplings and of masses. We deduce the optimal results:

$$f_{B_s B_s}(6) \simeq 16.3(1.3)_{t_c}(0.2)_\tau \text{ keV}, \quad f_{BB}^{sd} \simeq 1.116(13)_{t_c}(0)_\tau, \quad r_{BB}^{sd} \simeq 1.027(2)_{t_c}(1)_\tau, \quad (81)$$

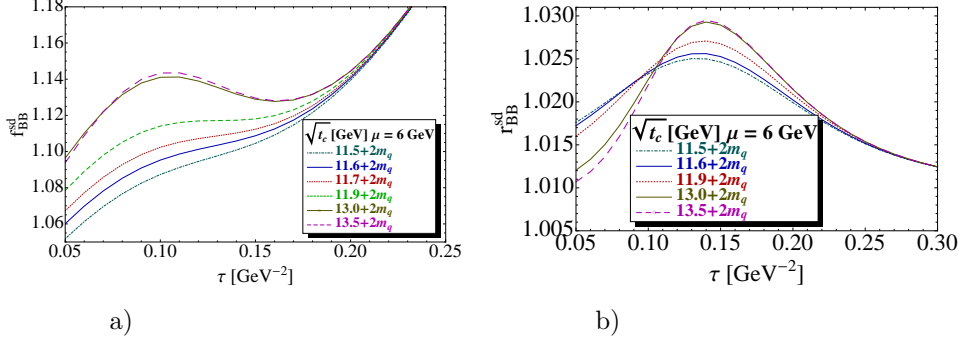


Fig. 11. **a)** SU3 ratio of couplings f_{BB}^{sd} at NLO as function of τ for different values of t_c , for $\mu = 6$ GeV and for the QCD parameters in Tables 3 and 4; **b)** The same as a) but for the SU3 ratio of masses r_{BB}^{sd} .

where the QCD corrections are given in Table 12. We have not considered the value of the mass from the figure but combine the accurate ratio with the value $M_{BB} = 10598(54)$ MeV (without QCD corrections) obtained in¹ from which we obtain:

$$M_{B_s B_s} = 10884(56)_M(21)_{t_c}(10)_{\tau} \cdots \text{ MeV}, \quad (82)$$

where \cdots denotes QCD corrections given in Table 12. Combining the SU3 ratio of couplings with the NLO value $f_{BB}(6) \simeq 16.2(1.6)$ keV from¹ runned at $\mu = 6$ GeV, one deduces:

$$f_{B_s B_s}(6) \simeq 18.1(1.8)_f(0.2)_{t_c}(0)_{\tau} \cdots \text{ keV}. \quad (83)$$

Taking the mean, we deduce:

$$f_{B_s B_s}(6) \simeq 16.9(1.1) \cdots \text{ keV} \implies f_{BB}^{sd} \simeq 1.043(12) \cdots, \quad (84)$$

The $\bar{B}_s^* B_s^*$ molecule state

In the same way as before, the extrema or inflexion points occur from $\sqrt{t_c} \simeq 11.6 + 2 m_q$ to $13 + 2 m_q$ GeV. The τ -stabilities are at 0.08 (resp. 0.13), about 0.12–0.16 (resp. 0.14) and 0.11 (resp. 0.13) GeV $^{-2}$ for the coupling, mass, SU3 ratio of couplings and of masses. We deduce the optimal results:

$$f_{B_s^* B_s^*}(6) \simeq 30.2(34)_{t_c}(1)_{\tau} \text{ keV}, \quad f_{B^* B^*}^{sd} \simeq 1.105(20)_{t_c}(6)_{\tau}, \quad r_{B^* B^*}^{sd} \simeq 1.028(2)_{t_c}(0)_{\tau}, \quad (85)$$

where the QCD corrections are given in Table 12. Using $M_{B^* B^*} = 10646(102)$ MeV from¹ we deduce:

$$M_{B_s^* B_s^*} = 10944(105)_M(21)_{t_c}(0)_{\tau} \text{ MeV}. \quad (86)$$

Combining the SU3 ratio of couplings with the NLO value $f_{B^* B^*}(6) \simeq 31(5)$ keV from¹ runned at $\mu = 6$ GeV, one deduces:

$$f_{B_s^* B_s^*}(6) \simeq 32.6(5.3)_f(0.7)_{t_c}(0)_{\tau} \text{ keV}. \quad (87)$$

Taking the mean value of the coupling, we obtain:

$$f_{B_s^* B_s^*}(6) \simeq 30.9(2.9) \cdots \text{ keV} \implies f_{B_s^* B_s^*}^{sd} \simeq 1.00(2) \cdots . \quad (88)$$

The $\bar{B}_{s0}^* B_{s0}^*$ molecule state

The different sum rules stabilize in the same range of t_c as in the previous 0^{++} cases. The τ -stabilities are at 0.08 (resp. 0.13), about 0.12–0.16 (resp. 0.14) and 0.11 (resp. 0.13) GeV^{-2} for the coupling, mass, SU3 ratio of couplings and of masses. We deduce the optimal results:

$$\begin{aligned} f_{B_{s0}^* B_{s0}^*}(6) &\simeq 11.7(3.7)_{t_c}(0.6)_\tau \text{ keV}, \quad f_{B_0^* B_0^*}^{sd} \simeq 1.258(73)_{t_c}(10)_\tau, \\ r_{B_0^* B_0^*}^{sd} &\simeq 1.050(7)_{t_c}(1)_\tau. \end{aligned} \quad (89)$$

Using $M_{B_0^* B_0^*} = 10649(113) \text{ MeV}$ from¹ we deduce:

$$M_{B_{s0}^* B_{s0}^*} = 11182(119)_M(74)_{t_c}(11)_\tau \text{ MeV}. \quad (90)$$

Combining the SU3 ratio of couplings with the NLO value $f_{B_0^* B_0^*}(6) \simeq 11.7(3.3) \text{ keV}$ from¹ runned at $\mu = 6 \text{ GeV}$, one deduces:

$$f_{B_{s0}^* B_{s0}^*}(6) \simeq 14.7(4.2)_f(0.9)_{t_c}(0.1)_\tau \text{ keV}. \quad (91)$$

Taking the mean value of the coupling, we obtain:

$$f_{B_{s0}^* B_{s0}^*}(6) \simeq 13.0(2.9) \cdots \text{ keV} \implies f_{B_0^* B_0^*}^{sd} \simeq 1.11(1) \cdots . \quad (92)$$

The $\bar{B}_{s1} B_{s1}$ and $\bar{B}_1 B_1$ molecule states

We perform a similar analysis. The behaviours of the different curves are very similar to the case of the $\bar{B}_s B_s$ molecule states. They present stabilites for $\sqrt{t_c} \simeq 11.6 + 2\bar{m}_s$ to $13.0 + 2\bar{m}_s$ GeV for $\tau \simeq 0.07 - 0.13$ (resp. 0.09–0.12) (resp. 0.09–0.12) GeV^{-2} for the coupling $f_{B_{s1} B_{s1}}$ (resp. SU3 ratio of couplings $f_{B_1 B_1}^{sd}$) (resp. SU3 ratio of masses $r_{B_1 B_1}^{sd}$) leading to the values at NLO:

$$f_{B_{s1} B_{s1}} \simeq 24(4) \cdots \text{ keV}, \quad f_{B_1 B_1}^{sd} \simeq 1.197(41) \cdots, \quad r_{B_1 B_1}^{sd} \simeq 1.040(1) \cdots, \quad (93)$$

where the quoted errors come from the correlated values of (t_c, τ) and \cdots are QCD corrections given in Table 5. The mass presents an inflexion which is difficult to localize. To fix the τ -values, we take the range where the SU3 ratio of masses optimizes, which corresponds to $\tau \simeq 0.09 - 0.12 \text{ GeV}^{-2}$. In this way, we obtain:

$$M_{B_{s1} B_{s1}} \simeq 10935(155) \cdots \text{ MeV}. \quad (94)$$

Using the previous values of the SU3 ratios, we can deduce for the $\bar{B}_1 B_1$ molecule at NLO:

$$f_{B_1 B_1} \simeq 20(3) \cdots \text{ keV}, \quad M_{B_1 B_1} \simeq 10514(149) \cdots \text{ MeV}. \quad (95)$$

7.2. The $(1^{+\pm})$ Beauty Axial-Vector Molecule States

Here, within our choice of interpolating currents, the (1^{++}) and (1^{+-}) are degenerate in masses like in the cases of charmonium and pseudoscalar channels and have the same couplings.

The $\bar{B}_s^ B_s$ molecule state*

The different sum rules stabilize in the same range of t_c as in the previous cases. The τ -stabilities are at 0.09 (resp. 0.135), 0.12 (resp. 0.15) and 0.13 (resp. 0.145) GeV^{-2} for the coupling, SU3 ratio of couplings and of masses. We deduce the optimal results:

$$f_{B_s^* B_s}(6) \simeq 16.6(1.6)_{t_c}(0.1)_\tau \text{ keV}, \quad f_{B^* B}^{sd} \simeq 1.114(17)_{t_c}(1)_\tau, \quad r_{B^* B}^{sd} \simeq 1.028(3)_{t_c}(1)_\tau. \quad (96)$$

Using $M_{B^* B} = 10673(150)$ MeV from¹ we deduce:

$$M_{B_s^* B_s} = 10972(154)_M(32)_{t_c}(11)_\tau \text{ MeV}. \quad (97)$$

Combining the SU3 ratio of couplings with the NLO value $f_{B^* B}(6) \simeq 16.5(5)$ keV from¹ runned at $\mu = 6$ GeV, one deduces:

$$f_{B_s^* B_s}(6) \simeq 18.4(5.6)_f(0.3)_{t_c}(0)_\tau \text{ keV}. \quad (98)$$

Taking the mean value of the coupling, we obtain:

$$f_{B_s^* B_s}(6) \simeq 16.7(1.5) \cdots \text{ keV} \implies f_{B^* B}^{sd} \simeq 1.01(1) \cdots. \quad (99)$$

The $\bar{B}_{s0}^ B_{s1}$ molecule state*

In this channel, only the coupling and the SU3 ratio of masses present net stabilities. The others present inflexion points which cannot be accurately localized. The τ -stabilities are at 0.04 (resp. 0.125), and 0.06 (resp. 0.115) GeV^{-2} for $\sqrt{t_c} \simeq 11.6 + 2 m_q$ (resp. $13 + 2 m_q$) GeV. We deduce the optimal results:

$$f_{B_{s0}^* B_{s1}}(6) \simeq 9.1(10)_{t_c}(14)_\tau \text{ keV}, \quad r_{B_0^* B_1}^{sd} \simeq 1.052(8)_{t_c}(3)_\tau. \quad (100)$$

Using $M_{B_0^* B_1} = 10679(132)$ MeV from¹ we deduce:

$$M_{B_{s0}^* B_{s1}} = 11234(139)_M(85)_{t_c}(32)_\tau \text{ MeV}. \quad (101)$$

Using the NLO value $f_{B_0^* B_1}(6) \simeq 11.3(1.6)$ keV from¹ runned at $\mu = 6$ GeV, one deduces:

$$f_{B_0^* B_1}^{sd} \simeq 0.80(11) \cdots. \quad (102)$$

7.3. The $(0^{-\pm})$ Beauty Pseudoscalar Molecule States

Here, within our choice of interpolating currents, the (0^{--}) and (0^{-+}) are degenerate in masses and have the same couplings. Here, we choose $\mu = 5.5$ GeV where inflexion point has been obtained for the non-strange channel.¹

Table 12. Different sources of errors for the estimate of the 0^+ and 1^+ $\bar{B}_s B_s$ -like molecule masses (in units of MeV) and couplings $f_{M_s M_s}(\mu)$ (in units of keV). We use $\mu = 6.0(5)$ GeV.

Inputs	$B_s B_s$		$B_s^* B_s^*$		$B_{s0}^* B_{s0}^*$		$B_{s1} B_{s1}$		$B_s^* B_s$		$B_{s0}^* B_{s1}$	
	ΔM	Δf	ΔM	Δf	ΔM	Δf	ΔM	Δf	ΔM	Δf	ΔM	Δf
<i>LSR parameters</i>												
(t_c, τ)	60.63	1.81	107.08	2.90	140.56	2.90	155	3.88	157.67	1.50	166.04	1.72
μ	5.14	0.0	7.30	0.56	3.46	0.04	9.30	1.31	7.29	0.03	6.20	0.0
<i>QCD inputs</i>												
M_Q	2.14	0.10	2.32	0.17	2.27	0.07	1.56	0.14	2.93	0.35	3.42	0.10
α_s	10.79	0.35	11.53	0.63	19.04	0.23	10.55	0.49	13.02	0.10	17.64	0.24
$N3LO$	1.54	0.21	0.84	0.35	11.76	0.27	3.71	0.35	0.00	0.23	14.91	0.11
$\langle\bar{q}q\rangle$	14.95	0.17	6.40	0.20	25.01	0.34	20.20	0.28	8.66	0.18	21.37	0.36
$\langle\alpha_s G^2\rangle$	0.51	0.02	0.70	0.02	3.52	0.05	0.55	0.04	0.03	0.0	1.70	0.0
M_0^2	11.63	0.15	11.67	0.23	22.24	0.20	10.22	0.23	7.12	0.18	22.75	0.25
$\langle\bar{q}q\rangle^2$	27.03	0.95	19.24	2.12	23.34	1.49	51.30	2.49	23.52	0.98	21.38	1.55
$\langle g^3 G^3 \rangle$	0.02	0.0	0.08	0.0	0.06	0.0	0.06	0.0	0.02	0.0	1.71	0.0
$d \geq 8$	22.0	0.83	76.0	2.78	171.5	0.57	42.9	1.09	110	0.22	116.5	0.10
<i>Total errors</i>	73.49	2.26	134.10	4.64	226.64	3.13	169.80	4.96	194.62	1.87	207.77	2.21

Table 13. Different sources of errors for the estimate of the 0^+ and 1^+ $\bar{B}B$ -like molecule SU(3) ratios of masses r_{MM}^{sd} and SU(3) ratios of couplings f_{MM}^{sd} . We use $\mu = 6.0(5)$ GeV.

Inputs	$B_s B_s$		$B_s^* B_s^*$		$B_{s0}^* B_{s0}^*$		$B_{s1} B_{s1}$		$B_s^* B_s$		$B_{s0}^* B_{s1}$	
	r^{sd}	f^{sd}	r^{sd}	f^{sd}	r^{sd}	f^{sd}	r^{sd}	f^{sd}	r^{sd}	f^{sd}	r^{sd}	f^{sd}
<i>LSR parameters</i>												
(t_c, τ)	0.002	0.012	0.002	0.02	0.007	0.01	0.001	0.050	0.003	0.01	0.009	0.11
μ	0.0	0.003	0.0	0.004	0.0	0.004	0.0	0.003	0.0	0.004	0.0	0.003
<i>QCD inputs</i>												
M_Q	0.0	0.0	0.0	0.0	0.0	0.0	0.0	0.0	0.0	0.0	0.0	0.003
α_s	0.0	0.0	0.0	0.0	0.0	0.0	0.0	0.001	0.0	0.0	0.0	0.003
$N3LO$	0.0	0.01	0.0	0.01	0.001	0.003	0.0	0.001	0.0	0.01	0.002	0.001
$\langle\bar{q}q\rangle$	0.001	0.001	0.0	0.001	0.002	0.002	0.001	0.0	0.0	0.001	0.002	0.002
$\langle\alpha_s G^2\rangle$	0.0	0.0	0.0	0.0	0.0	0.001	0.0	0.001	0.0	0.0	0.0	0.0
M_0^2	0.001	0.001	0.0	0.001	0.001	0.001	0.001	0.0	0.001	0.001	0.001	0.0
$\langle\bar{q}q\rangle^2$	0.001	0.032	0.001	0.029	0.002	0.047	0.001	0.049	0.001	0.030	0.002	0.032
$\langle g^3 G^3 \rangle$	0.0	0.0	0.0	0.0	0.0	0.0	0.0	0.0	0.0	0.0	0.0	0.0
$d \geq 8$	0.002	0.020	0.004	0.008	0.007	0.020	0.0	0.019	0.001	0.010	0.011	0.008
<i>Total errors</i>	0.004	0.041	0.005	0.033	0.011	0.051	0.002	0.073	0.004	0.032	0.014	0.036

The $\bar{B}_{s0}^* B_s$ molecule state

In this channel, the curves present new features where the coupling, its SU3 ratio and the mass present τ -minima as shown in Figs 12 and 13. The results are similar to the one of $\bar{B}_s^* B_s$. Stabilities are obtained from $\sqrt{t_c} \simeq 13.2 + 2 m_q$ to $15 + 2 m_q$ GeV. The τ -stabilities are at 0.04 (resp. 0.09), 0.07 (resp. 0.07) and 0.07 (resp. 0.095) GeV^{-2} for the coupling, SU3 ratio of couplings and the mass. We deduce the optimal results:

$$f_{B_{s0}^* B_s}(5.5) \simeq 59.8(6.7)_{t_c}(2.1)_\tau \text{ keV}, \quad f_{B_s^* B}^{sd} \simeq 1.009(23)_{t_c}(5)_\tau, \\ M_{B_{s0}^* B_s} \simeq 12725(197)_{t_c}(37)_\tau \text{ MeV}. \quad (103)$$

Using the NLO value $f_{B_0^*B}(5.5) \simeq 55(9)$ keV and $M_{B_0^*B} \simeq 12737(254)$ MeV from,¹ one deduces from $f_{B_0^*B}^{sd}$:

$$f_{B_{s0}^*B_s} \simeq 55.5(8.8)_f(1.3)_{t_c}(0.3)_\tau \cdots \text{keV}, r_{B_0^*B}^{sd} \simeq 1.00(2) \cdots. \quad (104)$$

Taking the mean value of the coupling and re-using $f_{B_0^*B}(5.5) \simeq 55(9)$ keV, we deduce the final estimate:

$$f_{B_{s0}^*B_s} \simeq 58.2(5.5) \cdots \text{keV} \implies f_{B_0^*B}^{sd} \simeq 1.058(23) \cdots. \quad (105)$$

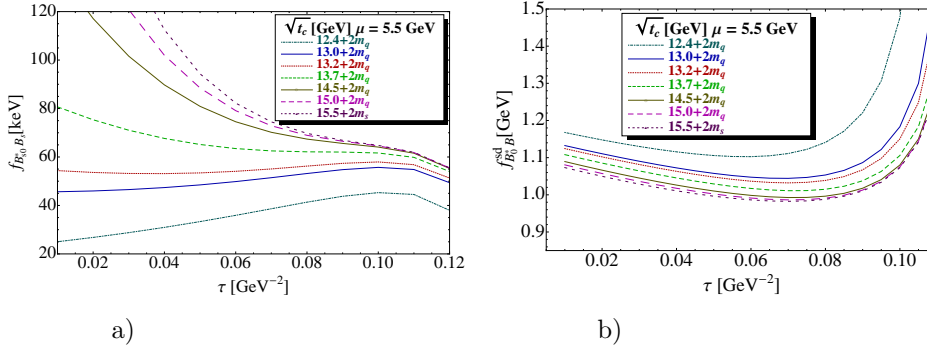


Fig. 12. **a)** The coupling $f_{B_{s0}^*B_s}$ at NLO as function of τ for different values of t_c , for $\mu = 5.5$ GeV and for the QCD parameters in Tables 3 and 4; **b)** The same as a) but for the SU3 ratio of couplings $f_{B_{s0}^*B_s}^{sd}$.

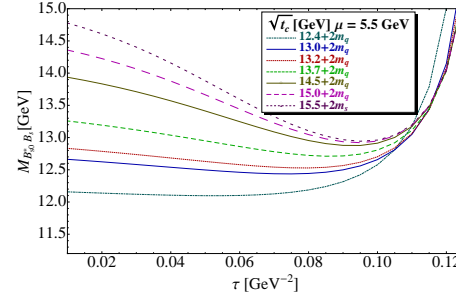


Fig. 13. $M_{B_{s0}^*B_s}$ at NLO as function of τ for different values of t_c , for $\mu = 5.5$ GeV and for the QCD parameters in Tables 3 and 4.

The $\bar{B}_s^*B_{s1}$ molecule state

The results are similar to the one of $\bar{B}_{s0}^*B_s$. Stabilities are obtained from $\sqrt{t_c} \simeq 13 + 2 m_q$ to $15 + 2 m_q$ GeV. The τ -stabilities are at 0.04 (resp. 0.09), 0.07 (resp. 0.07)

and 0.07 (resp. 0.09) GeV^{-2} for the coupling, SU3 ratio of couplings and the mass. We deduce the optimal results:

$$\begin{aligned} f_{B_s^* B_{s1}}(5.5) &\simeq 96.7(10.1)_{t_c}(4.3)_\tau \text{ keV}, \quad f_{B^* B_1}^{sd} \simeq 1.014(31)_{t_c}(10)_\tau, \\ M_{B_s^* B_{s1}} &\simeq 12726(264)_{t_c}(5)_\tau \text{ MeV}. \end{aligned} \quad (106)$$

Using the NLO value $f_{B^* B_1}(5.5) \simeq 105(15)$ keV and $M_{B^* B_1} \simeq 12794(228)$ MeV from,¹ one deduces:

$$f_{B_s^* B_{s1}}(5.5) \simeq 106.5(15.2)_f(3.3)_{t_c}(1.1)_\tau \text{ keV}, \quad r_{B^* B_1}^{sd} \simeq 1.00(3) \quad (107)$$

Taking the mean of the couplings, we obtain:

$$f_{B_s^* B_{s1}}(5.5) \simeq 100.2(9.0) \cdots \text{ keV} \implies f_{B^* B_1}^{sd} \simeq 0.96(3) \cdots \quad (108)$$

7.4. The (1^{--}) Beauty Vector Molecule States

The (1^{--}) $\bar{B}_{s0}^ B_s^*$ molecule state*

The behaviours of different curves are the same as in the case of the pseudoscalar ($0^{-\pm}$) molecules and will not be shown here. τ and t_c -stabilities are obtained about the same values as for the $B_s^* B_{s1}$ ($0^{-\pm}$) state at which we deduce the optimal results:

$$\begin{aligned} f_{B_{s0}^* B_s^*}(5.5) &\simeq 49.8(5.8)_{t_c}(1.8)_\tau \text{ keV}, \quad f_{B_0^* B^*}^{sd} \simeq 1.024(28)_{t_c}(7)_\tau, \\ M_{B_{s0}^* B_s^*} &\simeq 12715(258)_{t_c}(37)_\tau \text{ MeV}. \end{aligned} \quad (109)$$

Using the NLO value $f_{B_0^* B^*}(5.5) \simeq 54(9)$ keV and $M_{B_0^* B^*} \simeq 12756(261)$ MeV from,¹ one deduces from $f_{B_0^* B^*}^{sd}$:

$$f_{B_{s0}^* B_s^*} \simeq 55.3(9.2)_f(1.5)_{t_c}(0.4)_\tau \cdots \text{ keV}, \quad r_{B_0^* B^*}^{sd} \simeq 1.00(3). \quad (110)$$

Taking the mean value of the coupling and re-using $f_{B_0^* B^*}(5.5) \simeq 54(9)$ keV, we deduce the final estimate:

$$f_{B_{s0}^* B_s^*} \simeq 51.4(5.1) \cdots \text{ keV} \implies f_{B_0^* B^*}^{sd} \simeq 0.95(3) \cdots. \quad (111)$$

The (1^{--}) $\bar{B}_s B_{s1}$ molecule state

The behaviours of different curves are the same as in the case of the pseudoscalar ($0^{-\pm}$) molecules and will not be shown here. τ -stabilities are obtained at 0.055 (resp. 0.09), 0.07 (resp. 0.075) and 0.08 (resp. 0.095) GeV^{-2} for the coupling, SU3 ratio of couplings and the mass for $\sqrt{t_c} \simeq 13 + 2 m_q$ to $15 + 2 m_q$ GeV. We deduce the optimal results:

$$\begin{aligned} f_{B_s B_{s1}}(5.5) &\simeq 45.1(1.0)_{t_c}(0.2)_\tau \text{ keV}, \quad f_{B B_1}^{sd} \simeq 0.997(33)_{t_c}(8)_\tau, \\ M_{B_s B_{s1}} &\simeq 12615(221)_{t_c}(42)_\tau \text{ MeV}. \end{aligned} \quad (112)$$

Using the NLO value $f_{BB_1}(5.5) \simeq 54(10.6)$ keV and $M_{BB_1} \simeq 12734(249)$ MeV from,¹ one deduces:

$$f_{B_s B_{s1}} \simeq 53.8(10.6)_f(1.8)_{t_c}(0.4)_\tau \cdots \text{ keV}, \quad r_{BB_1}^{sd} \simeq 0.99(3) \cdots . \quad (113)$$

Taking the mean value of the coupling and re-using $f_{BB_1}(5.5) \simeq 54(10.6)$ keV, we deduce the final estimate:

$$f_{B_s B_{s1}} \simeq 45.1(1.0) \cdots \text{ keV} \implies f_{BB_1}^{sd} \simeq 0.83(3) \cdots . \quad (114)$$

7.5. The (1^{-+}) Beauty Vector Molecule States

The (1^{-+}) $\bar{B}_{s0}^ B_s^*$ molecule state*

The behaviours of different curves are the same as in the previous case of the pseudoscalar $(0^{-\pm})$ and 1^{--} vector molecules and will not be shown here. τ stabilities are obtained are obtained at 0.07–0.08 (resp. 0.09), 0.07 (resp. 0.07) and 0.09 (resp. 0.095) GeV $^{-2}$ for the coupling, the SU3 ratio of couplings and the mass for $\sqrt{t_c} \simeq 13.2 + 2 m_q$ to $15 + 2 m_q$ GeV. We obtain the optimal results:

$$\begin{aligned} f_{B_{s0}^* B_s^*}(5.5) &\simeq 50.3(3.4)_{t_c}(2.2)_\tau \text{ keV}, \quad f_{B_0^* B^*}^{sd} \simeq 0.99(1.3)_{t_c}(3)_\tau , \\ M_{B_{s0}^* B_s^*} &\simeq 12734(239)_{t_c}(92)_\tau \text{ MeV}. \end{aligned} \quad (115)$$

Using the NLO value $f_{B_0^* B^*}(5.5) \simeq 54(9)$ keV and $M_{B_0^* B^*} \simeq 12774(261)$ MeV from,¹ one deduces from $f_{B_0^* B^*}^{sd}$:

$$f_{B_{s0}^* B_s^*} \simeq 53.5(8.9)_f(0.7)_{t_c}(1.6)_\tau \cdots \text{ keV}, \quad r_{B_0^* B^*}^{sd} \simeq 1.00(3) . \quad (116)$$

Taking the mean value of the coupling and re-using $f_{B_0^* B^*}(5.5) \simeq 54(9)$ keV, we deduce the final estimate:

$$f_{B_{s0}^* B_s^*} \simeq 50.8(3.7) \cdots \text{ keV} \implies f_{B_0^* B^*}^{sd} \simeq 0.94(3) \cdots . \quad (117)$$

The (1^{-+}) $\bar{B}_s B_{s1}$ molecule state

The behaviours of different curves are the same as in the case of the pseudoscalar $(0^{-\pm})$ molecules and will not be shown here. τ -stabilities are obtained at 0.055 (resp. 0.09), 0.07 (resp. 0.075) and 0.08 (resp. 0.095) GeV $^{-2}$ for the coupling, SU3 ratio of couplings and the mass for $\sqrt{t_c} \simeq 13 + 2 m_q$ to $15 + 2 m_q$ GeV. We deduce the optimal results:

$$\begin{aligned} f_{B_s B_{s1}}(5.5) &\simeq 47.4(4.5)_{t_c}(1)_\tau \text{ keV}, \quad f_{BB_1}^{sd} \simeq 1.005(44)_{t_c}(12)_\tau , \\ M_{B_s B_{s1}} &\simeq 12602(234)_{t_c}(32)_\tau \text{ MeV}. \end{aligned} \quad (118)$$

Using the NLO value $f_{BB_1}(5.5) \simeq 53(10.6)$ keV and $M_{BB_1} \simeq 12790(249)$ MeV from,¹ one deduces:

$$f_{B_s B_{s1}} \simeq 53.3(10.6)_f(2.3)_{t_c}(0.6)_\tau \cdots \text{ keV}, \quad r_{BB_1}^{sd} \simeq 0.985(27) . \quad (119)$$

Taking the mean value of the coupling and re-using $f_{BB_1}(5.5) \simeq 54(10.6)$ keV, we deduce the final estimate:

$$f_{B_s B_{s1}} \simeq 48.3(4.2) \cdots \text{ keV} \implies f_{BB_1}^{sd} \simeq 0.894(41) \cdots . \quad (120)$$

Table 14. Different sources of errors for the estimate of the 0^- and 1^- $\bar{B}_s B_s$ -like molecule masses (in units of MeV) and couplings $f_{M_s M_s}$ (in units of keV). We use $\mu = 5.5(5)$ GeV.

Inputs	$\Delta M_{B_{s0}^* B_s}$	$\Delta f_{B_{s0}^* B_s}$	$\Delta M_{B_s^* B_{s1}}$	$\Delta f_{B_s^* B_{s1}}$	$\Delta M_{B_{s0}^* B_s^*}$	$\Delta f_{B_{s0}^* B_s^*}$	$\Delta M_{B_s B_{s1}}$	$\Delta f_{B_s B_{s1}}$
<i>LCSR parameters</i>								
(t_c, τ)	200.4	5.5	264.1	9.1	260.6	5.1	225.0	1.0
μ	11	1.13	12	2.15	11.6	1.39	12.4	1.04
<i>QCD inputs</i>								
M_Q	3.70	0.18	3.84	0.34	3.88	0.17	4.0	0.18
α_s	5.20	0.50	4.82	0.94	5.46	0.48	4.96	0.54
$N3LO$	15.12	0.70	10.71	1.26	14.21	0.56	13.23	0.35
$\langle \bar{q}q \rangle$	5.10	0.05	5.73	0.11	7.23	0.03	0.0	0.0
$\langle \alpha_s G^2 \rangle$	5.10	0.05	2.66	0.05	0.27	0.0	0.0	0.0
M_0^2	1.75	0.0	3.53	0.0	1.13	0.03	2.06	0.07
$\langle \bar{q}q \rangle^2$	35.65	1.51	33.8	3.18	32.15	1.11	42.95	1.51
$\langle g^3 G^3 \rangle$	0.15	0.0	0.17	0.0	0.15	0.0	0.16	0.0
$d \geq 8$	71.80	0.82	125	8.09	41.6	1.81	54.6	2.00
<i>Total errors</i>	216.80	3.38	294.73	11.03	266.66	3.86	236.26	2.97

Table 15. Different sources of errors for the direct estimate of the 0^- and 1^- $\bar{B}_s B_s$ -like molecule SU(3) ratio of couplings f_{MM}^{sd} . We use $\mu = 5.5(5)$ GeV.

Inputs	$\Delta f_{B_0^* B}^{sd}$	$\Delta f_{B^* B_1}^{sd}$	$\Delta f_{B_0^* B^*}^{sd}$	$\Delta f_{BB_1}^{sd}$
<i>LCSR parameters</i>				
(t_c, τ)	0.023	0.03	0.03	0.03
μ	0.001	0.001	0.006	0.002
<i>QCD inputs</i>				
M_Q	0.0	0.0	0.0	0.0
α_s	0.0	0.0	0.0	0.0
$N3LO$	0.003	0.001	0.004	0.004
$\langle \bar{q}q \rangle$	0.001	0.001	0.001	0.0
$\langle \alpha_s G^2 \rangle$	0.0	0.0	0.0	0.0
M_0^2	0.0	0.0	0.001	0.001
$\langle \bar{q}q \rangle^2$	0.016	0.020	0.012	0.017
$\langle g^3 G^3 \rangle$	0.0	0.0	0.0	0.0
$d \geq 8$	0.001	0.0	0.002	0.002
<i>Total errors</i>	0.028	0.036	0.033	0.035

8. The Heavy-light Beauty Four-Quark States

We do a similar analysis. The different sources of errors are given in Tables 16 and 17.

8.1. The $S_{sb}(0^+)$ Beauty Scalar State

In this case, the coupling stabilizes at $\tau \simeq 0.11$ (resp. 0.14) GeV $^{-2}$ from $\sqrt{t_c} = 11.9 + 2\bar{m}_q$ to $\sqrt{t_c} = 15 + 2\bar{m}_q$ GeV while the SU3 ratio of masses stabilizes at $\tau \simeq$

Table 16. Different sources of errors for the estimate of the four-quarks $[bs\bar{b}\bar{s}]$ pseudo (scalar) π_{sb} (S_{sb}) and axial (vector) A_{sb} (V_{sb}) masses (in units of MeV) and couplings (in units of keV). We use $\mu = 5.5(5)$ GeV.

Inputs	$\Delta M_{S_{sb}}$	$\Delta f_{S_{sb}}$	$\Delta M_{A_{sb}}$	$\Delta f_{A_{sb}}$	$\Delta M_{\pi_{sb}}$	$\Delta f_{\pi_{sb}}$	$\Delta M_{V_{sb}}$	$\Delta f_{V_{sb}}$
<i>LSR parameters</i>								
(t_c, τ)	21	1.4	24	0.9	203	6	264	6
μ	3.02	1.23	4.27	1.20	13.3	1.54	12.2	1.36
<i>QCD inputs</i>								
M_Q	5.53	0.13	2.70	0.12	3.79	0.24	3.90	0.20
α_s	13.81	0.46	12.80	0.44	5.67	0.66	4.83	0.54
$N3LO$	0.77	0.28	1.54	0.28	24.92	0.35	21.35	0.28
$\langle\bar{q}q\rangle$	18.37	0.25	18.33	0.26	5.00	0.08	5.91	0.08
$\langle\alpha_s G^2\rangle$	0.42	0.01	0.13	0.007	1.48	0.02	1.18	0.01
M_0^2	18.00	0.28	18.47	0.26	0.46	0.0	1.75	0.10
$\langle\bar{q}q\rangle^2$	6.16	0.89	12.26	0.82	35.35	5.68	35.34	3.36
$\langle g^3 G^3 \rangle$	0.06	0.0	0.0	0.001	0.14	0.0	0.15	0.0
$d \geq 8$	144.56	4.80	167.72	3.21	53.4	8.76	50.5	4.49
<i>Total errors</i>	149.23	5.27	172.41	3.69	214.78	11.80	272.36	7.56

Table 17. Different sources of errors for the direct estimate of the four-quarks $[bs\bar{b}\bar{s}]$ pseudo (scalar) π_{sb} (S_{sb}) and axial (vector) A_{sb} (V_{sb}) SU(3) ratio of masses r_M^{sd} and of couplings f_M^{sd} . We use $\mu = 5.5(5)$ GeV.

Inputs	$\Delta r_{S_b}^{sd}$	$\Delta f_{S_b}^{sd}$	$\Delta r_{A_b}^{sd}$	$\Delta f_{A_b}^{sd}$	$\Delta f_{\pi_b}^{sd}$	$\Delta f_{V_b}^{sd}$
<i>LSR parameters</i>						
(t_c, τ)	0.002	0.016	0.002	0.02	0.03	0.04
μ	0.0	0.003	0.0	0.004	0.002	0.002
<i>QCD inputs</i>						
M_Q	0.0	0.0	0.0	0.0	0.0	0.0
α_s	0.0	0.007	0.0	0.001	0.0	0.0
$N3LO$	0.003	0.004	0.003	0.004	0.003	0.005
$\langle\bar{q}q\rangle$	0.001	0.002	0.001	0.003	0.001	0.001
$\langle\alpha_s G^2\rangle$	0.0	0.001	0.0	0.0	0.0	0.0
M_0^2	0.001	0.002	0.001	0.001	0.0	0.001
$\langle\bar{q}q\rangle^2$	0.001	0.012	0.001	0.019	0.056	0.044
$\langle g^3 G^3 \rangle$	0.0	0.0	0.0	0.0	0.0	0.0
$d \geq 8$	0.003	0.013	0.004	0.015	0.016	0.006
<i>Total errors</i>	0.0050	0.026	0.006	0.032	0.065	0.060

0.17(resp. 0.17) GeV $^{-2}$ for the same range of t_c -values. The SU3 ratio of couplings stabilizes for $\tau \simeq 0.09$ (resp. 0.14) GeV $^{-2}$ from $\sqrt{t_c} = 12.9 + 2\bar{m}_q$ to $\sqrt{t_c} = 15 + 2\bar{m}_q$ GeV. We obtain the optimal results at NLO:

$$f_{S_{sb}} \simeq 21.7(1.4)_{t_c}(0.1)_\tau \cdots \text{ keV}, \quad f_{S_b}^{sd} \simeq 0.919(17)_{t_c}(1)_\tau \cdots, \\ r_{S_b}^{sd} \simeq 1.044(2)_{t_c}(0.3)_\tau \cdots. \quad (121)$$

Using $f_{S_b} \simeq 17(0.14)$ keV and $M_{S_b} \simeq 10653(0.1)$ MeV from,¹ we can also deduce:

$$f_{S_b}^{sd} \simeq 0.78(4) \cdots, \quad M_{S_{sb}} \simeq 11122(21) \cdots \text{ MeV}. \quad (122)$$

Taking the mean of the SU3 ratio of couplings, we obtain our final estimate:

$$f_{S_b}^{sd} \simeq 0.898(16) \cdots \implies f_{S_{sb}} \simeq 15.27(0.30) \cdots \text{ keV} \quad (123)$$

8.2. The $A_b(1^+)$ Beauty Axial-Vector State

Here the coupling stabilizes at $\tau \simeq 0.10$ (resp. 0.14) GeV^{-2} from $\sqrt{t_c} = 11.9 + 2\bar{m}_q$ to $\sqrt{t_c} = 15 + 2\bar{m}_q$ GeV while the SU3 ratio of masses stabilizes at $\tau \simeq 0.18$ (resp. 0.16) GeV^{-2} for the same range of t_c -values. We obtain the optimal results at NLO:

$$f_{A_{sb}} \simeq 21.9(1.2)_{t_c}(0.1)_\tau \cdots \text{ keV}, \quad r_{A_b}^{sd} \simeq 1.042(2)_{t_c}(0.3)_\tau \cdots. \quad (124)$$

Using $f_{A_b} \simeq 18(0.9)$ keV and $M_{A_b} \simeq 10701(9)$ MeV from,¹ we deduce:

$$f_{A_b}^{sd} \simeq 0.82(6) \cdots, \quad M_{A_{sb}} \simeq 11150(24) \cdots \text{ MeV}. \quad (125)$$

Taking the mean of the previous SU3 ratio of couplings with the one from the direct determination obtained at $\tau \simeq 0.09$ (resp. 0.14) GeV^{-2} from $\sqrt{t_c} = 12.9 + 2\bar{m}_q$ GeV to $\sqrt{t_c} = 15 + 2\bar{m}_q$ GeV :

$$f_{A_b}^{sd} \simeq 0.92(2)_{t_c}(1)_\tau \cdots, \quad (126)$$

we deduce:

$$f_{A_b}^{sd} \simeq 0.91(2) \cdots \implies f_{A_{sb}} \simeq 16.4(0.9) \cdots \text{ keV} \quad (127)$$

where f_{A_b} has been used for deriving the last equation.

8.3. The $\pi_{sb}(0^-)$ Beauty Pseudoscalar State

The coupling presents τ -stabilities from $\sqrt{t_c} = 13.2 + 2\bar{m}_q$ GeV to $\sqrt{t_c} = 15 + 2\bar{m}_q$ GeV and for $\tau=0.045$ (resp. 0.09) GeV^{-2} . Within these range of t_c -values, the mass stabilizes for $\tau \simeq 0.08$ (resp. 0.095) GeV^{-2} and the ratio of couplings for $\tau \simeq 0.08$ (resp. 0.09) GeV^{-2} . We obtain:

$$\begin{aligned} f_{\pi_{sb}} &\simeq 60(7)_{t_c}(2)_\tau \cdots \text{ keV}, \\ f_{\pi_b}^{sd} &\simeq 0.91(2)_{t_c}(3)_\tau \cdots, \quad M_{\pi_{sb}} \simeq 12730(197)_{t_c}(48)_\tau \text{ MeV}. \end{aligned} \quad (128)$$

Using the values: $M_{\pi_b} = 12920(235)$ MeV and $f_{\pi_b} = 83(9)$ keV from,¹ we can deduce:

$$r_{\pi_b}^{sd} \simeq 0.985(24) \cdots, \quad f_{\pi_{sb}} \simeq 75.5(82)_f(17)_{t_c}(25)_\tau \cdots \text{ keV}. \quad (129)$$

Taking the mean of $f_{\pi_{sb}}$ and re-using $f_{\pi_b} = 83(9)$ keV, we deduce the final estimate:

$$f_{\pi_{sb}} \simeq 66(6) \cdots \text{ keV} \implies f_{\pi_b}^{sd} \simeq 0.80(3) \cdots, \quad (130)$$

where the error comes from the direct determination of the SU3 ratio.

8.4. The $V_{sb}(1^-)$ Beauty Vector State

The behaviours of the corresponding curves are very similar to the previous ones. The coupling presents τ -stabilities from $\sqrt{t_c} = 13.0 + 2\bar{m}_q$ to $\sqrt{t_c} = 15.0 + 2\bar{m}_q$ GeV and for $\tau=0.04$ (resp. 0.09) GeV^{-2} . Within these range of t_c -values, the mass

stabilizes for $\tau \simeq 0.07$ (resp. 0.09) GeV^{-2} and the ratio of couplings for $\tau \simeq 0.06$ (resp. 0.07) GeV^{-2} . We obtain:

$$\begin{aligned} f_{V_{sb}} &\simeq 57(7)_{t_c}(2)_\tau \cdots \text{ keV ,} \\ f_{V_b}^{sd} &\simeq 1.03(3)_{t_c}(2)_\tau \cdots , \quad M_{V_{sb}} \simeq 12716(260)_{t_c}(48)_\tau \text{ MeV.} \end{aligned} \quad (131)$$

Using the NLO values: $M_{V_b} = 12770(214)$ MeV and $f_{V_b} \simeq 62(9)$ keV from,¹ we can deduce:

$$r_{V_b}^{sd} \simeq 1.00(3) \cdots , \quad f_{V_{sb}} \simeq 64(9)_f(2)_{t_c}(1)_\tau \cdots \text{ keV .} \quad (132)$$

Taking the mean of $f_{V_{sb}}$ and re-using $f_{V_b} \simeq 62(9)$ keV, we deduce the final estimate:

$$f_{V_{sb}} \simeq 60(6) \cdots \text{ keV} \implies f_{V_b}^{sd} \simeq 0.97(4) \cdots , \quad (133)$$

where the error of $f_{V_b}^{sd}$ comes from the direct determination.

9. Summary Tables

Our different results for the masses, couplings and their SU3 ratios are summarized in the Tables below. The SU3 ratios have been obtained either from a direct determination or/and by taking the ratio of masses (couplings) from this paper and the ones in the chiral limit from.¹ We complete Table 18 by the revised values of the $\bar{D}_0^* D_0^*$ and $\bar{D}_0^* D_1$ masses and couplings and by the new value of the $\bar{D}_1 D_1$ ones.

9.1. Charm States

Molecules

Table 18. $\bar{D}D$ -like molecules couplings, masses and their corresponding SU3 ratios from LSR within stability criteria at NLO to N2LO of PT. We include revised estimates of the $\bar{D}_0^* D_0^*$, $\bar{D}_0^* D_1$ couplings and masses and new one for $\bar{D}_1 D_1$. The errors are the quadratic sum of the ones in Tables 5 to 8.

Channels	$f_M^{sd} \equiv f_{M_s}/f_M$		f_{M_s} [keV]		$r_M^{sd} \equiv M_{M_s}/M_M$		M_{M_s} [MeV]	
	NLO	N2LO	NLO	N2LO	NLO	N2LO	NLO	N2LO
Scalar(0^{++})								
$\bar{D}_s D_s$	0.95(3)	0.98(4)	156(17)	167(18)	1.069(4)	1.070(4)	4169(48)	4169(48)
$\bar{D}_s^* D_s^*$	0.93(3)	0.95(3)	265(31)	284(34)	1.069(3)	1.075(3)	4192(200)	4196(200)
$\bar{D}_{s0}^* D_{s0}^*$	0.88(6)	0.89(6)	85(12)	102(14)	1.069(69)	1.058(68)	4277(134)	4225(132)
$\bar{D}_{s1} D_{s1}$	0.906(33)	0.930(34)	209(28)	229(31)	1.097(7)	1.090(7)	4187(62)	4124(61)
$\bar{D}_0^* D_0^*$	—	—	97(15)	114(18)	—	—	4003(227)	3954(224)
$\bar{D}_1 D_1$	—	—	236(32)	274(37)	—	—	3838(57)	3784(56)
Axial($1^{+\pm}$)								
$\bar{D}_s^* D_s$	0.93(3)	0.97(3)	143(16)	156(17)	1.070(4)	1.073(4)	4174(67)	4188(67)
$\bar{D}_{s0}^* D_{s1}$	0.90(1)	0.82(1)	87(14)	110(18)	1.119(24)	1.100(24)	4269(205)	4275(206)
$\bar{D}_0^* D_1$	—	—	96(15)	112(17)	—	—	3849(182)	3854(182)
Pseudo($0^{-\pm}$)								
$\bar{D}_{s0}^* D_s$	0.94(5)	0.90(4)	225(24)	232(25)	0.970(50)	0.946(40)	5604(223)	5385(214)
$\bar{D}_s^* D_{s1}$	0.93(4)	0.90(4)	455(34)	508(38)	0.970(50)	0.972(34)	5724(195)	5632(192)
Vector(1^{--})								
$\bar{D}_{s0}^* D_s^*$	0.87(4)	0.86(4)	208(11)	216(11)	0.980(33)	0.956(32)	5708(184)	5571(180)
$\bar{D}_s D_{s1}$	0.97(3)	0.93(3)	202(12)	213(13)	0.970(33)	0.951(31)	5459(122)	5272(120)
Vector(1^{-+})								
$\bar{D}_{s0}^* D_s^*$	0.98(5)	0.92(5)	219(17)	231(18)	0.963(32)	0.948(32)	5699(184)	5528(179)
$\bar{D}_s D_{s1}$	0.92(3)	0.88(3)	195(13)	212(14)	0.959(34)	0.955(34)	5599(155)	5487(152)

Four-quark

Table 19. 4-quark couplings, masses and their corresponding SU3 ratios from LSR within stability criteria at NLO and N2LO of PT. The errors are the quadratic sum of the ones in Tables 10 and 11. The * indicates that the value does not come from a direct determination.

Channels	$f_M^{sd} \equiv f_{M_s}/f_M$		f_{M_s} [keV]		$r_M^{sd} \equiv M_{M_s}/M_M$		M_{M_s} [MeV]	
	NLO	N2LO	NLO	N2LO	NLO	N2LO	NLO	N2LO
c-quark								
$S_{sc}(0^+)$	0.91(4)	0.98(4)	161(17)	187(19)	1.085(11)	1.086(11)	4233(61)	4233(61)
$A_{sc}(1^+)$	0.80(4)	0.87(4)	141(15)	160(17)	1.081(4)	1.082(4)	4205(112)	4209(112)
$\pi_{sc}(0^-)$	0.88(7)	0.86(7)	256(29)	267(30)	0.97(3)*	0.96(3)*	5671(181)	5524(176)
$V_{sc}(1^-)$	0.91(10)	0.87(10)	245(31)	258(33)	0.96(4)*	0.96(4)*	5654(239)	5539(234)

9.2. Beauty States

Molecules

Table 20. $\bar{B}B$ -like molecules couplings, masses and their corresponding SU3 ratios from LSR within stability criteria at NLO to N2LO of PT. The errors are the quadratic sum of the ones in Tables 12 to 15. The * indicates that the value does not come from a direct determination.

Channels	$f_M^{sd} \equiv f_{M_s}/f_M$		f_{M_s} [keV]		$r_M^{sd} \equiv M_{M_s}/M_M$		M_{M_s} [MeV]	
	NLO	N2LO	NLO	N2LO	NLO	N2LO	NLO	N2LO
Scalar(0^{++})								
$\bar{B}_s B_s$	1.04(4)	1.15(4)	17(2)	20(2)	1.027(4)	1.029(4)	10884(74)	10906(74)
$\bar{B}_s^* B_s^*$	1.00(3)	1.12(3)	31(5)	36(6)	1.028(5)	1.029(5)	10944(134)	10956(134)
$\bar{B}_{s0}^* B_{s0}^*$	1.11(5)	1.07(5)	13(3)	17(4)	1.050(11)	1.034(11)	11182(227)	11014(224)
$\bar{B}_{s1} B_{s1}$	1.197(73)	1.214(74)	24(5)	29(6)	1.040(2)	1.035(2)	10935(170)	10882(169)
$\bar{B}_1 B_1$	—	—	20(3)	28.6(4)	—	—	10514(149)	10514(149)
Axial($1^{+\pm}$)								
$\bar{B}_s^* B_s$	1.01(3)	1.18(4)	17(2)	20(2)	1.028(4)	1.030(4)	10972(195)	10972(195)
$\bar{B}_{s0}^* B_{s1}$	0.80(4)	0.79(4)	9(2)	11(3)	1.052(14)	1.031(14)	11234(208)	11021(204)
Pseudo($0^{-\pm}$)								
$\bar{B}_{s0}^* B_s$	1.06(3)	1.02(3)	58(3)	68(4)	1.00(3)*	1.00(3)*	12725(217)	12509(213)
$\bar{B}_s^* B_{s1}$	0.96(4)	0.95(4)	100(11)	118(13)	1.00(3)*	1.00(3)*	12726(295)	12573(292)
Vector(1^{--})								
$\bar{B}_{s0}^* B_s^*$	0.95(3)	0.90(3)	51(4)	59(5)	1.00(3)*	0.99(3)*	12715(267)	12512(263)
$\bar{B}_s B_{s1}$	0.83(4)	0.77(3)	45(3)	50(3)	0.99(3)*	0.99(3)*	12615(236)	12426(233)
Vector(1^{-+})								
$\bar{B}_{s0}^* B_s^*$	0.94(3)	0.92(3)	51(5)	59(6)	1.00(3)*	0.99(3)*	12734(262)	12479(257)
$\bar{B}_s B_{s1}$	0.89(4)	0.85(3)	48(5)	55(6)	0.99(3)*	0.98(3)*	12602(247)	12350(242)

Four-quark

Table 21. 4-quark couplings, masses and their corresponding SU3 ratios from LSR within stability criteria at NLO and N2LO of PT. The errors are the quadratic sum of the ones in Tables 10 and 17.

Channels	$f_M^{sd} \equiv f_{M_s}/f_M$		f_{M_s} [keV]		$r_M^{sd} \equiv M_{M_s}/M_M$		M_{M_s} [MeV]	
	NLO	N2LO	NLO	N2LO	NLO	N2LO	NLO	N2LO
b-quark								
$S_{sb}(0^+)$	0.78(3)	0.83(3)	22(5)	26(6)	1.044(4)	1.048(4)	11122(149)	11133((149)
$A_{sb}(1^+)$	0.92(3)	0.98(3)	22(4)	26(5)	1.042(6)	1.046(6)	11150(172)	11172(172)
$\pi_{sb}(0^-)$	0.80(7)	0.76(4)	66(12)	71(13)	0.985(2)*	0.975(2)*	12730(215)	12374(209)
$V_{sb}(1^-)$	0.97(6)	0.90(6)	64(8)	68(9)	0.996(3)*	0.984(30)*	12716(272)	12411(266)

10. Comments and Conclusions

Comparison of the lowest order QCD expressions

We compare numerically the different LO QCD expressions of the spectral functions up to dimension-six from different authors. For definiteness, we consider the examples of the 0^{++} and 1^{++} with some specific channels where the results from the QSSR analysis are listed in Table 22.

– $D_s^* D_s^*$ molecule states

Table 22. Comparison with some existing lowest order (LO) results for the 0^{++} and 1^+ charm molecules and four-quark states with hidden strange quarks from QCD Laplace Sum Rules within the same choice of interpolating currents. The experimental candidates are listed in Table 1.

Charm States	Mass[MeV]	Beauty States	Mass[MeV]	PT Order	References
Scalar (0^{++}) Molecules					
$\bar{D}_s D_s$					
4169(48)	$\bar{B}_s B_s$	10906(74)	N2LO	<i>This work</i>	¹²⁵
3910(100)			LO		
$\bar{D}_s^* D_s^*$					
4196(200)	$\bar{B}_s^* B_s^*$	10956(134)	N2LO	<i>This work</i>	¹²⁶
4140(90)			LO		¹²⁵
4130(100)			LO		
4480(170)		11240(180)	LO		¹²⁷
4380(160)			LO		¹²⁸
$\bar{D}_{s0}^* D_{s0}^*$					
4225(132)	$\bar{B}_{s0}^* B_{s0}^*$	11014(224)	N2LO	<i>This work</i>	¹²⁹
4580(100)		11350(90)	LO		
$\bar{D}_{s1} D_{s1}$					
4124(61)	$\bar{B}_{s1} B_{s1}$	10882(169)	N2LO	<i>This work</i>	¹²⁹
4660(120)		11390(130)	LO		
Four-quarks					
$S_{sc}[\bar{c}\bar{s}cs]$					
4.233(61)	$S_{sb}[\bar{b}\bar{s}bs]$	11133(149)	N2LO	<i>This work</i>	¹³⁰
4180(190)		10010(210)	LO		
Axial (1^+) Molecules					
$\bar{D}_s^* D_s$					
4188(67)	$\bar{B}_s^* B_s$	10972(195)	N2LO	<i>This work</i>	¹²⁸
3980(150)			LO		¹²⁵
4010(100)		10710(110)	LO		
$\bar{D}_{s0}^* D_{s1}$					
4275(206)	$\bar{B}_{s0}^* B_{s1}$	11021(204)	N2LO	<i>This work</i>	¹²⁹
4640(100)		11380(90)	LO		
Four-quarks					
$A_{sc}[\bar{c}\bar{s}cs]$					
4209(112)	$A_{sb}[\bar{b}\bar{s}bs]$	11172(172)	N2LO	<i>This work</i>	¹³¹
4240(100)		10340(90)	LO		¹³²
3950(90)			LO		¹³²
4183(115)			LO		¹³³

There is a complete agreement with our results and the ones in.^{126,127} For the four-quark condensates, we retain the linear m_s -corrections while m_s^2 corrections are included in.^{126,127}

– 0^{++} four-quarks states

Our results are compared with the ones in.¹³⁰ There is a discrepancy at high s as shown in Fig. 14, which originates from the fact that we only keep the linear m_s corrections.

– 1^{++} four-quarks states

We compare in Figs. 15 to 17 our results with the ones from.^{131,132} One can notice that the disagreement among different expressions occurs mainly at high values of s . The disagreement for the four-quark condensate in Fig. 17 at low s of our result with the one from¹³² by a factor 2.

However, due to the few informations given by the authors on the derivation of

their QCD expressions, it is difficult to trace back the exact origin of such discrepancies. Hopefully, within the accuracy of the approach, such discrepancies affect only slightly the final results listed in Table 22 if the errors are taken properly.

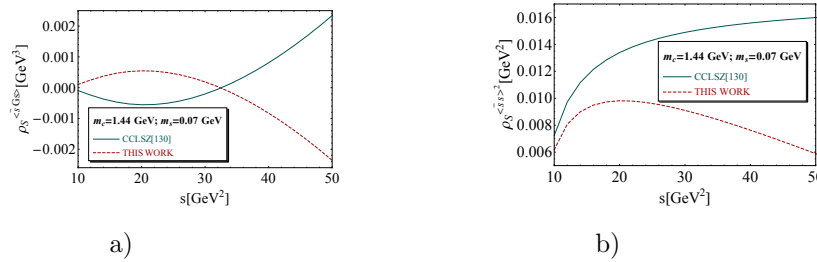


Fig. 14. Comparison of the Wilson coefficients of the 0^{++} four-quark spectral functions for different values of s and for given values of m_c and m_s : **a)** mixed condensate; **b)** four-quark condensate.

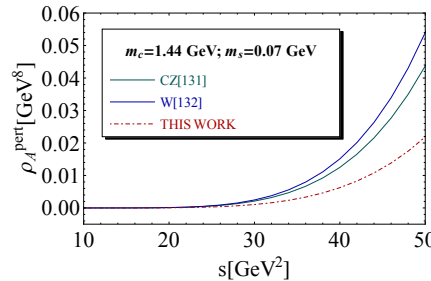


Fig. 15. Comparison of the perturbative expression of the 1^{++} four-quark spectral functions for different values of s and for given values of m_c and m_s .

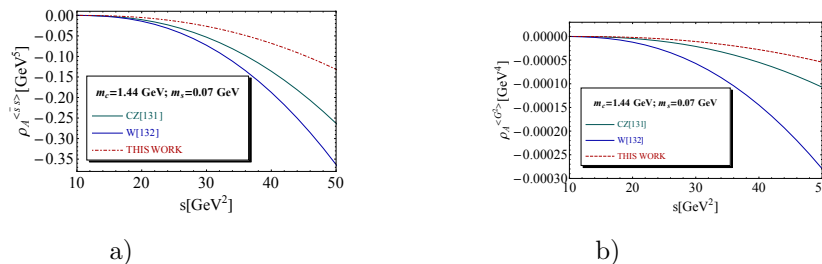


Fig. 16. Comparison of the Wilson coefficients of the 1^{++} four-quark spectral functions for different values of s and for given values of m_c and m_s : **a)** $\langle \bar{s}s \rangle$ condensate; **b)** $\alpha_s G^2$ condensate.

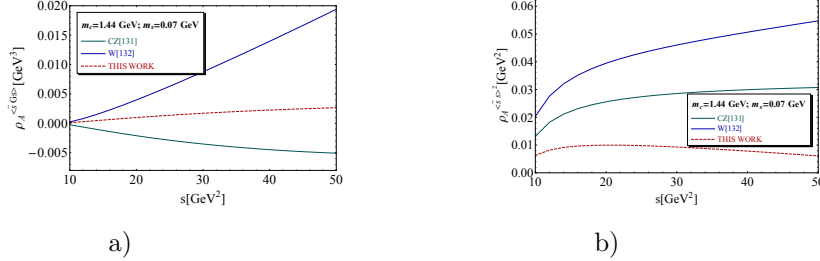


Fig. 17. Comparison of the Wilson coefficients of the 1^{++} four-quark spectral functions for different values of s and for given values of m_c and m_s : **a)** mixed condensate; **b)** four-quark condensate.

Comparison with some previous lowest order QSSR results

We list in Table 22 some previous results for the 0^{++} and 1^{++} charm states obtained from QSSR at lowest order (LO) of perturbative QCD for the scalar and axial-vector channels. The comparison is only informative as it is known that the LO results suffer from the ill-defined definition of the heavy quark mass used in the analysis at this order. Most of the authors use the running mass value which is not justified when one implicitly uses the QCD expression obtained within the on-shell scheme. The difference between some results is also due to the way for extracting the optimal information from the analysis (different choices of t_c and τ). Here, we use well-defined based stability criteria verified from the example of the harmonic oscillator in quantum mechanics and from different well-known hadronic channels. Another source of discrepancy in the four-quark channels is the choice of the interpolating currents. We have taken the simplest choice of currents and used the optimal choice ($k = 0$) determined in our earlier works.^{23,24} The results obtained in^{23,24} by matching the Laplace sum rules with Finite Energy moments at N2LO will not be reported in the Table as this way of doing may lead to erroneous results due to the high-sensitivity of the Finite Energy moments on the continuum contribution. There, we also use the range of values spanned by the running and the pole mass (which one should do at LO) in the analysis.

Confrontation with experiments

We compare our results of the scalar 0^{++} and axial-vector 1^{++} charm states obtained by using the lowest dimension currents with the experimental X candidates given in Table 1. We conclude from the previous analysis that:

- The 0^{++} $X(4700)$ experimental candidate might be identified with a $\bar{D}_{s0}^* D_{s0}^*$ molecule ground state.
- The interpretation of the 0^{++} candidates as pure 4-quark ground states is not favoured by our result.
- The masses of 1^{++} $X(4147)$ and $X(4273)$ are compatible within the error with the one of the $\bar{D}_s^* D_s$ molecule state and with the one of the axial-vector A_c 4-quark state.

- Our predictions suggest the presence of 0^{++} $\bar{D}_s D_s$ and $\bar{D}_s^* D_s^*$ molecule states in the range $(4121 \sim 4396)$ MeV and a $D_{s0}^* D_{s1}$ state around 4841 MeV.
- We present new predictions for the $0^{-\pm}, 1^{-\pm}$ and for different beauty states which can be tested in future experiments.
- Noting that the QCD continuum model smears all higher mass states, one may approximately expect that their masses are in the vicinity of the value of the continuum threshold. In most case, the optimization region starts from 300 (resp. 600) MeV above the lowest ground state mass. Then, one expects that the radial excitations might be visible in these regions if they couple strongly enough to the interpolating currents.

Theoretical Results and Perspectives

- Our previous results show that the SU3 breakings are relatively small for the masses (≤ 10 (resp. 3)% for the charm (resp. bottom) channels while its can be large for the couplings ($\leq 20\%$). This can be understood as, in the ratios of sum rules, the corrections tend to cancel out.
- The approach cannot clearly separate (within the errors) some molecule states from the four-quark ones of a given quantum number.
- Like in the chiral limit case,¹ we also observe that the couplings behave as $1/m_b^{3/2}$ (resp. $1/m_b$) for the $1^+, 0^+$ (resp. $1^-, 0^-$) molecules and four-quark states which can be compared with $f_B \sim 1/m_b^{1/2}$ for open beauty mesons. These results which are important for further building of an effective theory for these exotic states can be tested by lattice calculations.
- A natural extension of our analysis is the estimate of the meson widths. We plan to do this project in a future work.

Acknowledgements

We thank A. Rabemananjara for participating at the early stage of this work.

Appendix A. SU3 Breakings to the Molecule Spectral Functions

They are defined from Eq. 2 as: $\frac{1}{\pi} \text{Im} \Pi_{mol}^{(1)}(t)$ for spin 1 particles and $\frac{1}{\pi} \text{Im} \psi_{mol}^{(s,p)}(t)$ from Eq. 3 for spin 0 ones and normalized in the same way as the spectral functions in Ref.¹. In the following, we shall give the SU3 breaking corrections (denoted by $\delta\rho$) to the spectral functions obtained in the chiral limit ($m_q = 0$)¹. We shall use the same notations and definitions:

$$\begin{aligned} Q &\equiv c, b, & x = M_Q^2/t, & v = \sqrt{1 - 4x}, \\ \mathcal{L}_v &= \text{Log}_{(1-v)}^{(1+v)}, & \mathcal{L}_+ = \text{Li}_2\left(\frac{1+v}{2}\right) - \text{Li}_2\left(\frac{1-v}{2}\right). \end{aligned}$$

Appendix A.1. $(0^{++}) \bar{D}_s D_s, \bar{B}_s B_s$ Molecules

$$\begin{aligned}\delta\rho_{m_s}^{pert}(s) &= -\frac{m_s M_Q^7}{2^{11} \pi^6} \left[v \left(60 + \frac{130}{x} - \frac{18}{x^2} - \frac{1}{x^3} \right) + \right. \\ &\quad \left. 12\mathcal{L}_v \left(10x - 4 - 6 \operatorname{Log}(x) - \frac{6}{x} + \frac{1}{x^2} \right) - 144\mathcal{L}_+ \right] \\ \delta\rho_{m_s}^{\langle \bar{s}s \rangle}(s) &= -\frac{m_s M_Q^4 \langle \bar{s}s \rangle}{2^8 \pi^4} \left[v \left(24 + \frac{22}{x} - \frac{1}{x^2} \right) + 12\mathcal{L}_v \left(4x - 5 \right) \right] \\ \delta\rho_{m_s}^{\langle \bar{s}Gs \rangle}(s) &= \frac{m_s M_Q^2 \langle \bar{s}Gs \rangle}{2^7 \pi^4} \left[v \left(10 + \frac{1}{x} \right) + 3\mathcal{L}_v \left(4x - 3 \right) \right] \\ \delta\rho_{m_s}^{\langle \bar{s}s \rangle^2}(s) &= -\frac{m_s M_Q \rho \langle \bar{s}s \rangle^2}{2^5 \pi^2} v(1+s\tau) \\ \delta\rho_{m_s}^{\langle \bar{s}s \rangle \langle \bar{s}Gs \rangle}(s) &= \frac{(m_s/M_Q) \langle \bar{s}s \rangle \langle \bar{s}Gs \rangle}{3 \cdot 2^7 \pi^2} v \left(6 + 6s\tau - 6s^2\tau^2 + 5s^3\tau^3 x \right)\end{aligned}$$

Appendix A.2. $(0^{++}) D_s^* D_s^*, B_s^* B_s^*$ Molecules

$$\begin{aligned}\delta\rho_{m_s}^{pert}(s) &= -\frac{m_s M_Q^7}{2^{10} \pi^6} \left[v \left(60 + \frac{130}{x} - \frac{18}{x^2} - \frac{1}{x^3} \right) + \right. \\ &\quad \left. 12\mathcal{L}_v \left(10x - 4 - 6 \operatorname{Log}(x) - \frac{6}{x} + \frac{1}{x^2} \right) - 144\mathcal{L}_+ \right] \\ \delta\rho_{m_s}^{\langle \bar{s}s \rangle}(s) &= -\frac{m_s M_Q^4 \langle \bar{s}s \rangle}{2^6 \pi^4} \left[v \left(24 + \frac{22}{x} - \frac{1}{x^2} \right) + 12\mathcal{L}_v \left(4x - 5 \right) \right] \\ \delta\rho_{m_s}^{\langle \bar{s}Gs \rangle}(s) &= \frac{m_s M_Q^2 \langle \bar{s}Gs \rangle}{2^6 \pi^4} v \left(8 - \frac{1}{x} \right) \\ \delta\rho_{m_s}^{\langle \bar{s}s \rangle^2}(s) &= -\frac{m_s M_Q \rho \langle \bar{s}s \rangle^2}{2^4 \pi^2} v(1+s\tau) \\ \rho^{m_s \cdot \langle \bar{s}s \rangle \langle \bar{s}Gs \rangle}(s) &= \frac{(m_s/M_Q) \langle \bar{s}s \rangle \langle \bar{s}Gs \rangle}{3 \cdot 2^6 \pi^2} v x \left(12s^2\tau^2 + 5s^3\tau^3 \right)\end{aligned}$$

Appendix A.3. $(0^{++}) D_{s0}^* D_{s0}^*, B_{s0}^* B_{s0}^*$ Molecules

$$\begin{aligned}\delta\rho_{m_s}^{pert}(s) &= \frac{m_s M_Q^7}{2^{11} \pi^6} \left[v \left(60 + \frac{130}{x} - \frac{18}{x^2} - \frac{1}{x^3} \right) + \right. \\ &\quad \left. 12\mathcal{L}_v \left(10x - 4 - 6 \operatorname{Log}(x) - \frac{6}{x} + \frac{1}{x^2} \right) - 144\mathcal{L}_+ \right] \\ \delta\rho_{m_s}^{\langle\bar{s}s\rangle}(s) &= -\frac{m_s M_Q^4 \langle\bar{s}s\rangle}{2^8 \pi^4} \left[v \left(24 + \frac{22}{x} - \frac{1}{x^2} \right) + 12\mathcal{L}_v \left(4x - 5 \right) \right] \\ \delta\rho_{m_s}^{\langle\bar{s}Gs\rangle}(s) &= \frac{m_s M_Q^2 \langle\bar{s}Gs\rangle}{2^7 \pi^4} \left[v \left(10 + \frac{1}{x} \right) + 3\mathcal{L}_v \left(4x - 3 \right) \right] \\ \delta\rho_{m_s}^{\langle\bar{s}s\rangle^2}(s) &= \frac{m_s M_Q \rho \langle\bar{s}s\rangle^2}{2^5 \pi^2} v(1 + s\tau) \\ \delta\rho_{m_s}^{\langle\bar{s}s\rangle \langle\bar{s}Gs\rangle}(s) &= -\frac{(m_s/M_Q) \langle\bar{s}s\rangle \langle\bar{s}Gs\rangle}{3 \cdot 2^7 \pi^2} v \left(6 + 6s\tau - 6s^2\tau^2 + 5s^3\tau^3 x \right)\end{aligned}$$

Appendix A.4. $(0^{++}) D_{s1}D_{s1}, B_{s1}B_{s1}$ Molecules

$$\begin{aligned}
\rho^{pert}(s) &= \frac{M_Q^8}{5 \cdot 2^{12} \pi^6} \left[v \left(480 + \frac{1460}{x} - \frac{274}{x^2} - \frac{38}{x^3} + \frac{1}{x^4} \right) + \right. \\
&\quad \left. 120 \mathcal{L}_v \left(8x - 1 - 6 \operatorname{Log}(x) - \frac{8}{x} + \frac{2}{x^2} \right) - 1440 \mathcal{L}_+ \right] \\
\delta \rho_{m_s}^{pert}(s) &= \frac{m_s M_Q^7}{2^{10} \pi^6} \left[v \left(60 + \frac{130}{x} - \frac{18}{x^2} - \frac{1}{x^3} \right) + \right. \\
&\quad \left. 12 \mathcal{L}_v \left(10x - 4 - 6 \operatorname{Log}(x) - \frac{6}{x} + \frac{1}{x^2} \right) - 144 \mathcal{L}_+ \right] \\
\rho^{\langle \bar{s}s \rangle}(s) &= -\frac{M_Q^5 \langle \bar{s}s \rangle}{2^6 \pi^4} \left[v \left(6 - \frac{5}{x} - \frac{1}{x^2} \right) + 6 \mathcal{L}_v \left(2x - 2 + \frac{1}{x} \right) \right] \\
\delta \rho_{m_s}^{\langle \bar{s}s \rangle}(s) &= -\frac{m_s M_Q^4 \langle \bar{s}s \rangle}{2^6 \pi^4} \left[v \left(24 + \frac{22}{x} - \frac{1}{x^2} \right) - 12 \mathcal{L}_v \left(5 - 4x \right) \right] \\
\rho^{\langle G^2 \rangle}(s) &= \frac{M_Q^4 \langle g_s^2 G^2 \rangle}{3 \cdot 2^{10} \pi^6} \left[v \left(6 - \frac{5}{x} - \frac{1}{x^2} \right) + 6 \mathcal{L}_v \left(2x - 2 + \frac{1}{x} \right) \right] \\
\rho^{\langle \bar{s}Gs \rangle}(s) &= -\frac{3 M_Q^3 \langle \bar{s}Gs \rangle}{2^7 \pi^4} \left[\frac{v}{x} - 2 \mathcal{L}_v \right] \\
\delta \rho_{m_s}^{\langle \bar{s}Gs \rangle}(s) &= \frac{m_s M_Q^2 \langle \bar{s}Gs \rangle}{2^6 \pi^4} v \left[8 - \frac{1}{x} \right] \\
\rho^{\langle \bar{s}s \rangle^2}(s) &= \frac{M_Q^2 \rho^{\langle \bar{s}s \rangle^2} v}{4 \pi^2} \\
\delta \rho_{m_s}^{\langle \bar{s}s \rangle^2}(s) &= \frac{m_s M_Q \rho^{\langle \bar{s}s \rangle^2}}{2^4 \pi^2} v (3 - s \tau) \\
\rho^{\langle G^3 \rangle}(s) &= -\frac{M_Q^2 \langle g_s^3 G^3 \rangle}{3 \cdot 2^{12} \pi^6} \left[v \left(6 - \frac{25}{x} + \frac{1}{x^2} \right) + 6 \mathcal{L}_v \left(2x + 2 + \frac{1}{x} \right) \right] \\
\rho^{\langle \bar{s}s \rangle \langle \bar{s}Gs \rangle}(s) &= -\frac{M_Q^2 \langle \bar{s}s \rangle \langle \bar{s}Gs \rangle}{8 \pi^2} v s \tau^2 \\
\delta \rho_{m_s}^{\langle \bar{s}s \rangle \langle \bar{s}Gs \rangle}(s) &= \frac{m_s M_Q \langle \bar{s}s \rangle \langle \bar{s}Gs \rangle}{3 \cdot 2^6 \pi^2} v \tau \left[12 s \tau + 5 s^2 \tau^2 \right]
\end{aligned}$$

Appendix A.5. $(1^{+\pm}) D_s^* D_s, B_s^* B_s$ Molecules

$$\begin{aligned}\delta\rho_{m_s}^{pert}(s) &= -\frac{m_s M_Q^7}{5 \cdot 2^{14} \pi^6} \left[v \left(420x + 1270 + \frac{4174}{x} - \frac{617}{x^2} - \frac{36}{x^3} \right) + \right. \\ &\quad \left. 60\mathcal{L}_v \left(14x^2 + 40x - 12 - 36 \text{Log}(x) - \frac{40}{x} + \frac{7}{x^2} \right) - 4320\mathcal{L}_+ \right] \\ \delta\rho_{m_s}^{\langle \bar{s}s \rangle}(s) &= \frac{m_s M_Q^4 \langle \bar{s}s \rangle}{2^{10} \pi^4} \left[v \left(12x - 94 - \frac{74}{x} + \frac{3}{x^2} \right) + 24\mathcal{L}_v \left(x^2 - 8x + 9 \right) \right] \\ \delta\rho_{m_s}^{\langle \bar{s}Gs \rangle}(s) &= -\frac{m_s M_Q^2 \langle \bar{s}Gs \rangle}{3 \cdot 2^8 \pi^4} \left[v \left(6x - 37 + \frac{1}{x} \right) + 6\mathcal{L}_v \left(2x^2 - 6x + 3 \right) \right] \\ \delta\rho_{m_s}^{\langle \bar{s}s \rangle^2}(s) &= -\frac{m_s M_Q \rho \langle \bar{s}s \rangle^2}{2^6 \pi^2} v(1 + 2s\tau) \\ \delta\rho_{m_s}^{\langle \bar{s}s \rangle \langle \bar{s}Gs \rangle}(s) &= -\frac{(m_s/M_Q) \langle \bar{s}s \rangle \langle \bar{s}Gs \rangle}{3 \cdot 2^8 \pi^2} v \left[s\tau \left(13x - 12 \right) + s^2\tau^2 \left(x + 6 \right) - 10s^3\tau^3 x \right]\end{aligned}$$

Appendix A.6. $(1^{+\pm}) D_{s0}^* D_{s1}, B_{s0}^* B_{s1}$ Molecules

$$\begin{aligned}\delta\rho_{m_s}^{pert}(s) &= \frac{m_s M_Q^7}{5 \cdot 2^{14} \pi^6} \left[v \left(420x + 1270 + \frac{4174}{x} - \frac{617}{x^2} - \frac{36}{x^3} \right) + \right. \\ &\quad \left. 60\mathcal{L}_v \left(14x^2 + 40x - 12 - 36 \text{Log}(x) - \frac{40}{x} + \frac{7}{x^2} \right) - 4320\mathcal{L}_+ \right] \\ \delta\rho_{m_s}^{\langle \bar{s}s \rangle}(s) &= \frac{m_s M_Q^4 \langle \bar{s}s \rangle}{2^{10} \pi^4} \left[v \left(12x - 94 - \frac{74}{x} + \frac{3}{x^2} \right) + 24\mathcal{L}_v \left(x^2 - 8x + 9 \right) \right] \\ \delta\rho_{m_s}^{\langle \bar{s}Gs \rangle}(s) &= -\frac{m_s M_Q^2 \langle \bar{s}Gs \rangle}{3 \cdot 2^8 \pi^4} \left[v \left(6x - 37 + \frac{1}{x} \right) + 6\mathcal{L}_v \left(2x^2 - 6x + 3 \right) \right] \\ \delta\rho_{m_s}^{\langle \bar{s}s \rangle^2}(s) &= \frac{m_s M_Q \rho \langle \bar{s}s \rangle^2}{2^6 \pi^2} v(1 + 2s\tau) \\ \delta\rho_{m_s}^{\langle \bar{s}s \rangle \langle \bar{s}Gs \rangle}(s) &= \frac{(m_s/M_Q) \langle \bar{s}s \rangle \langle \bar{s}Gs \rangle}{3 \cdot 2^8 \pi^2} v \left[s\tau \left(13x - 12 \right) + s^2\tau^2 \left(x + 6 \right) - 10s^3\tau^3 x \right]\end{aligned}$$

Appendix A.7. $(0^{-\pm}) D_s^* D_{s1}, B_s^* B_{s1}$ Molecules

$$\begin{aligned}\delta\rho_{m_s}^{pert}(s) &= 0 \\ \delta\rho_{m_s}^{\langle \bar{s}s \rangle}(s) &= \frac{m_s M_Q^4 \langle \bar{s}s \rangle}{2^6 \pi^4} \left[v \left(24 + \frac{2}{x} + \frac{1}{x^2} \right) + 12\mathcal{L}_v \left(4x - 3 \right) \right] \\ \delta\rho_{m_s}^{\langle \bar{s}Gs \rangle}(s) &= -\frac{m_s M_Q^2 \langle \bar{s}Gs \rangle}{2^6 \pi^4} v \left(4 + \frac{1}{x} \right) \\ \delta\rho_{m_s}^{\langle \bar{s}s \rangle^2}(s) &= 0 \\ \delta\rho_{m_s}^{\langle \bar{s}s \rangle \langle \bar{s}Gs \rangle}(s) &= 0\end{aligned}$$

Appendix A.8. $(0^{-\pm}) D_{s0}^* D_s, D_{s0}^* D_s$ Molecules

$$\begin{aligned}\delta\rho_{m_s}^{pert}(s) &= 0 \\ \delta\rho_{m_s}^{\langle\bar{s}s\rangle}(s) &= \frac{m_s M_Q^4 \langle\bar{s}s\rangle}{2^8 \pi^4} \left[v \left(24 + \frac{2}{x} + \frac{1}{x^2} \right) + 12\mathcal{L}_v \left(4x - 3 \right) \right] \\ \delta\rho_{m_s}^{\langle\bar{s}Gs\rangle}(s) &= -\frac{m_s M_Q^2 \langle\bar{s}Gs\rangle}{2^7 \pi^4} \left[v \left(8 - \frac{1}{x} \right) + 3\mathcal{L}_v \left(4x - 1 \right) \right] \\ \delta\rho_{m_s}^{\langle\bar{s}s\rangle^2}(s) &= 0 \\ \delta\rho_{m_s}^{\langle\bar{s}s\rangle\langle\bar{s}Gs\rangle}(s) &= 0\end{aligned}$$

Appendix A.9. $(1^{--}) D_{s0}^* D_s^*, B_{s0}^* B_s^*$ Molecules

$$\begin{aligned}\delta\rho_{m_s}^{pert}(s) &= 0 \\ \delta\rho_{m_s}^{\langle\bar{s}s\rangle}(s) &= \frac{m_s M_Q^4 \langle\bar{s}s\rangle}{2^9 \pi^4} \left[v \left(60 + \frac{20}{x} + \frac{1}{x^2} \right) + 12\mathcal{L}_v \left(10x - 9 \right) \right] \\ \delta\rho_{m_s}^{\langle\bar{s}Gs\rangle}(s) &= \frac{m_s M_Q^2 \langle\bar{s}Gs\rangle}{3 \cdot 2^8 \pi^4} \left[v \left(6x - 50 - \frac{1}{x} \right) + 3\mathcal{L}_v \left(4x^2 - 18x + 9 \right) \right] \\ \delta\rho_{m_s}^{\langle\bar{s}s\rangle^2}(s) &= 0 \\ \delta\rho_{m_s}^{\langle\bar{s}s\rangle\langle\bar{s}Gs\rangle}(s) &= -\frac{(m_s/M_Q)\langle\bar{s}s\rangle\langle\bar{s}Gs\rangle}{3 \cdot 2^7 \pi^2} v \left[3 - s\tau(x - 3) + s^2\tau^2(14x - 3) \right]\end{aligned}$$

Appendix A.10. $(1^{-+}) D_{s0}^* D_s^*, B_{s0}^* B_s^*$ Molecules

$$\begin{aligned}\delta\rho_{m_s}^{pert}(s) &= -\frac{m_s M_Q^7}{5 \cdot 2^{13} \pi^6} \left[v \left(420x - 1130 - \frac{1026}{x} + \frac{103}{x^2} + \frac{4}{x^3} \right) + \right. \\ &\quad \left. 60\mathcal{L}_v \left(14x^2 - 40x + 20 + 12 \text{Log}(x) + \frac{8}{x} - \frac{1}{x^2} \right) + 1440\mathcal{L}_+ \right] \\ \delta\rho_{m_s}^{\langle\bar{s}s\rangle}(s) &= -\frac{m_s M_Q^4 \langle\bar{s}s\rangle}{2^8 \pi^4} \left[v \left(6x + 19 + \frac{1}{x} + \frac{1}{x^2} \right) + 6\mathcal{L}_v \left(2x^2 + 6x - 5 \right) \right] \\ \delta\rho_{m_s}^{\langle\bar{s}Gs\rangle}(s) &= \frac{m_s M_Q^2 \langle\bar{s}Gs\rangle}{3 \cdot 2^8 \pi^4} \left[v \left(18x + 20 + \frac{1}{x} \right) + 9\mathcal{L}_v \left(4x^2 + 2x - 1 \right) \right] \\ \delta\rho_{m_s}^{\langle\bar{s}s\rangle^2}(s) &= \frac{m_s M_Q \rho \langle\bar{s}s\rangle^2}{2^5 \pi^2} v \\ \delta\rho_{m_s}^{\langle\bar{s}s\rangle\langle\bar{s}Gs\rangle}(s) &= -\frac{(m_s/M_Q)\langle\bar{s}s\rangle\langle\bar{s}Gs\rangle}{2^7 \pi^2} v \left[1 + s\tau(4x - 3) - s^2\tau^2(3x - 1) \right]\end{aligned}$$

Appendix A.11. $(1^{--}) D_s D_{s1}, B_s B_{s1}$ Molecules

$$\begin{aligned}\delta\rho_{m_s}^{pert}(s) &= 0 \\ \delta\rho_{m_s}^{\langle\bar{s}s\rangle}(s) &= 0 \\ \delta\rho_{m_s}^{\langle\bar{s}Gs\rangle}(s) &= \frac{3m_s M_Q^2 \langle\bar{s}Gs\rangle}{2^7 \pi^4} \left[v + \mathcal{L}_v(2x - 1) \right] \\ \delta\rho_{m_s}^{\langle\bar{s}s\rangle^2}(s) &= 0 \\ \delta\rho_{m_s}^{\langle\bar{s}s\rangle\langle\bar{s}Gs\rangle}(s) &= -\frac{(m_s/M_Q)\langle\bar{s}s\rangle\langle\bar{s}Gs\rangle}{2^6 \pi^2} v(s^2 \tau^2 x)\end{aligned}$$

Appendix A.12. $(1^{+}) D_s D_{s1}, B_s B_{s1}$ Molecules

$$\begin{aligned}\delta\rho_{m_s}^{pert}(s) &= \frac{m_s M_Q^7}{5 \cdot 2^{13} \pi^6} \left[v \left(420x - 1130 - \frac{1026}{x} + \frac{103}{x^2} + \frac{4}{x^3} \right) + \right. \\ &\quad \left. 60\mathcal{L}_v \left(14x^2 - 40x + 20 + 12 \text{Log}(x) + \frac{8}{x} - \frac{1}{x^2} \right) + 1440\mathcal{L}_+ \right] \\ \delta\rho_{m_s}^{\langle\bar{s}s\rangle}(s) &= -\frac{m_s M_Q^4 \langle\bar{s}s\rangle}{2^9 \pi^4} \left[v \left(12x + 98 + \frac{22}{x} + \frac{3}{x^2} \right) + 24\mathcal{L}_v(x^2 + 8x - 7) \right] \\ \delta\rho_{m_s}^{\langle\bar{s}Gs\rangle}(s) &= \frac{m_s M_Q^2 \langle\bar{s}Gs\rangle}{3 \cdot 2^7 \pi^4} \left[v \left(6x + 26 + \frac{1}{x} \right) + 3\mathcal{L}_v(4x^2 + 6x - 3) \right] \\ \delta\rho_{m_s}^{\langle\bar{s}s\rangle^2}(s) &= -\frac{m_s M_Q \rho^{\langle\bar{s}s\rangle^2}}{2^5 \pi^2} v \\ \delta\rho_{m_s}^{\langle\bar{s}s\rangle\langle\bar{s}Gs\rangle}(s) &= \frac{(m_s/M_Q)\langle\bar{s}s\rangle\langle\bar{s}Gs\rangle}{3 \cdot 2^7 \pi^2} v \left[s\tau(13x - 12) - s^2 \tau^2(17x - 6) \right]\end{aligned}$$

Appendix B. Four-Quark States Spectral Functions

The spectral functions corresponding to the four-quark interpolating currents given in Table 9 read:

Appendix B.1. (0^+) Scalar State

$$\begin{aligned}\rho_S^{m_s}(s) &= -\frac{(1-k^2)m_s M_c^7}{3 \cdot 2^9 \pi^6} \left[v \left(60 + \frac{130}{x} - \frac{18}{x^2} - \frac{1}{x^3} \right) + \right. \\ &\quad \left. 12\mathcal{L}_v \left(10x - 4 - 6 \log x - \frac{6}{x} + \frac{1}{x^2} \right) - 144 \mathcal{L}_+ \right] \\ \rho_S^{m_s \cdot \langle \bar{s}s \rangle}(s) &= -\frac{(1+k^2)m_s M_c^4 \langle \bar{s}s \rangle}{3 \cdot 2^6 \pi^4} \left[v \left(24 + \frac{22}{x} - \frac{1}{x^2} \right) + 12\mathcal{L}_v \left(4x - 5 \right) \right] \\ \rho_S^{m_s \cdot \langle \bar{s}Gs \rangle}(s) &= \frac{(1+k^2)m_s M_c^2 \langle \bar{s}Gs \rangle}{3 \cdot 2^7 \pi^4} \left[v \left(28 + \frac{1}{x} \right) + 6\mathcal{L}_v \left(4x - 3 \right) \right] \\ \rho_S^{m_s \cdot \langle \bar{s}s \rangle^2}(s) &= -\frac{(1-k^2)m_s M_c \rho \langle \bar{s}s \rangle^2}{3 \cdot 2^3 \pi^2} v(1+s\tau) \\ \rho_S^{m_s \cdot \langle \bar{s}s \rangle \langle \bar{s}Gs \rangle}(s) &= \frac{(1-k^2)(m_s/M_c) \langle \bar{s}s \rangle \langle \bar{s}Gs \rangle}{3^2 \cdot 2^5 \pi^2} v \left[3 + 3s\tau - 3s^2\tau^2 + 5xs^3\tau^3 \right]\end{aligned}$$

Appendix B.2. (1^+) Axial-vector State

$$\begin{aligned}\rho_A^{m_s}(s) &= -\frac{(1-k^2)m_s M_c^7}{5 \cdot 3 \cdot 2^{12} \pi^6} \left[v \left(420x + 1270 + \frac{4174}{x} - \frac{617}{x^2} - \frac{36}{x^3} \right) + \right. \\ &\quad \left. 60\mathcal{L}_v \left(14x^2 + 40x - 12 - 36 \log x - \frac{40}{x} + \frac{7}{x^2} \right) - 4320 \mathcal{L}_+ \right] \\ \rho_A^{m_s \cdot \langle \bar{s}s \rangle}(s) &= \frac{(1+k^2)m_s M_c^4 \langle \bar{s}s \rangle}{3 \cdot 2^8 \pi^4} \left[v \left(12x - 94 - \frac{74}{x} + \frac{3}{x^2} \right) + 24\mathcal{L}_v \left(x^2 - 8x + 9 \right) \right] \\ \rho_A^{m_s \cdot \langle \bar{s}Gs \rangle}(s) &= -\frac{(1+k^2)m_s M_c^2 \langle \bar{s}Gs \rangle}{3 \cdot 2^7 \pi^4} \left[v \left(2x - 19 + \frac{1}{x} \right) + 2\mathcal{L}_v \left(2x^2 - 6x + 3 \right) \right] \\ \rho_A^{m_s \cdot \langle \bar{s}s \rangle^2}(s) &= -\frac{(1-k^2)m_s M_c \rho \langle \bar{s}s \rangle^2}{3 \cdot 2^4 \pi^2} v(1+2s\tau) \\ \rho_A^{m_s \cdot \langle \bar{s}s \rangle \langle \bar{s}Gs \rangle}(s) &= \frac{(1-k^2)(m_s/M_c) \langle \bar{s}s \rangle \langle \bar{s}Gs \rangle}{3^2 \cdot 2^6 \pi^2} v \left[3s\tau(2 - 3x) - 3s^2\tau^2(1 + x) + 10xs^3\tau^3 \right]\end{aligned}$$

Appendix B.3. (0^-) Pseudoscalar State

$$\begin{aligned}\rho_P^{m_s}(s) &= 0 \\ \rho_P^{m_s \cdot \langle \bar{s}s \rangle}(s) &= \frac{(1+k^2)m_s M_c^4 \langle \bar{s}s \rangle}{3 \cdot 2^6 \pi^4} \left[v \left(24 + \frac{2}{x} + \frac{1}{x^2} \right) + 12\mathcal{L}_v \left(4x - 3 \right) \right] \\ \rho_P^{m_s \cdot \langle \bar{s}Gs \rangle}(s) &= -\frac{(1+k^2)m_s M_c^2 \langle \bar{s}Gs \rangle}{3 \cdot 2^7 \pi^4} \left[v \left(20 - \frac{1}{x} \right) + 6\mathcal{L}_v \left(4x - 1 \right) \right] \\ \rho_P^{m_s \cdot \langle \bar{s}s \rangle^2}(s) &= 0 \\ \rho_P^{m_s \cdot \langle \bar{s}s \rangle \langle \bar{s}Gs \rangle}(s) &= 0\end{aligned}$$

Appendix B.4. (1^-) Vector State

$$\begin{aligned}\rho_V^{m_s}(s) &= -\frac{(1-k^2)m_s M_c^7}{5 \cdot 3 \cdot 2^{12} \pi^6} \left[v \left(420x - 1130 - \frac{1026}{x} + \frac{103}{x^2} + \frac{4}{x^3} \right) + \right. \\ &\quad \left. 60\mathcal{L}_v \left(14x^2 - 40x + 20 + 12 \log x + \frac{8}{x} - \frac{1}{x^2} \right) + 1440 \mathcal{L}_+ \right] \\ \rho_V^{m_s \cdot \langle \bar{s}s \rangle}(s) &= \frac{(1+k^2)m_s M_c^4 \langle \bar{s}s \rangle}{3 \cdot 2^8 \pi^4} \left[v \left(12x + 98 + \frac{22}{x} + \frac{3}{x^2} \right) + 24\mathcal{L}_v \left(x^2 + 8x - 7 \right) \right] \\ \rho_V^{m_s \cdot \langle \bar{s}Gs \rangle}(s) &= -\frac{(1+k^2)m_s M_c^2 \langle \bar{s}Gs \rangle}{3 \cdot 2^7 \pi^4} \left[v \left(2x + 17 + \frac{1}{x} \right) + 2\mathcal{L}_v \left(2x^2 + 6x - 3 \right) \right] \\ \rho_V^{m_s \cdot \langle \bar{s}s \rangle^2}(s) &= \frac{(1-k^2)m_s M_c \rho \langle \bar{s}s \rangle^2}{3 \cdot 2^4 \pi^2} v \\ \rho_V^{m_s \cdot \langle \bar{s}s \rangle \langle \bar{s}Gs \rangle}(s) &= \frac{(1-k^2)(m_s/M_c) \langle \bar{s}s \rangle \langle \bar{s}Gs \rangle}{3 \cdot 2^6 \pi^2} v \left[s\tau(2-3x) - s^2\tau^2(1-3x) \right]\end{aligned}$$

References

1. R. Albuquerque, S. Narison, F. Fanomezana, A. Rabemananjara, D. Rabetiarivony and G. Randriamananjara, *Int. J. Mod. Phys. A* **31** (2016) no. 36, 1650196.
2. R. Albuquerque, S. Narison, A. Rabemananjara and D. Rabetiarivony, *Int. J. Mod. Phys. A* **31** (2016) no. 17, 1650093.
3. F. Fanomezana, S. Narison and A. Rabemananjara, *Nucl. Part. Phys. Proc.* **258-259** (2015) 152.
4. F. Fanomezana, S. Narison and A. Rabemananjara, *Nucl. Part. Phys. Proc.* **258-259** (2015) 156.
5. M.A. Shifman, A.I. Vainshtein and V.I. Zakharov, *Nucl. Phys.* **B147** (1979) 385.
6. M.A. Shifman, A.I. Vainshtein and V.I. Zakharov, *Nucl. Phys.* **B147** (1979) 448.
7. S. Narison, E. de Rafael, *Phys. Lett.* **B103** (1981) 57.
8. J.S. Bell and R.A. Bertlmann, *Nucl. Phys.* **B227** (1983) 435.
9. R.A. Bertlmann, *Acta Phys. Austriaca* **53** (1981) 305.
10. R.A. Bertlmann and H. Neufeld, *Z. Phys.* **C27** (1985) 437.
11. R.A. Bertlmann, G. Launer and E. de Rafael, *Nucl. Phys.* **B250** (1985) 61.
12. R.A. Bertlmann, C.A. Dominguez, M. Loewe, M. Perrottet and E. de Rafael, *Z. Phys.* **C39** (1988) 231.
13. S. Narison, *QCD as a theory of hadrons*, Cambridge Monogr. Part. Phys. Nucl. Phys. Cosmol. **17** (2002) 1 [hep-ph/0205006].
14. S. Narison, *QCD spectral sum rules*, World Sci. Lect. Notes Phys. **26** (1989) 1.
15. S. Narison, *Phys. Rept.* **84** (1982) 263.
16. S. Narison, *Acta Phys. Pol.* **B26** (1995) 687.
17. S. Narison, hep-ph/9510270 (1995).
18. L.J. Reinders, H. Rubinstein and S. Yazaki, *Phys. Rept.* **127** (1985) 1.
19. E. de Rafael, hep-ph/9802448.
20. R.D. Matheus, S. Narison, M. Nielsen and J.M. Richard, *Phys. Rev.* **D75** (2007) 014005.
21. J. M. Dias, S. Narison, F.S. Navarra, M. Nielsen and J. M. Richard, *Phys. Lett.* **B703** (2011) 274.
22. S. Narison, F.S. Navarra and M. Nielsen, *Phys. Rev.* **D83** (2011) 016004.

23. R.M. Albuquerque, F. Fanomezana, S. Narison and A. Rabemananjara, *Phys. Lett.* **B715** (2012) 129-141.
24. R.M. Albuquerque, F. Fanomezana, S. Narison and A. Rabemananjara, *Nucl. Phys. Proc. Suppl.* **234** (2013) 158-161.
25. F. S. Navarra, M. Nielsen, S. H. Lee, *Phys. Rep.* **497** (2010) 41.
26. H.-X. Chen et al., *Phys. Rep.* **631** (2016) 1.
27. R. Albuquerque, PhD thesis, arXiv:1306.4671 [hep-ph] (2013).
28. R. Albuquerque, S. Narison, D. Rabetiarivony and G. Randriamananjara, talks given at QCD17-Montpellier and HEPMAD17-Antananarivo, arXiv:1801.03073 [hep-ph] (to appear as *Nucl. Part. Phys. Proc. and ECONF-SLAC*).
29. S. Narison, *Phys. Lett.* **B673** (2009) 30.
30. G. Launer, S. Narison and R. Tarrach, *Z. Phys.* **C26** (1984) 433.
31. Y. Chung et al., *Z. Phys.* **C25** (1984) 151.
32. H.G. Dosch, *Non-Perturbative Methods*, Montpellier, France, 1985 ed. S. Narison (World Scientific, Singapore, 1985).
33. H.G Dosch, M. Jamin and S. Narison, *Phys. Lett.* **B220** (1989) 251.
34. S. Narison and R. Tarrach, *Phys. Lett.* **B125** (1983) 217.
35. S. Narison and V.I. Zakharov, *Phys. Lett.* **B679** (2009) 355.
36. T. Skwarnicki [LHCb collaboration] talk given at Meson2016.
37. T. Aaltonen et al. [CDF Collaboration], *Phys. Rev. Lett.* **102** (2009) 242002.
38. T. Aaltonen et al. [CDF Collaboration], arXiv:1101.6058 [hep-ex] (2011).
39. S. Chatrchyan et al. [CMS Collaboration], *Phys. Lett.* **B734** (2014) 261.
40. V.M Abazov et al. [D0 Collaboration], *Phys. Rev.* **D89** (2014) 012004.
41. C.P Shen et al. [BELLE Collaboration], *Phys. Rev. Lett.* **104** (2010) 112004.
42. R. Tarrach, *Nucl. Phys.* **B183** (1981) 384.
43. R. Coquereaux, *Annals of Physics* **125** (1980) 401.
44. P. Binetruy and T. Sücker, *Nucl. Phys.* **B178** (1981) 293.
45. S. Narison, *Phys. Lett.* **B197** (1987) 405.
46. S. Narison, *Phys. Lett.* **B216** (1989) 191.
47. N. Gray, D.J. Broadhurst, W. Grafe, and K. Schilcher, *Z. Phys.* **C48** (1990) 673.
48. L.V. Avdeev and M. Yu. Kalmykov, *Nucl. Phys.* **B502** (1997) 419.
49. J. Fleischer, F. Jegerlehner, O.V. Tarasov, and O.L. Veretin, *Nucl. Phys.* **B539** (1999) 671.
50. K.G. Chetyrkin and M. Steinhauser, *Nucl. Phys.* **B573** (2000) 617.
51. K. Melnikov and T. van Ritbergen, *Phys. Lett.* **B482** (2000) 99.
52. F. S. Navarra, M. Nielsen, J.M. Dias and C.M. Zanetti, *Nucl. Part. Phys. Proc.* **258-259** (2015) 145.
53. W. Chen, T. G. Steele, H.-X. Chen and S.-L. Zhu, *Phys. Rev.* **D92** (2015) 054002.
54. A. Pich and E. de Rafael, *Phys. Lett.* **B158** (1985) 477.
55. A. Pich, *Phys. Lett.* **B206** (1988) 322.
56. S. Narison and A. Pivovarov, *Phys. Lett.* **B327** (1994) 341.
57. K. Hagiwara, S. Narison and D. Nomura, *Phys. Lett.* **B540** (2002) 233.
58. D.J. Broadhurst, *Phys. Lett.* **B101** (1981) 423.
59. K.G. Chetyrkin and M. Steinhauser, *Phys. Lett.* **B502** (2001) 104.
60. K.G. Chetyrkin and M. Steinhauser, *Eur. Phys. J.* **C21** (2001) 319 and references therein.
61. P. Gelhausen et al., *Phys. Rev.* **D88** (2013) 014015, Erratum: ibid. **D89** (2014) 099901, Erratum: ibid. **D91** (2015) 099901.
62. K. Chetyrkin, S. Narison and V.I. Zakharov, *Nucl. Phys.* **B550** (1999) 353.
63. S. Narison and V.I. Zakharov, *Phys. Lett.* **B522** (2001) 266.

64. V.I. Zakharov, *Nucl. Phys. Proc. Suppl.* **164** (2007) 240.
65. S. Narison, *Nucl. Phys. Proc. Suppl.* **164** (2007) 225.
66. S. Narison and G. Veneziano, *Int. J. Mod. Phys. A* **4** (1989) 2751.
67. S. Narison, *Nucl. Phys. B* **509** (1998) 225.
68. S. Narison, *Nucl. Phys. Proc. Suppl.* **64** (1998) 210.
69. V. De Alfaro, S. Fubini, G. Furlan and C. Rossetti, *Currents in Hadron Physics*, Elsevier (1973) 1-866.
70. S. Narison, *Phys. Lett.* **B210** (1988) 238.
71. S. Narison, *Phys. Lett.* **B337** (1994) 166.
72. S. Narison, *Phys. Lett.* **B322** (1994) 327.
73. S. Narison, *Phys. Lett.* **B387** (1996) 162.
74. S. Narison, *Phys. Lett.* **B358** (1995) 113.
75. S. Narison, *Phys. Rev. D* **74** (2006) 034013.
76. S. Narison, *Phys. Lett.* **B466** (1999) 345.
77. S. Narison, *Phys. Lett.* **B605** (2005) 319.
78. S. Narison, *Phys. Lett.* **B668** (2008) 308.
79. R.M. Albuquerque and S. Narison, *Phys. Lett.* **B694** (2010) 217.
80. R.M. Albuquerque, S. Narison and M. Nielsen, *Phys. Lett.* **B684** (2010) 236.
81. W. Lucha, D. Melikhov and S. Simula, *Phys. Lett.* **B735** (2014) 12.
82. S. Narison, *Phys. Lett.* **B718** (2013) 1321.
83. S. Narison, *Nucl. Phys. Proc. Suppl.* **234** (2013) 187.
84. E. de Rafael, *Nucl. Phys. Proc. Suppl.* **96** (2001) 316.
85. S. Peris, B. Phily and E. de Rafael, *Phys. Rev. Lett.* **86** (2001) 14.
86. S. Narison, *Phys. Lett.* **B520** (2001) 115.
87. S. Narison, *Nucl. Phys. Proc. Suppl.* **258-259** (2015) 189 and references therein.
88. S. Narison, *Nucl. Phys. Proc. Suppl.* **270-272** (2016) 143 and references therein.
89. J. Rosner and S. Stone, arXiv:1509.02220 [hep-ph] (2015).
90. S. Aoki et al., FLAG working group, *Eur. Phys. J.* **C74** (2014) 2890.
91. S. Narison, *Phys. Lett.* **B721** (2013) 269.
92. S. Narison, *Phys. Lett.* **B738** (2014) 346.
93. S. Narison, *Int. J. Mod. Phys. A* **30** (2015) no.20, 1550116.
94. S. Narison, *Int. Mod. Phys. A* **33** (2018) 1850045.
95. P.M. Stevenson, *Nucl. Phys.* **B868** (2013) 38.
96. S. J. Brodsky, G. P. Lepage and P. B. Mackenzie, *Phys. Rev. D* **28** (1983) 228.
97. X.-G. Wu et al., *Rep. Prog. Phys.* **78** (2015) 126201.
98. A.L. Kataev and S.V. Mikhailov, *Phys. Rev. D* **91** (2015) no.1, 014007.
99. J. -L. Kneur and A. Neveu, *Phys. Rev. D* **88** (2013) 074025.
100. E. Braaten, S. Narison and A. Pich, *Nucl. Phys.* **B373** (1992) 581.
101. S. Narison and A. Pich, *Phys. Lett.* **B211** (1988) 183.
102. H.G. Dosch and S. Narison, *Phys. Lett.* **B417** (1998) 173.
103. S. Narison, *Phys. Lett.* **B216** (1989) 191.
104. S. Narison, arXiv:hep-ph/0202200 (2002).
105. S. Narison, *Phys. Lett.* **B693** (2010) 559; Erratum ibid 705 (2011) 544.
106. S. Narison, *Phys. Lett.* **B706** (2011) 412.
107. S. Narison, *Phys. Lett.* **B707** (2012) 259.
108. B.L. Ioffe and K.N. Zyablyuk, *Eur. Phys. J.* **C27** (2003) 229.
109. B.L. Ioffe, *Prog. Part. Nucl. Phys.* **56** (2006) 232.
110. Particle Data Group (C.Patrignani *et al.*), *Chin. Phys. C* **40** (2016) 100001.
111. B.L. Ioffe, *Nucl. Phys.* **B188** (1981) 317.
112. B.L. Ioffe, *Nucl. Phys.* **B191** (1981) 591.

113. A.A.Ovchinnikov and A.A.Pivovarov, *Yad. Fiz.* **48** (1988) 1135.
114. S. Narison, *Phys. Lett.* **B300** (1993) 293.
115. S. Narison, *Phys. Lett.* **B361** (1995) 121.
116. F.J. Yndurain, *Phys. Rept.* **320** (1999) 287.
117. S. Narison, *Phys. Lett.* **B361** (1995) 121.
118. S. Narison, *Phys. Lett.* **B624** (2005) 223.
119. S. Narison, *Phys. Lett.* **B387** (1996) 162.
120. E.G. Floratos, S. Narison and E. de Rafael, *Nucl. Phys.* **B155** (1979) 155.
121. A. Pich and A. Rodriguez-Sánchez, *Phys. Rev.D* **94** n°3 (2016) 034027 .
122. S. Bethke, *Nucl. Part. Phys. Proc.* **282-284** (2017) 149.
123. G. S. Bali, C. Bauer and A. Pineda, *Phys. Rev. Lett.* **113** (2014) 092001.
124. T. Lee, *Phys. Rev.* **D82**(2010)114021.
125. J. R. Zhang and M. Q. Huang, *J. Phys.* **G37** (2010) 025005.
126. R. M. Albuquerque, M. E. Bracco and M. Nielsen, *Phys. Lett.* **B678** (2009) 186.
127. Z. G. Wang, Z. C. Liu and X. H. Zhang, *Eur. Phys. J.* **C 64** (2009) 373.
128. C.-F. Qiao and L. Tang, *Eur. Phys. J.* **C74** (2014) 2810.
129. J. R. Zhang and M. Q. Huang, *Commun.Theor. Phys.* **54**(2010) 1075.
130. W. Chen, H.X Chen, X. Liu, T.G Steele and S. L. Zhu, *Phys. Rev.D* **96** n°11 (2017) 114017.
131. W. Chen and S. L Zhu, *Phys.Rev.* **D83** (2011) 034010.
132. Z. G.Wang, *Eur. Phys. J.* **C 77** (2017) n°3, 174.
133. S.S. Agaev, K. Azizi and H. Sundu, *Phys.Rev.* **D95** (2017) n°11, 114003